On positive braids and monodromy groups of plane curve singularities

Inaugural dissertation
of the Faculty of Science,
University of Bern

presented by

Livio Clemente Emilio Ferretti

from Italy

Supervisor of the doctoral thesis:
Prof. Dr. Sebastian Baader

University of Bern

On positive braids and monodromy groups of plane curve singularities

Inaugural dissertation
of the Faculty of Science,
University of Bern

presented by

Livio Clemente Emilio Ferretti

from Italy

Supervisor of the doctoral thesis:
Prof. Dr. Sebastian Baader
University of Bern

Accepted by the Faculty of Science.

Bern, 29.06.2023

The Dean
Prof. Dr. Marco Herwegh

Acknowledgements

First of all, I wish to thank my advisor Sebastian Baader for his guidance and support through my PhD studies. His enthusiasm and positivity in research, his interest for Mathematics as a whole, the freedom he always gave me during my studies were invaluable and deeply shaped my mathematical views. On a different level, he contributed in making my experience in Bern so enjoyable, be it by teaching me backgammon in front of a cup of coffee, playing chess or sharing good wine while playing the piano together.

This thesis was refereed by David Cimasoni and Marco Golla; I am very grateful to both of them for reading the manuscript. More generally, they both were, in different ways, very inspirational and supportive from even before the beginning of my PhD studies. I am glad they accepted to referee my thesis, thus somehow closing a circle.

During those years, I had the chance to collaborate and discuss with various people, from which I learned a lot and that I wish to thank: Valeriano Aiello, Lukas Lewark, Filip Misev and Levi Ryffel. I also had many interesting mathematical conversations with Elia Bubani, Gaofeng Huang, Julia Münch, Simon Santschi and Alejandro Vargas. Besides, special thanks to Peter Feller for giving a very interesting CUSO lecture, Livio Liechti for organising an exciting reading group in Teichmüller theory, and Damaris Meier for co-founding and co-organising our Bern-Fribourg graduate seminar.

Those years of studies were somehow split in two. I want to thank all my housemates in Köniz for trying to keep a semblance of normality through the pandemic and making the home-office be more bearable, and all the people at the Mathematical Institute for trying to go back to actual normality and bringing back a nice environment at Alpeneggstrasse.

Finally, thanks to all of my friends in Geneva and in Italy for keeping the contacts in spite of the distance and not asking too many questions about maths, my current housemates for the nice time together, my family for their unconditional support, and Julia for too many things to write here.

Contents

Chapter 1

Introduction

This thesis is situated at the intersection of knot theory, singularity theory and surface topology. It contains most of the results obtained during my PhD studies; part of them, mainly from Chapter 4, appeared in [37]. In this introduction, we will recall the context from which this research originated and shortly present the main results.

Singularity theory and topology have always been strongly related. If at the beginning of the 20th century topological investigations of singularities of complex curves and the development of knot theory proceeded in parallel, the interactions between complex algebraic geometry and topology were further explored in higher dimensions starting from the sixties, thanks to the work of some of the masters of modern topology, such as Hirzebruch, Milnor and Brieskorn, to name just a few.

The key concept to connect singularity theory and topology is the one of links of singularities. If $f : \mathbb{C}^n \to \mathbb{C}$ is a polynomial in n variables and $X = f^{-1}(0) \subset \mathbb{C}^n$ the associated hypersurface, for a point $p \in X$ the link of p in X is $L_p(f) = X \cap S^{2n-1}(p; r)$, where $S^{2n-1}(p; r)$ is a sphere centered at p of sufficiently small radius r. If p is either a smooth point of X or an isolated critical point, its link is a compact smooth manifold of real dimension $2n - 3$. In the following, we will assume that all critical points are isolated. While the link of a smooth point is clearly a standard, unknotted sphere, links of isolated singular points provide many examples of interesting topological spaces, which are often amenable to study because of their rather concrete nature. In fact, this is already the case for some of the simplest spaces: (homology) spheres. For example, while for $n \geq 4$ Milnor proved that no non-trivial homology sphere can arise as the link of a singularity [64], Brieskorn showed that interesting knotted spheres can appear [20]. Famously, Hirzebruch first realized that some of those spheres naturally carry an exotic smooth structure, and his student Brieskorn later proved that every odd dimensional exotic sphere bounding a parallelizable manifold could be exhibited as the link of an

isolated singularity [49],[18]. In dimension $n = 3$, the situation is radically different. By a result of Mumford, no non-trivially knotted 3-sphere can be the link of an isolated surface singularity [65]; on the other hand, homology 3-spheres are abundant among links of singularities, and the examples coming from singularity theory for instance eventually led to a greater understanding of the homology cobordism group of homology 3-spheres [39],[41],[38]. Ideas obviously also traveled in the other direction, and topological methods were successfully applied to solve problems of singularity theory. A first, fundamental result in this direction is the Cone Structure Theorem, saying that locally around an isolated critical point p the hypersurface $X = f^{-1}(0)$ is homeomorphic to the cone over the link $L_p(f)$, so that the embedded link type of $L_p(f) \subset S^{2n-1}$ completely determines the local topology of the singularity [64]. Moreover, in many cases even the intrinsic topology of the link itself is enough to extract important information on the singularities. For example, Mumford characterized smooth points of normal complex surfaces in terms of the fundamental group of their links [65], and Neumann vastly generalized it by showing that the minimal resolution of a normal surface singularity is determined by the topology of the link (and in fact in most cases simply by the fundamental group of the link) [66].

In this thesis, we will only be interested in the classical case of isolated complex curve singularities. In this context, the link of an isolated critical point is a classical link $L \subset S^3$. As we have already mentioned, links of plane curve singularities were studied in great detail in the first few decades of the 20th century, and both the classical field of singularity theory and the then rather new field of knot theory took great profit from this interaction. We would like to illustrate those exchanges with the following example, that we discovered thanks to Durfee's interesting historical survey [35]. It dates back to some seminars given by Wirtinger in 1905, and was later written down by his student Brauner in [17]. Wirtinger was interested in studying complex surfaces using branched coverings over the plane $\mathbb{C}^2$, in analogy to the successful description of complex curves as branched covers of the complex line $\mathbb{C}$. To do so, he needed to understand the branching set and what he called the *branching group* of a branch point: in modern terminology, this is the local monodromy around a branch point p, i.e. the action of the fundamental group of the complement of the branching set in a neighbourhood of p as permutations of the sheets of the covering. The case of complex curves is simple: the branching set is discrete, and the local monodromy group is always cyclic. In the case of surfaces, difficulties arise: the branching set is a potentially singular complex curve, and the local monodromy can be complicated. Wirtinger explicitly considered the surface defined by the equation

$$f(x, y, z) = z^3 - 3xz + 2y = 0$$

and projected it on the xy-plane. This projection is a 3-sheeted cover branched over the curve $C = \{(x, y) \in \mathbb{C}^2 \mid y^2 = x^3\}$. Smooth points of C have two preimages, and by finding appropriate local coordinates Wirtinger proved that the local monodromy group around such a point is always cyclic (of course, from our modern viewpoint this follows immediately from the fact that the local fondamental group around a smooth point of C is itself cyclic). On the other hand, the branching around the critical point 0 of C is more complicated. Wirtinger understood that the intersection of C with a small ball centered at 0 is a cone over the trefoil knot, discovered what we now call the *Wirtinger relation* and used it to deduce that the local monodromy group around 0 is not cyclic, but in fact the whole symmetric group on 3 elements. That is, by his interest in complex geometry and singularities Wirtinger was led to discoveries of fundamental importance in knot theory, which he then successfully applied to solve problems in singularity theory.

Brauner subsequently systematically studied knots of irreducible plane curve singularities, showed that they are iterated cables of torus knots and explained how the cabling coefficients could be computed from the so-called characteristic Puiseux pairs of the singularity. Shortly after, various authors considered the case of reducible singularities, proving that their links are determined by the knot type of each component and the pairwise linking numbers, and showing that the linking number of two components is equal to the so-called intersection multiplicity between the corresponding branches of the singularity. It follows that the isotopy class of the link is completely determined by those classical algebro-geometric invariants: the characteristic pairs of each branch and the pairwise intersection multiplicities. Finally, Burau [25] used the recently introduced Alexander polynomial to prove that knots obtained from singularities with different characteristic pairs are indeed different, thus getting a complete knot-theoretical characterization of those classical invariants (this result was also obtained with different methods by Zariski [79]). From the cone structure theorem, it follows that both the link of the singularity and the classical invariants are complete topological invariants.

Having such an explicit, complete topological classification of plane curve singularities in terms of the associated links, the question remains of how to extract topological information from the links and use it to understand topological invariants intrinsic to singularity theory. In the most ideal case, one would hope to express singularity invariants as specialization of link invariants. However, this is often very hard. For example, the discovery of the HOMFLY-PT polynomial was needed to prove that the multiplicity of a singularity corresponds to the braid index of the associated link [78], while the identifications of the so-called Milnor number and δ-invariant of a singularity with, respectively, the minimal first Betti number and the unknotting number of the link, both

conjectured by Milnor [64], were first obtained as a consequence of the famous proof of the Thom conjecture by Kronheimer and Mrowka [54].

The present thesis fits in this general framework. Inspired by some constructions of singularity theory, our goal is to define analogue objects for positive braids and, by working in this wider context (any link of a singularity turns out to be a positive braid closure), deduce results for the original singularities.

Summary of results:

The first object of consideration is the local fundamental group of the discriminant complement, and a recently proposed, conjectural braid-theoretic generalization of it. We will now introduce the minimum necessary to present our results, and refer to Chapter 2 for a more detailed discussion. Basically, to any plane curve singularity $f : \mathbb{C}^2 \to \mathbb{C}$ one can associate a space $\mathbb{C}^\mu$, which parametrizes deformations of the singularity; we will call it the *versal deformation space*. Here, $\mu = \mu(f)$ is the *Milnor number* that we mentioned earlier. The original singularity f corresponds to $0 \in \mathbb{C}^\mu$. Now, a generic deformation of f will in fact give a smooth curve; the points of the versal deformation space corresponding to singular curves form an algebraic hypersurface $\Delta \subset \mathbb{C}^\mu$, called the *discriminant*. Both the discriminant, a highly singular hypersurface stratified according to the type of the corresponding deformation of f, and the discriminant complement $\mathbb{C}^\mu \setminus \Delta$ - parametrizing smooth deformations of f - have drawn a lot of attention, but proved to be very intricate. Being interested in small deformations, one would typically first consider the local topology around the origin, i.e. inside a small ball B_ε centered at 0. For ε suitably small, this is in fact independent of ε. In particular, the local fundamental group $\pi_1(B_\varepsilon \setminus \Delta)$ has attracted a lot of research, as it appears to be very rich, but is to date only understood in a handful of very specific cases; even the question of its topological invariance, asked by Brieskorn 50 years ago [23], is still unanswered.

Our investigations started from [13], in which Baader and Lönne defined secondary braid groups. Those are groups associated to positive braids, defined explicitly in terms of generators and relations. The presentation of a secondary braid group is inspired by the presentation of the local fundamental group of the discriminant complement of some known singularities, and indeed in those cases the secondary braid group appears as a braid-theoretical generalization of the local fundamental group. Baader and Lönne then took the first steps towards proving that the secondary braid group is a topological invariant of the braid closure, but, analogously to the case of local fundamental groups, serious difficulties arise and a general proof of invariance is still out of reach. The first result of this thesis is a proof of invariance in the special case of positive braids on 3 strands.

Theorem 1.1. *If two positive* 3*-braids have isotopic closures, their secondary braid groups are isomorphic.*

Going back to singularities, the (local) discriminant complement $B_\varepsilon \setminus \Delta$ is the base of a smooth fibre bundle, with fibre a smooth complex curve. In particular, this induces a monodromy representation of $\pi_1(B_\varepsilon \setminus \Delta)$ in the mapping class group of the fibre, whose image is called the *geometric monodromy group* of f. Again, we refer to Chapter 2 for the details of the definition. The geometric monodromy group is known to be a topological invariant of the singularity, generated by finitely many Dehn twists around some curves on the fibre surface called vanishing cycles. As this fibration in fact determines the topology of the singularity, various forms of monodromy have been intensively studied, and important results were obtained in the homological setting [5]. However, the geometric monodromy group has proved evasive: for a long time, results were only known for so called simple singularities [68],[77], and important, general results have only been obtained recently [70].

Inspired by this definition of the geometric monodromy group as a quotient of the local fundamental group of the discriminant complement, in the second part of this thesis we associate to every positive braid β a group $MG(\beta)$ that we call the *monodromy group* of the braid. It is defined as the group generated by the Dehn twists around a certain family of curves on the unique minimal genus Seifert surface of the braid closure, and it is naturally a quotient of the secondary braid group. First, we prove that the monodromy group of a positive braid is indeed a generalization of the geometric monodromy group of a singularity.

Theorem 1.2. *Let $f : \mathbb{C}^2 \to \mathbb{C}$ define an isolated plane curve singularity and $L(f)$ be the link of f. Then there exists a positive braid β representing $L(f)$ such that the geometric monodromy group of f is equal to $MG(\beta)$.*

To study monodromy groups of positive braids, we use the theory of framed mapping class groups. This theory belongs to a family of techniques that were developed in recent years to study the action of the mapping class group of a surface on various tangential structures - in the present case, framings - and successfully applied to study monodromy groups appearing in a variety of settings, including singularities [70]. We will carefully discuss framed mapping class groups in Chapter 2; for the time being, it suffices to mention that to every framing on a surface one can associate a framed mapping class group, and that such framed mapping class groups turn out to be generated by finitely many Dehn twists around curves with a prescribed intersection pattern [27]. Our first step is to construct an explicit framing on the minimal genus Seifert surface of a positive braid, and prove that the monodromy group of the braid is

contained in the associated framed mapping class group. The reverse inclusion is harder, and we can prove it provided the surface has connected boundary.

Theorem 1.3. *Let β be a prime positive braid not of type A_n and whose closure is a knot. Up to finitely many exceptions, the monodromy group of β is a framed mapping class group.*

In fact, our proof of Theorem 1.3 also applies to many (but not all) positive braids whose closure is a link, including links of singularities. In particular, we obtain the following result, that was already proved by Cuadrado and Salter in [70].

Theorem 1.4. *Let $f : \mathbb{C}^2 \to \mathbb{C}$ be an isolated plane curve singularity not of type A_n or D_n. Up to finitely many exceptions, the geometric monodromy group of f is a framed mapping class group.*

It is important to mention that the two infinite families of braids of type A_n and D_n that we exclude from Theorems 1.3 and 1.4 are in fact the only cases where the monodromy group was already explicitly known: it is isomorphic to the Artin group of the corresponding type [68]. Those groups are not isomorphic to any framed mapping class group, so their exclusion is a necessity, rather than a limitation of any sort. On the other hand, the remaining finitely many exceptions are due to technical reasons, and we still expect the results of Theorems 1.3 and 1.4 to hold in those cases.

Framed mapping class groups are determined by the value of the framing on the boundary components of the surface and a certain Arf invariant associated to the framing. In the case of a surface Σ with connected boundary, the value of the framing on the boundary is always equal to the Euler characteristic of Σ, so that the framed mapping class group is determined simply by the genus of Σ and the Arf invariant of the framing. In our specific case, we are able to identify the Arf invariant of the framing with the classical Arf invariant of the boundary knot. We thus obtain the following corollaries, expressing the geometric monodromy group of an irreducible singularity in terms of well known invariants of its knot.

Corollary 1.1. *Let β be a prime positive braid not of type A_n and whose closure is a knot K. Up to finitely many exceptions, the monodromy group of β is an invariant of K, determined by its genus and Arf invariant.*

Corollary 1.2. *Let f be an irreducible isolated plane curve singularity that is not of type A_n and let $K(f)$ be the knot of the singularity. For all but finitely many such singularities, the geometric monodromy group of f is determined by the genus and the Arf invariant of $K(f)$.*

In particular, it follows that the geometric monodromy group of a singularity is in fact a very weak invariant, as most singularities with the same Milnor number have isomorphic monodromy groups. Moreover, given two singularities with the same Milnor number we now have a simple method for determining whether their geometric monodromy groups are isomorphic.

Finally, we will shortly discuss how the techniques used to understand monodromy groups of positive braids can be applied to the more general study of groups generated by finitely many Dehn twists. Those methods work particularly well for surfaces constructed by plumbing Hopf bands, where we look at the group generated by the Dehn twists around the core curves of the Hopf bands. Note that the monodromy group of a positive braid is indeed of that form. It turns out that also in this more general setting it is possible to define an explicit framing on the surface, whose framed mapping class group contains all the Dehn twists we are interested in, and that, if the boundary of the surface is connected, the Arf invariant of the framing coincides with the Arf invariant of the boundary knot. We will study in detail the case of arborescent Hopf plumbings.

Theorem 1.5. *Let Σ be a surface constructed by plumbing Hopf bands according to a tree T, and $\mathcal{C} = \{c_1, \dots, c_l\}$ be the core curves of the Hopf bands. If Σ has connected boundary and $l \geq 10$, the group*

$$G(\mathcal{C}) = \langle T_{c_1}, \dots, T_{c_l} \rangle \leqslant \mathrm{MCG}(\Sigma)$$

is uniquely determined by T. For every fixed l, there are only three possible groups: either $T = A_l$ and $G(\mathcal{C})$ is the braid group B_{l+1}, or $G(\mathcal{C})$ is one of two framed mapping class groups, distinguished by the Arf invariant of the boundary knot.

Structure of the thesis: In Chapter 2 we will collect the necessary preliminaries concerning singularity theory, framed mapping class groups and positive braids. In Chapter 3 we discuss secondary braid groups and prove Theorem 1.1. Chapter 4 is the core of this thesis: we define the monodromy group of a positive braid and prove Theorems 1.2, 1.3 and 1.4, together with the related corollaries. Finally, in Chapter 5 we consider groups generated by finitely many Dehn twists, discuss their relation to Artin groups and prove Theorem 1.5.

Chapter 2

Preliminaries

The goal of this chapter is to concisely present the context in which this thesis fits and introduce the main tools used in the following. We will assume familiarity with classical knot theory, as presented for instance in [58] or [26], as well as with the basics on mapping class groups [36].

1 Plane curve singularities

In this section, we will recall some classical notions from the theory of plane curve singularities. Those serve mainly to provide context and as a motivation for the following chapters. Our main references are the books [7, 8], [24] and [64].

An *isolated plane curve singularity*, shortly *singularity*, is a germ of holomorphic function $f : (\mathbb{C}^2, 0) \to (\mathbb{C}, 0)$ with an isolated critical point at the origin. In what follows, we will mainly be interested in the topology of the singular curve $C(f) = f^{-1}(0)$ around the critical point. More precisely:

Definition 2.1. Two singularities f and g are *topologically equivalent* if there are neighbourhoods U and V of 0 in $\mathbb{C}^2$ and a homeomorphism

$$\phi : (U, 0) \to (V, 0)$$

such that $\phi(U \cap C(f)) = V \cap C(g)$.

Since the ring $\mathbb{C}\{x, y\}$ of convergent power series is factorial, f can be uniquely decomposed (up to units) as a product of irreducible factors,

$$f = f_1 \dots f_n.$$

At the level of the singular curve, this corresponds to a decomposition into irreducible components,

$$C(f) = C(f_1) \cup \dots \cup C(f_n).$$

We call those irreducible components the *branches* of the singularity.

Remark 2.1. Even though a singularity f is defined to be an analytic function germ, for concrete examples it is always enough to consider polynomials. Indeed, by a theorem of Levinson [57], there exist local coordinates around $0 \in \mathbb{C}^2$ for which f is a polynomial.

1.1 The link of a singularity and Milnor's fibration

Let f be a singularity. For a suitably small radius $r > 0$, the sphere $S^3_r \subset \mathbb{C}^2$ centered at 0 intersects the singular curve $C = f^{-1}(0)$ transversally; the intersection $L(f) = C \cap S^3_r$ is therefore a link in the 3-sphere, called the link of the singularity. The number of components of $L(f)$ is equal to the number of branches of f. Links of singularities are well understood: they are iterated cables of the unknot, and the cabling coefficients that can appear are completely classified in terms of the so-called Puiseux inequalities. Moreover, it is well known that the isotopy type of $L(f)$ completely determines the topological type of the singularity; in fact, for reducible singularities it is enough to know the knot type of each component and all the linking numbers, see [24, §8.3].

Example 2.1 (Simple singularities)**.** Important examples of singularities are the so-called *simple* singularities, famously classified by Arnold [6]. We will often refer to them as ADE singularities. Those consist of two infinite families and three exceptional singularities, namely:

- A_n: $f(x, y) = y^2 - x^{n+1}$ for $n \geq 1$;
- D_n: $f(x, y) = xy^2 + x^{n-1}$ for $n \geq 4$;
- E_6: $f(x, y) = y^3 - x^4$;
- E_7: $f(x, y) = x^3 + xy^3$;
- E_8: $f(x, y) = y^3 - x^5$

The link of the A_n singularity is $L(A_n) = T_{2,n}$, the torus link on two strands. Similarly, $L(E_6) = T_{3,4}$ and $L(E_8) = T_{3,5}$. Braids representing the links of the remaining simple singularities are shown in Example 2.4.

In [64], Milnor proved that the map

$$\frac{f}{|f|} : S^3_r \setminus L(f) \to S^1$$

is a locally trivial fibration, called the *Milnor fibration*. Singularity links are therefore fibred links, with fibre a surface $\Sigma(f)$ called the *Milnor fibre*. The

first Betti number $\mu = \mu(f)$ of the Milnor fibre is called the *Milnor number* of f. The fibration induces a monodromy diffeomorphism of the fibre, which is only defined up to isotopy and hence gives a mapping class in $\mathrm{MCG}(\Sigma(f))$, called the *geometric monodromy* of the singularity. The geometric monodromy is an important invariant, which determines the topology of the singularity and has been intensively studied in the context of singularity theory.

Milnor's fibration also has an alternative definition, which is originally due to Brieskorn. Indeed, for small enough $\varepsilon > 0$ and $|z| < \varepsilon$ ($z \in \mathbb{C}$), the non-singular level set $f^{-1}(z)$ also intersects the sphere $S^3_r \subset \mathbb{C}^2$ transversally. It now follows from the Ehresmann fibration theorem that the restriction of f to

$$f : B^4_r \cap f^{-1}(D_\varepsilon \setminus \{0\}) \to D_\varepsilon \setminus \{0\}$$

is a locally trivial fibration, where $D_\varepsilon \subset \mathbb{C}$ denotes the disk of radius ϵ and $B^4_r \subset \mathbb{C}^2$ the ball of radius r. In particular, the restriction of this bundle to the circle $S^1_\varepsilon = \partial(D_\varepsilon)$ also gives a locally trivial fibration over the circle

$$f : B^4_r \cap f^{-1}(S^1_\varepsilon) \to S^1_\varepsilon,$$

which Milnor proved to be equivalent to the Milnor fibration [64]. Hence, the Milnor fibre $\Sigma(f)$ is diffeomorphic to the regular curve $f^{-1}(z) \cap B^4_r$ for any $z \in \mathbb{C} \setminus \{0\}$ with $|z| \leq \varepsilon$. From now on, we will mostly use this second version of the Milnor fibration.

1.2 The geometric monodromy group

To study the topology of the Milnor fibration, it is convenient to consider perturbations of f. In the following lines, we fix r and ε suitably small, as before. We will use perturbations of the form $\tilde{f} = f + \lambda g$, with $g : \mathbb{C}^2 \to \mathbb{C}$ linear and $\lambda \in \mathbb{C}$. For $|\lambda|$ small enough, the level set $\tilde{f}^{-1}(z)$ is transverse to the sphere S^3_r for any $|z| \leq \varepsilon$ and all the critical points of $\tilde{f}$ in B^4_r are mapped to critical values in the interior of the disk D_ε. Besides, one can prove that, for any regular value z with $|z| \leq \varepsilon$, the regular curve $\tilde{f}^{-1}(z) \cap B^4_r$ is diffeomorphic to the corresponding regular curve of f, that is to the Milnor fibre. Moreover, an easy application of Sard's theorem gives the following:

Lemma 2.1. *For almost all linear maps $g : \mathbb{C}^2 \to \mathbb{C}$, the perturbation $\tilde{f} = f + \lambda g$ is Morse, i.e. only has non-degenerate critical points with distinct critical values.*

Proof. We take $\tilde{f}(x_1, x_2) = f(x_1, x_2) - \sum v_i x_i$ with $(v_1, v_2) \in \mathbb{C}^2$. One easily notices that the critical points of $\tilde{f}$ are precisely the preimages of (v_1, v_2) for the gradient ∇f, and that if such a critical point of $\tilde{f}$ is degenerate, then

it is a critical point of ∇f, so that (v_1, v_2) is a critical value of ∇f. By Sard's theorem, almost all values (v_1, v_2) are non-critical for ∇f, which means that almost all such perturbations $\tilde{f}$ only have non-degenerate critical points. Moreover, the set of regular values of ∇f is open, so by an additional small linear perturbation of $\tilde{f}$ we can ensure that all the critical values of $\tilde{f}$ are pairwise distinct, i.e. $\tilde{f}$ is Morse. □

Let us now assume that $\tilde{f}$ is Morse. There are finitely many critical points of $\tilde{f}$ in B^4_r, mapped to distinct critical values $z_1, \ldots, z_n \in D_\varepsilon$. Once again, by the Ehresmann fibration theorem we have a fibration

$$\tilde{f} : B^4_r \cap \tilde{f}^{-1}(D_\varepsilon \setminus \{z_1, \ldots, z_n\}) \to D_\varepsilon \setminus \{z_1, \ldots, z_n\}$$

with fibre $\Sigma(f)$. Fixing a regular value $z_0 \in \partial(D_\varepsilon)$ as base point, we therefore get a monodromy representation $\rho_{\tilde{f}} : \pi_1(D_\varepsilon \setminus \{z_1, \ldots, z_n\}, z_0) \to \mathrm{MCG}(\Sigma(f))$, where $\mathrm{MCG}(\Sigma(f))$ denotes the mapping class group of the Milnor fibre.

Definition 2.2. The *geometric monodromy group* Γ_f of a singularity f is the image in $\mathrm{MCG}(\Sigma_f)$ of the monodromy representation

$$\rho = \rho_{\tilde{f}} : \pi_1(D_\varepsilon \setminus \{z_1, \ldots, z_n\}, z_0) \to \mathrm{MCG}(\Sigma(f))$$

for any Morse perturbation $\tilde{f}$ of f.

It is not difficult to show that the geometric monodromy group does not depend on the choice of the Morse perturbation $\tilde{f}$. It can also be proved that the geometric monodromy group is in fact a topological invariant of the singularity.

Having chosen $\tilde{f}$ to be Morse allows us to use Picard-Lefschetz theory (i.e. complex Morse theory) to study the topology of the Milnor fibration. More precisely, consider a path $u : [0, 1] \to D_\varepsilon$ with $u(0) = z_0$, $u(1) = z_i, i \neq 0$ and not passing through any critical value of $\tilde{f}$ except at $t = 1$. To such a path we can associate a loop $\gamma \in \pi_1(D_\varepsilon \setminus \{z_1, \ldots, z_n\}, z_0)$ by following u from z_0 to z_i, turning once anticlockwise around z_i and going back to z_0 along u. Using local coordinates around the non-degenerate critical point p_i corresponding to z_i, one can see that there exists a unique simple closed curve c on $\Sigma(f) = \tilde{f}^{-1}(z_0)$ that gets contracted to p_i when $\Sigma(f)$ is transported to the singular level-set $\tilde{f}^{-1}(z_i)$ along u. We call this curve the *vanishing cycle* corresponding to u. The isotopy type of a vanishing cycle c (as a curve on the Milnor fibre) does not depend on the choice of perturbation $\tilde{f}$.

Theorem 2.1 (Picard-Lefschetz; see [8], §1&2)**.**
Let u be a path as above, $\gamma \in \pi_1(D_\varepsilon \setminus \{z_1, \ldots, z_n\}, z_0)$ the associated loop and

c the vanishing cycle corresponding to u. The monodromy along γ is given by the right Dehn twist around c, i.e.

$$\rho(\gamma) = T_c.$$

To end this discussion, consider now a family of paths u_i for $i = 1, \ldots, n$, each joining the base point z_0 to the corresponding z_i. We assume that all those paths are not self-intersecting and pairwise disjoint (except at the common starting point z_0). Under those conditions, we say that the set of the corresponding vanishing cycles $\{c_i\}$ is *distinguished*.

Theorem 2.2 (Milnor; see [8], Theorem 2.1, and [64], Theorem 6.5)**.** *A distinguished set of vanishing cycles forms a basis of $H_1(\Sigma(f))$. In particular, the number of critical points of $\tilde{f}$ in $B_r^4 \cap \tilde{f}^{-1}(D_\varepsilon)$ equals the Milnor number $\mu(f)$.*

Of course, after perturbing f to $\tilde{f}$, the monodromy around $\partial(D_\varepsilon)$, considered as a loop based at z_0, is still equal to the geometric monodromy of f. A choice of a distinguished set of vanishing cycles therefore induces a decomposition of the geometric monodromy as a product of Dehn twists, where each such Dehn twist appears exactly once in an appropriate order. To sum up, we have the following:

Corollary 2.1. *The geometric monodromy group of a singularity f is generated by $\mu(f)$ Dehn twists; the geometric monodromy decomposes as a product of those generators and is therefore an element of the geometric monodromy group.*

Miniversal deformations and the discriminant

The geometric monodromy group admits an alternative definition, involving the so-called versal deformations of a singularity. A *deformation* of a singularity f is a germ of holomorphic function $F : (\mathbb{C}^2 \oplus \mathbb{C}^l, 0) \to (\mathbb{C}, 0)$ such that $F(x, 0) = f(x)$. The space $\mathbb{C}^l$ is the *base* of the deformation. A deformation F is called *versal* if every other deformation of f is equivalent, in a certain natural sense, to a restriction of F. It can be proved that versal deformations exist. In fact, there exists a unique (up to diffeomorphism of the base) versal deformation with base of minimal dimension, that we call *miniversal*. The dimension of the base of the miniversal deformation is equal to the Milnor number $\mu(f)$. For a detailed discussion of those notions, we refer to [7].

So, let $F(x, \lambda)$ be a miniversal deformation of a singularity f, where $x \in \mathbb{C}^2$ and $\lambda \in \mathbb{C}^\mu$. We will be interested in the level sets

$$V_\lambda = \{x \in \mathbb{C}^2 \mid F(x, \lambda) = 0, ||x|| \leq r\},$$

where r is chosen suitably small. For $\lambda = 0$, this is nothing else than the singular curve $C(f) \cap B_r^4$. Recalling that, for any r small enough, the curve $C(f)$ is transverse to the sphere S_r^3, it follows that there exists some $\delta > 0$ such that for all $||\lambda|| \leq \delta$ the curve $\{x \in \mathbb{C}^2 \mid F(x, \lambda) = 0\}$ is also transverse to S_r^3. In particular, if the level set V_λ is smooth, then it is diffeomorphic to the Milnor fibre of f. We will now restrict our considerations to the ball $B_\delta = \{\lambda \in \mathbb{C}^\mu \mid ||\lambda|| \leq \delta\}$ in the base of the deformation.

Definition 2.3. The *discriminant* of the singularity f is the space

$$\Delta = \Delta_\delta = \{\lambda \in \mathbb{C}^\mu \mid ||\lambda|| \leq \delta, V_\lambda \text{ is not smooth}\}.$$

It can be shown that the topological type of the pair $(B_\delta, \Delta_\delta)$ does not depend on δ (for δ sufficiently small) nor on the choice of miniversal deformation. Moreover, the discriminant is a set of complex codimension 1 in B_δ. The space $B_\delta \setminus \Delta$ is the base of a locally trivial fibration

$$\begin{aligned} \{(x, \lambda) \in \mathbb{C}^2 \oplus \mathbb{C}^\mu \mid x \in V_\lambda, ||\lambda|| \leq \delta, \lambda \notin \Delta\} &\to B_\delta \setminus \Delta \\ (x, \lambda) &\mapsto \lambda \end{aligned}$$

with fibre $V_\lambda \cong \Sigma(f)$. As usual, we get a monodromy representation

$$\pi_1(B_\delta \setminus \Delta) \to \mathrm{MCG}(\Sigma(f)).$$

Theorem 2.3 (see [8], Theorem 3.1.)**.** *The image of the monodromy representation* $\pi_1(B_\delta \setminus \Delta) \to \mathrm{MCG}(\Sigma(f))$ *in* $\mathrm{MCG}(\Sigma(f))$ *coincides with the geometric monodromy group of* f*.*

In the proof of Theorem 2.3, one shows that the monodromy representation $\rho : \pi_1(D_\varepsilon \setminus \{z_1, \ldots, z_\mu\}, z_0) \to \mathrm{MCG}(\Sigma(f))$ used in the original definition of the geometric monodromy group factors through

$$\rho : \pi_1(D_\varepsilon \setminus \{z_1, \ldots, z_\mu\}, z_0) \twoheadrightarrow \pi_1(B_\delta \setminus \Delta) \to \mathrm{MCG}(\Sigma(f)).$$

In particular, this exposes a natural set of μ generators of $\pi_1(B_\delta \setminus \Delta)$, but this latter group also has non-trivial relations.

Example 2.2. By results of Brieskorn and Arnold([19], [21] and [6], see also [22]), for a simple singularity of type ADE the fundamental group of the discriminant complement is isomorphic to the Artin group of the same type.

In [68], Perron and Vannier showed that the monodromy representation is injective for simple singularities of type A_n and D_n, and conjectured the same to be true for the other simple singularities. This was later disproved by Wajnryb in [77]. In fact, Portilla Cuadrado and Salter recently proved that

this representation is never injective if f is not of type A_n or D_n and the Milnor fibre $\Sigma(f)$ has genus $g \geq 7$, see [70].

Here, it is important to point out that the topological type of the discriminant, that is of the pair (B_δ, Δ), is not a topological invariant of the singularity, as first showed by Pham [69]. The question of the invariance of $\pi_1(B_\delta \setminus \Delta)$ was asked by Brieskorn in 1972 [23], but it is still unanswered. To the best of our knowledge, the strongest result in this direction is by Lönne, who proved invariance for singularities of multiplicity at most 3, see [62].

1.3 A'Campo's divides

The various definitions of the geometric monodromy group that we have just discussed are conceptually clear, but difficult to use for concrete computations. However, there exists an easy combinatorial model to construct the Milnor fiber of a singularity together with a distinguished basis of vanishing cycles. This was obtained by A'Campo using the theory of divides.

Definition 2.4. A *divide* $\mathcal{D}$ is a generic relative immersion of finitely many intervals in the unit disk $(D^2, \partial(D^2))$.

Here, *generic* means that the only singularities are double points and that the intervals meet the boundary $\partial(D^2)$ transversally. Examples of divides can be seen in Figure 2.1 and Figure 4.4.

Divides were first introduced by A'Campo ([2], [3]) and Gusein-Zade ([44], [45]), who independently proved that they could be associated in a natural way to singularities and used them for studying properties of the monodromy. Roughly speaking, their construction goes as follows: first, up to topological equivalence one can assume that the singularity f is in real form, i.e. the defining equation of each branch has real coefficients. Using a resolution of the singularity, one can then construct a special perturbation $\tilde{f}$ called a *real morsification*. The divide of the singularity is now simply the real part of the perturbed curve $\tilde{f}^{-1}(0)$ inside the Milnor ball; that is, we consider the disk $D^2 = B^4_r \cap \mathbf{R}^2$ and $\mathcal{D} = \tilde{f}^{-1}(0) \cap D^2$.

Example 2.3 (Geometric monodromy group of simple singularities)**.** Using this construction, A'Campo proved that a simple singularity has a basis of distinguished vanishing cycles consisting of curves whose intersection pattern is the corresponding ADE Dynkin diagram; that is, the geometric monodromy group of an ADE singularity is generated by the Dehn twists around curves with the corresponding intersection pattern [2].

Later on, in [4],[1] A'Campo associated to any divide $\mathcal{D}$ a link $L(\mathcal{D})$, constructed as follows. Consider the tangent bundle of the unit disk,

$$TD^2 = \{(x, v) \mid x \in D^2, v \in T_x D^2\}.$$

The sphere S^3 can be seen as the unit sphere in TD^2,

$$S^3 = \{(x, v) \in TD^2 \mid |x|^2 + |v|^2 = 1\}.$$

Now let $\mathcal{D} \subset D^2$ be a divide, the link of $\mathcal{D}$ is defined as

$$L(\mathcal{D}) = \{(x, v) \in S^3 \mid x \in \mathcal{D}, v \in T_x\mathcal{D}\} \subset S^3.$$

This gives a link whose number of components is equal to the number of intervals in the divide. In [1], A'Campo proved that if the divide is connected, then the associated link is fibred. Moreover, by studying the monodromy of those fibred links, in [4] he showed that if the divide was obtained from a singularity, then the associated link $L(\mathcal{D})$ is ambient isotopic to the link of the singularity. In this latter case, he also provided an easy graphical algorithm to construct a model of the Milnor fibre on which a distinguished system of vanishing cycles is visible. We say that a *face* of a divide $\mathcal{D}$ is a connected component of $D^2 \setminus \mathcal{D}$ which does not intersect the boundary of D^2. Let n be the number of intervals in $\mathcal{D}$, δ be the number of crossings and r the number of faces. The Milnor fibre will be a surface with first Betti number $\mu = \delta + r$ and n boundary components. The distinguished vanishing cycles will be given by one curve per crossing and one curve per face. The surface is constructed as follows: first, replace every crossing of $\mathcal{D}$ with a small circle, to get a trivalent graph. Now, realize every edge of this new graph by a half-twisted band. This gives a surface composed of twisted cylinders, corresponding to the crossings of $\mathcal{D}$, connected by half-twisted bands corresponding to the edges of $\mathcal{D}$. The vanishing cycle associated to a crossing is given by the core curve of the corresponding cylinder, the vanishing cycle of a face is given by the core curves of the bands bounding the face. An example of this construction is shown in Figure 2.1. To sum up, we then have the following theorem:

Theorem 2.4. *Let f be an isolated plane curve singularity, $\mathcal{D}$ a divide associated to f and $\Sigma(f)$ the surface constructed from $\mathcal{D}$ with the previous procedure. Then $\Sigma(f)$ is the Milnor fibre of f and the family of curves forms a basis of distinguished vanishing cycles. In particular, the geometric monodromy group Γ_f is the subgroup of $\mathrm{MCG}(\Sigma(f))$ generated by the Dehn twists around those vanishing cycles constructed on $\Sigma(f)$. This does not depend on the choice of the divide $\mathcal{D}$.*

Remark 2.2. A'Campo's construction only leads to a combinatorial model of the Milnor fibre which is not embedded. A graphical procedure to construct a diagram of the link of a divide and the associated embedded fibre surface has been given by Hirasawa in [48].

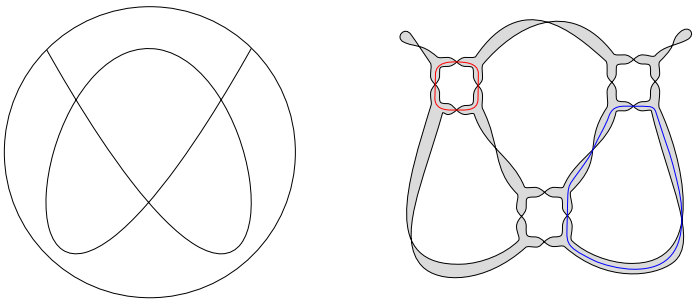

Figure 2.1: A divide and the associated surface with some of the vanishing cycles. This is a divide of the E_6 singularity; one can check using A'Campo's definition (with the help of Hirasawa's algorithm [48]) that the corresponding link $L(\mathcal{D})$ is indeed the torus knot $T_{3,4}$.

2 Framed mapping class groups

In recent years, there has been an increasing interest in the study of tangential structures on surfaces, such as framings or so-called r-spin structures, and of the action of the mapping class group on such structures. This has led to important advances in the understanding of monodromy groups arising in a variety of settings, see for instance [74], [28], [46], [47] and [27]. Most importantly for this thesis, in [70] Portilla Cuadrado and Salter proved that the geometric monodromy group of any isolated plane curve singularity of genus at least 5 and not of type A_n and D_n is a so-called framed mapping class group. In this section we will briefly recall the basics of the theory of framed surfaces, concentrating in particular on the action of the mapping class group on such structures, as investigated in [27] and [71]. In what follows, we will adhere to the notations and conventions of [27], but we will restrict only to the case of surfaces with connected boundary.

Let $\Sigma = \Sigma_{g,1}$ be a connected, compact, oriented surface of genus g with one boundary component. A *framing* ϕ on Σ is a trivialization of the tangent bundle $T\Sigma$. With the fixed orientation (and a choice of a Riemannian metric), a framing is determined by a nowhere-vanishing vector field ξ_ϕ on Σ. Two framings are *isotopic* if the associated vector fields are homotopic through nowhere-vanishing vector fields.

To a framing one can associate a *winding number function*, computing the holonomy of a simple closed curve. If $c : \mathbb{S}^1 \to \Sigma$ is a $\mathcal{C}^1$ embedding, one can define

$$\phi(c) = \int_{\mathbb{S}^1} d\angle(\dot{c}(t), \xi_\phi(c(t))) \in \mathbb{Z}.$$

This defines a map from the set of simple closed curves on Σ to $\mathbb{Z}$, which

is clearly invariant under isotopy of ϕ and c. It is not hard to see that the converse also holds: the isotopy class of a framing on Σ is determined by its winding number function, and actually by the value on finitely many curves (see [31], Theorem 5.6 and [71], Prop.2.4). Thanks to this, we will use the term "framing" indifferently to refer to the isotopy class of the vector field ξ_ϕ or to the associated winding number function ϕ.

Remark 2.3. Since we are only considering surfaces with connected boundary, it follows from the Poincaré-Hopf index theorem that for any framing ϕ on Σ, if the boundary $\partial\Sigma$ is oriented with the surface on its left, then $\phi(\partial\Sigma) = \chi(\Sigma)$.

Remark 2.4. The winding number function induced by a framing is nothing else than a cohomology class on the unit tangent bundle of Σ which evaluates to 1 on the oriented fibre S^1; see [31, 32] and [51] for a detailed study of generalized winding number functions.

The action of the mapping class group: The mapping class group of Σ acts on the set of isotopy classes of framings by pullback, via $f \cdot \phi(c) = \phi(f^{-1}(c))$, for $f \in \mathrm{Mod}(\Sigma)$ and c a simple closed curve.

Definition 2.5. Let (Σ, ϕ) be a framed surface. The *framed mapping class group*

$$\mathrm{MCG}(\Sigma, \phi) = \{f \in \mathrm{MCG}(\Sigma) \mid f \cdot \phi = \phi\}$$

is the stabilizer of the isotopy class of ϕ.

Of particular interest is the action of Dehn twists.

Lemma 2.2 ([51])**.** *Let (Σ, ϕ) be a framed surface and a, x oriented simple closed curves on Σ, then*

$$\phi(T_a(x)) = \phi(x) + \langle x, a\rangle \phi(a),$$

where $\langle \cdot, \cdot \rangle$ denotes the algebraic intersection number.

We say that a nonseparating simple closed curve a on (Σ, ϕ) is *admissible* if $\phi(a) = 0$. As a consequence of Lemma 2.2 we have that a nonseparating simple closed curve $a \subset \Sigma$ is admissible if and only if the corresponding Dehn twist preserves ϕ. Calderon and Salter proved that, for big enough genus, the framed mapping class group is generated by those admissible twists:

Proposition 2.1 ([27], Prop. 5.11)**.** *If (Σ, ϕ) is a framed surface of genus $g \geq 5$,*

$$\mathrm{MCG}(\Sigma, \phi) = \langle T_a \mid a \text{ admissible for } \phi \rangle.$$

But more is true. The framed mapping class group is generated by finitely many admissible twists around curves with prescribed intersection pattern. Again following [27]:

Definition 2.6. Let $\mathcal{C} = \{c_1, \cdots, c_k\}$ be a collection of curves on a surface Σ, pairwise in minimal position and intersecting at most once. We say that such a configuration:

- *spans the surface* if Σ deformation retracts onto the union of curves in $\mathcal{C}$;
- is *arboreal* if its intersection graph is a tree, and *E-arboreal* if moreover it contains the Dynkin diagram E_6 as a subtree.

Definition 2.7. Let $\mathcal{C} = \{c_1, \cdots, c_k, c_{k+1}, \cdots, c_l\}$ be a collection of curves on a surface Σ. Let us denote by S_1 a regular neighbourhood of c_1 and by S_j a regular neighbourhood of $S_{j-1} \cup c_j$, for $j > 1$. We say that $\mathcal{C}$ is an *h-assemblage of type E* if:

- $\{c_1, \cdots, c_k\}$ is an E-arboreal spanning configuration on $S_k \subset \Sigma$, and S_k has genus h;
- For $j > k$, $c_j \cap S_{j-1}$ is a single arc;
- $S_l = \Sigma$.

Proposition 2.2 ([27], Theorem B)**.** *Let (Σ, ϕ) be a framed surface and $\mathcal{C} = \{c_1, \cdots, c_l\}$ an h-assemblage of type E on Σ of genus $h \geq 5$. If all the curves in $\mathcal{C}$ are admissible for ϕ, then*

$$\mathrm{MCG}(\Sigma, \phi) = \langle T_c \mid c \in \mathcal{C} \rangle.$$

An h-assemblage $\mathcal{C} = \{c_1, \cdots, c_k, c_{k+1}, \cdots, c_l\}$ should be thought of as a way of sequentially constructing the surface Σ. One starts from an E-arboreal spanning configuration on a subsurface $S \subset \Sigma$ and performs a sequence of stabilisations to build up the whole surface Σ. In particular, we only have conditions on the pairwise intersection numbers for the curves $\{c_1, \cdots, c_k\}$ of the original E-arboreal spanning configuration, but for $j > k$ no constraints are imposed on the intersections of c_j with any of the other curves.

As we already mentioned, Proposition 2.2 was applied by Portilla Cuadrado and Salter to the context of singularity theory:

Theorem 2.5 ([70], Theorem A)**.** *Let f be an isolated plane curve singularity whose Milnor fibre $\Sigma(f)$ has genus $g \geq 5$. If f is not of type A_n or D_n, then the geometric monodromy group Γ_f is a framed mapping class group (for some natural relative framing on $\Sigma(f)$).*

The orbit space of this action was studied by Randal-Williams in [71]. It is classified by the Arf invariant. More precisely, it follows from work of Johnson [52] that the function $(\phi + 1) \bmod 2$ is a quadratic refinement of the mod 2 intersection form on $H_1(\Sigma, \mathbb{Z}/2\mathbb{Z})$. We can therefore define $\mathcal{A}(\phi)$ to be the Arf invariant of this quadratic refinement. Concretely, let us denote by $i(\cdot, \cdot)$ the geometric intersection number and take a collection of oriented simple closed curves $\{x_1, y_1, \ldots, x_g, y_g\}$ such that $\langle x_i, x_j \rangle = \langle y_i, y_j \rangle = 0$ and $\langle x_i, y_j \rangle = i(x_i, y_j) = \delta_{i,j}$. We then have

$$\mathcal{A}(\phi) = \sum_{i=1}^{g} (\phi(x_i) + 1)(\phi(y_i) + 1) \mod 2.$$

This is independent of the choice of the curves $\{x_1, y_1, \ldots, x_g, y_g\}$.

Proposition 2.3 ([71], Theorem 2.9)**.** *Let $g \geq 2$. The action of the mapping class group on the set of isotopy classes of framings on $\Sigma = \Sigma_{g,1}$ has exactly two orbits, distinguished by the Arf invariant.*

As a consequence, for a given surface Σ there are at most two conjugacy classes of framed mapping class groups as subgroups of $\mathrm{MCG}(\Sigma)$, distinguished by the Arf invariant.

Some properties: In spite of the important results that we just mentioned, algebraic properties of framed mapping class groups are still largely unknown. For instance, we do not know any presentation of such groups. A priori, given two framings with different Arf invariant, it could even be possible that the two corresponding framed mapping class groups are abstractly isomorphic (yet without being conjugate in the ambient mapping class group). In [71] Randal-Williams used his results on the orbits of the action of the mapping class group on the space of framings to prove some form of homological stability for framed mapping class groups. In particular, he obtained the following:

Proposition 2.4 ([71], Corollary 3.2)**.** *For every framed surface (Σ, ϕ) of genus $g \geq 7$, the abelianization of $\mathrm{MCG}(\Sigma, \phi)$ is $\mathbb{Z}/24\mathbb{Z}$.*

Another interesting property was shown by Calderon and Salter. As a step in proving Proposition 2.2, they proved that, on a framed surface $\Sigma = \Sigma_{g,1}$ of genus $g \geq 5$ with one boundary component, all Dehn twists about separating simple closed curves are contained in the framed mapping class group ([27], Prop. 4.1). In particular, this is the case for the boundary twist, which is a central element of the mapping class group. One immediately gets the following corollary:

Proposition 2.5. *If $g \geq 5$, the framed mapping class group* $\mathrm{MCG}(\Sigma_{g,1}, \phi)$ *has a non-trivial center.*

Remark 2.5 (Caveat). In this section we only stated results for surfaces with connected boundary, in terms of *absolute* framings. For general surfaces, the whole theory is still valid, but needs to be formulated for *relative* framings, i.e. only allowing isotopies that are trivial on the boundary. In this more general context, the framed mapping class group is the stabilizer of the *relative* isotopy class of a framing, and one needs to also take into account the action on arcs, getting so-called relative winding number functions. The orbit space is now classified by a generalized Arf invariant together with the values of the framing on the different boundary components. However, if the boundary is connected the absolute and relative theories are equivalent and we can use this slightly simpler formulation.

3 Positive braids

We will now recall some important facts about the combinatorics and geometry of positive braids. Let

$$B_N = \langle \sigma_1, \dots, \sigma_{N-1} \mid \sigma_i\sigma_j = \sigma_j\sigma_i \text{ if } |i-j| \geq 2, \sigma_i\sigma_{i+1}\sigma_i = \sigma_{i+1}\sigma_i\sigma_{i+1} \rangle$$

denote the braid group on N strands.

Definition 2.8.

- A word w in the alphabet $\{\sigma_1, \dots, \sigma_{N-1}\}$ is positive if only positive powers of the generators appear in w.
- A braid $\beta \in B_N$ is positive if it is represented by a positive word.

By a theorem of Garside [42], the monoid B_N^+ of positive braid words embeds in the braid group B_N. That is, two positive words represent the same braid if and only if they are related through a sequence of positive words obtained by applying the defining relations, without ever introducing the inverse of a generator. We can hence equivalently consider a positive braid as an element of the positive monoid B_N^+. We will usually represent a positive braid word on N strands with a *brick diagram*, a plane graph with N vertical lines connected by horizontal segments corresponding to the crossings. Since all the crossings are positive, one can reconstruct the braid from the brick diagram.

Positive braid links: The closure of a positive braid is called a *positive braid link*. Every link of an isolated plane curve singularity is in fact a positive braid link. A classical result of Stallings says that non-split positive braid links are fibred, thus generalizing Milnor's fibration [75]. Notice that, if β is a positive braid word, its closure $\hat{\beta}$ is non-split if and only if every generator σ_i appears at least once in β. Moreover, the fibre surface can easily be constructed directly from the positive word, by taking a disk for each strand of β and, for each generator σ_i in β, gluing a half-twisted band between the i-th and $(i+1)$-th disks. Being the fibre surface, this is in particular the unique genus minimizing Seifert surface of $\hat{\beta}$. The brick diagram of β naturally embeds in this surface as a retract.

Example 2.4 (Links of ADE type)**.** In what follows, we will say that a positive braid link is:

- of *type* A_n if it isotopic to the closure of the braid σ_1^{n+1}
- of *type* D_n if it isotopic to the closure of the braid $\sigma_1^{n-2}\sigma_2\sigma_1^2\sigma_2$
- of *type* E_6, E_7, or E_8 if it isotopic to the closure of the braid $\sigma_1^3\sigma_2\sigma_1^3\sigma_2$, $\sigma_1^4\sigma_2\sigma_1^3\sigma_2$, or $\sigma_1^5\sigma_2\sigma_1^3\sigma_2$, respectively.

Those are precisely the links of the singularities of same type. Moreover, they are the only prime positive braid links with maximal signature (that is, with the absolute value of the signature equal to twice the 3-genus) [9].

Linking graphs: Let β be a positive braid word and denote the fibre surface of $\hat{\beta}$, constructed as above, by Σ_β. Let g be its genus and n the number of boundary components. On Σ_β there is a standard family of $2g+n-1$ curves γ_i, oriented counterclockwise, which are in one-to-one correspondence with the *bricks*, i.e. the innermost rectangles, of the brick diagram of β and form a basis of the first homology of Σ_β. See Figure 2.2 for an example of Σ_β with the corresponding curves for $\beta = \sigma_3\sigma_1\sigma_2\sigma_1^2\sigma_3\sigma_2$. The intersection pattern of those standard curves can be read off directly from the brick diagram, in the so called linking graph:

Definition 2.9. Let β be a positive braid word. Its *linking graph* is a planar graph whose vertices are the bricks of the brick diagram of β; two vertices are connected by an edge if and only if the corresponding bricks are arranged as the two bricks of the braids σ_i^3, $\sigma_i\sigma_{i+1}\sigma_i\sigma_{i+1}$ or $\sigma_{i+1}\sigma_i\sigma_{i+1}\sigma_i$.

Notice that two vertices of the linking graph are connected with an edge if and only if the corresponding curves intersect each other. It is also worth mentioning that since positive braid links are visually prime by [34], a positive braid link is prime if and only if its linking graph is connected.

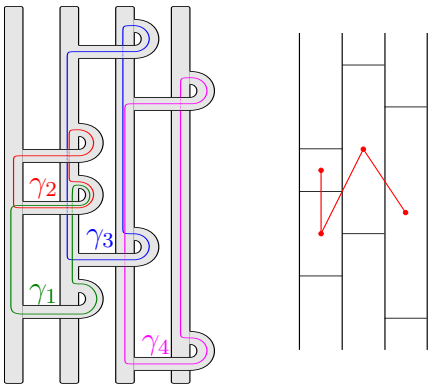

Figure 2.2: The fibre surface of $\sigma_3\sigma_1\sigma_2\sigma_1^2\sigma_3\sigma_2$, its brick diagram and the corresponding linking graph.

Example 2.5. The linking graphs of the positive braids words representing the links of type ADE in Example 2.4 are the simply laced Dynkin diagrams of the corresponding type.

Comparing Example 2.3 and Example 2.5, one immediately notices that, at least in the case of simple singularities, there is a striking similarity between the distinguished vanishing cycles on the Milnor fibre and the combinatorics of the corresponding positive braids and their linking graphs . This analogy is one of the main driving principles of this thesis, and will be further explored in the following chapters.

Linking graphs also have an additional important property: they come with a natural orientation of the edges, which induces an orientation of the innermost cycles, i.e. the boundary cycles of bounded regions. Indeed, in a linking graph there are two types of edges: vertical ones, corresponding to pairs of bricks in the same column, and diagonal ones, corresponding to pairs of bricks in adjacent columns. We will simply orient vertical edges downwards and diagonal edges upwards. Now, every bounded region of the linking graph has a triangular shape, bounded by a certain number of vertical edges, all lying in the same column, and exactly two diagonal edges connecting to a distinguished vertex to the right or to the left. It is easy to see that the orientation of the edges induces a compatible orientation on the boundaries of the regions; the boundary is oriented anticlockwise if the distinguished vertex is on the right, and clockwise otherwise. Linking graphs of positive braids were studied in great detail in [12], where it is shown that the embedded, oriented linking graph of a prime positive braid word determines the link type of the closure.

Chapter 3

Secondary braid groups of positive 3-braids

Secondary braid groups of positive braids were defined by Baader and Lönne in [13] as a combinatorial analogue of the fundamental group of discriminant complements of isolated plane curve singularities. Their main motivation came from the similarities between the combinatorial structure of positive braids and that of isolated plane curve singularities, as discussed in Chapter 2, together with the results of Lönne showing how to explicitly compute, in some very specific cases, a presentation of the fundamental group of the discriminant complement from such combinatorial data [61], [60]. In particular, they proved that for braids of type ADE and for braids of minimal braid index whose closure is a torus link $T_{p,q}$ the secondary braid group is isomorphic to the fundamental group of the discriminant complement of the corresponding singularities (simple singularities in the former case, Brieskorn-Pham singularities $f(x, y) = x^p + y^q$ in the latter).

Secondary braid groups are defined in terms of generators and relations starting from any positive word in the standard generators of the braid group, see Section 1. In [13], Baader and Lönne showed that the secondary braid group is invariant under braid relation, i.e. is associated to the positive braid itself rather than the positive word representing it, and elementary conjugation. As a consequence, they deduce the conjugation invariance for positive braids containing a power of the half-twist. However, general conjugation invariance and link invariance is still out of reach. The goal of this chapter is to prove invariance in the restricted class of positive braids on 3 strands. That is, we have the following:

Theorem 3.1. *If two positive* 3*-braids have isotopic closures, their secondary braid groups are isomorphic.*

It is interesting to notice that this theorem fits nicely with the results of [62],

where the topological invariance of the fundamental group of the discriminant complement is proved for singularities of multiplicity at most 3. Indeed, the multiplicity of a singularity is equal to the braid index of the associated link [78].

The chapter is structured as follows. In Section 1 we will define the secondary braid group of a positive braid and state the required invariance properties. To prove Theorem 3.1, we will prove the conjugation invariance in B_3^+ and use the classification of 3-braids by Birman and Menasco [15] to deduce link invariance. This will be done in Section 2 and Section 3 respectively.

1 Secondary braid groups

The definition of secondary braid groups is based on linking graphs. Recall from Chapter 2, Section 3 that linking graphs have a natural orientation of the innermost cycles, i.e. the boundary cycles of bounded regions: every bounded region of the linking graph has a triangular shape with a distinguished vertex; the boundary is oriented anticlockwise if the distinguished vertex is on the right, and clockwise otherwise. We can now proceed with the definition of secondary braid groups, following [13].

Definition 3.1. Let β be a positive braid word and Γ its linking graph. Let $v_1, \ldots, v_k$ be the vertices of Γ. The *secondary braid group* ${}^2B(\beta)$ of β is the group generated by the elements $s_1, \ldots, s_k$, corresponding to the vertices of Γ, with the following relations:

- Braid relation: if the vertices v_i, v_j are joined by an edge,

$$s_i s_j s_i = s_j s_i s_j;$$

- Commutation: if the vertices v_i, v_j are not joined by an edge,

$$s_i s_j = s_j s_i;$$

- Cycle relation: If $v_{i_n} \to \cdots \to v_{i_1} \to v_{i_n}$ are the vertices around a bounded region of Γ, taken in cyclic order following the orientation of the boundary cycle, we have

$$s_{i_n} s_{i_{n-1}} \ldots s_{i_2} s_{i_1} s_{i_n} s_{i_{n-1}} \ldots s_{i_4} s_{i_3} =$$
$$s_{i_{n-1}} s_{i_{n-2}} \ldots s_{i_2} s_{i_1} s_{i_n} s_{i_{n-1}} \ldots s_{i_3} s_{i_2}.$$

If the linking graph Γ is empty, we will define the secondary braid group ${}^2B(\beta)$ to be the trivial group.

It should not be surprising that the cycle relation is equivalent to any shifted version of it, provided that the braid and commutation relations hold. In other words, the point v_{i_n} from which we start enumerating the vertices $v_{i_n} \to \cdots \to v_{i_1}$ around a region does not matter, as long as we keep following the orientation. This is explained in detail in [13].

Baader and Lönne then proved the following important invariance properties:

Proposition 3.1 ([13])**.**

I. ***Braid relation invariance****: Let α and β be positive braid words related by a braid relation $\sigma_i\sigma_{i+1}\sigma_i \to \sigma_{i+1}\sigma_i\sigma_{i+1}$, then*

$$^2B(\alpha) \cong {}^2B(\beta).$$

II. ***Elementary conjugation invariance****: Let ω be a positive braid word, then*

$$^2B(\omega\sigma_i) \cong {}^2B(\sigma_i\omega).$$

2 Conjugation invariance

To prove the conjugation invariance of the secondary braid group for braids on three strands we will heavily rely on the solution to the word and conjugation problems in the braid group found by Garside [42], together with some useful improvements by Elrifai and Morton [72]. In what follows, B_N denotes the braid group on N strands, with generators $\sigma_1, \dots \sigma_{N-1}$; for two braids $\alpha, \beta \in B_N$, $\alpha \sim \beta$ means that α and β are conjugate in B_N.

Definition 3.2. Let B_N^+ be the monoid of positive braids on N strands.

- The *positive half-twist* is the positive braid

$$\Delta = (\sigma_1 \cdots \sigma_{N-1})(\sigma_1 \cdots \sigma_{N-2}) \cdots (\sigma_1\sigma_2)\sigma_1 \in B_N^+;$$

- A positive braid $\beta_1 \in B_N^+$ *contains the half-twist* if there exists $\beta_2 \in B_N^+$ such that $\beta_1 = \Delta\beta_2$.

In [42], Garside proved that every braid $\beta \in B_N$ has a normal form $\beta = \Delta^{k_\beta}\tilde{\beta}$, where $k_\beta \in \mathbb{Z}$ is called the *power* of β and $\tilde{\beta}$ is a positive braid that does not contain the half-twist. Notice that requiring $\tilde{\beta}$ to not contain the half-twist is equivalent to requiring k_β to be the maximal integer for which such a decomposition exists. In particular, a braid β is positive if and only if $k_\beta \geq 0$, and a positive braid contains the half-twist if and only if $k_\beta \geq 1$.

Since the positive braid $\tilde{\beta}$ is uniquely defined, this normal form solves the word problem in the braid group.

As for the conjugacy problem, given a braid $\beta \in B_N$ Garside defines the *summit power*

$$P(\beta) = \max\{k_\alpha \mid \alpha \in B_N, \alpha \sim \beta\}$$

and the *summit set*

$$S(\beta) = \{\alpha \in B_N \mid \alpha \sim \beta, k_\alpha = P(\beta)\}.$$

He then shows that the summit set of a braid is finite and can be constructed algorithmically in finite time, thus solving the conjugacy problem. Moreover, he proves that any two braids in the summit set are related by a sequence of conjugations by positive divisors of Δ without ever leaving the summit set.

In [72], Elrifai and Morton improved Garside's algorithm for the conjugacy problem. Most importantly for this note, they prove that, starting from a braid β, one can get to its summit set by so-called *cycling*, an operation which can be realized by a sequence of elementary conjugations.

Proposition 3.2. *Let $\beta_1, \beta_2 \in B_3^+$. If $\beta_1 \sim \beta_2$, then ${}^2B(\beta_1) \cong {}^2B(\beta_2)$.*

Proof. Take $\beta_1, \beta_2 \in B_3^+$, $\beta_1 \sim \beta_2$. Since the secondary braid group is invariant under elementary conjugation, up to cycling we can assume that β_1 and β_2 are in the summit set. In particular, we can assume that β_2 is obtained from β_1 by conjugation by a positive divisor of Δ. If $P(\beta_1) \geq 1$, a conjugation by a divisor of Δ can be realized by elementary conjugations and the result follows. Indeed, suppose that $\beta_2 = \alpha^{-1}\beta_1\alpha$ with α a positive divisor of the half-twist, i.e. $\Delta = \alpha\gamma$ for some positive braid γ. Now, if $P(\beta_1) \geq 1$ we can write $\beta_1 = \Delta\tilde{\beta}_1 = \alpha\gamma\tilde{\beta}_1$, and we get $\beta_2 = \alpha^{-1}(\alpha\gamma\tilde{\beta}_1)\alpha = \gamma\tilde{\beta}_1\alpha$, which is indeed realized by elementary conjugations.

Therefore, we can assume that $P(\beta_1) = 0$. Up to the symmetry $\sigma_1 \leftrightarrow \sigma_2$ (which clearly leaves the secondary braid group invariant, as it induces an isomorphism of linking graphs) we are left with three possibilities: either $\beta_1 = \sigma_1^{a_1}\sigma_2^{b_1}\cdots\sigma_1^{a_n}\sigma_2^{b_n}$ with $a_i, b_i \geq 2$, $\beta_1 = \sigma_1^{a_1}\sigma_2^{b_1}\cdots\sigma_1^{a_n}\sigma_2^{b_n}\sigma_1^{a_{n+1}}$ with $a_1, a_{n+1} \geq 1, a_i \geq 2$ for $i \notin \{1, n+1\}$ and $b_i \geq 2$, or $\beta_1 = \sigma_1^m$. We then have to prove that, after conjugating such a β_1 by a positive divisor of the half-twist, we either get a non-positive braid or one with the same secondary braid group. Notice that in B_3 the only non-trivial positive divisors of Δ are the following five braids: $\sigma_1, \sigma_2, \sigma_1\sigma_2, \sigma_2\sigma_1$ and Δ.

We will now treat in detail the case $\beta_1 = \sigma_1^{a_1}\sigma_2^{b_1}\cdots\sigma_1^{a_n}\sigma_2^{b_n}$ with $a_i, b_i \geq 2$ and $\beta_2 = \alpha^{-1}\beta_1\alpha$; the other cases follow from analogous computations.

- $\alpha = \sigma_1$: this is just an elementary conjugation.

- $\alpha = \sigma_2$:

$$\begin{aligned}\alpha^{-1}\beta\alpha &= \sigma_2^{-1}\sigma_1^{a_1}\sigma_2^{b_1}\cdots\sigma_1^{a_n}\sigma_2^{b_n+1}\\ &= \Delta^{-1}\sigma_2\sigma_1^{a_1+1}\sigma_2^{b_1}\cdots\sigma_1^{a_n}\sigma_2^{b_n+1}.\end{aligned}$$

  Now, $\sigma_2\sigma_1^{a_1+1}\sigma_2^{b_1}\cdots\sigma_1^{a_n}\sigma_2^{b_n+1}$ is a positive braid that does not contain the half-twist, so $\Delta^{-1}\sigma_2\sigma_1^{a_1+1}\sigma_2^{b_1}\cdots\sigma_1^{a_n}\sigma_2^{b_n+1}$ is in Garside's normal form and the braid it represents is not positive.

- $\alpha = \Delta$: conjugating by the half-twist simply results in a reflection along the vertical axis, which leaves the secondary braid group invariant.

- $\alpha = \sigma_1\sigma_2$:

$$\begin{aligned}\alpha^{-1}\beta\alpha &= \sigma_1\Delta^{-1}\beta\Delta\sigma_1^{-1}\\ &= \sigma_1\sigma_2^{a_1}\sigma_1^{b_1}\cdots\sigma_2^{a_n}\sigma_1^{b_n}\sigma_1^{-1},\end{aligned}$$

  is a composition of a reflection along the vertical axis and an elementary conjugation, both of which leave the secondary braid group invariant.

- $\alpha = \sigma_2\sigma_1$:

$$\begin{aligned}\alpha^{-1}\beta\alpha &= \sigma_1^{-1}\sigma_2^{-1}\sigma_1^{a_1}\sigma_2^{b_1}\cdots\sigma_1^{a_n}\sigma_2^{b_n+1}\sigma_1\\ &= \Delta^{-1}\sigma_1^{a_1+1}\sigma_2^{b_1}\cdots\sigma_1^{a_n}\sigma_2^{b_n+1}\sigma_1.\end{aligned}$$

  The result is in normal form, hence it is not a positive braid.

□

3 Link invariance

At this point, one might be tempted to invoke Markov's theorem and use Proposition 3.2 to directly deduce the invariance of the secondary braid group, as it is clearly invariant under Markov stabilization. However, there exist positive 3-braids that are not conjugate in B_3 but become conjugate after one stabilization. To effectively be able to apply Markov's theorem, we would need conjugation invariance for braids with more strands. Instead, we will use Birman-Menasco's classification of links that are closures of 3-braids [15, 14].

Definition 3.3. We say that:

- a 3-braid $\beta \in B_3$ *admits a flype* if β is conjugate to $\sigma_1^u\sigma_2^v\sigma_1^w\sigma_2^\epsilon$, where $u, v, w \in \mathbb{Z}$ and $\epsilon = \pm 1$.

- a *flype* on a flype-admissible braid is the operation

$$\sigma_1^u\sigma_2^v\sigma_1^w\sigma_2^\epsilon \to \sigma_1^u\sigma_2^\epsilon\sigma_1^w\sigma_2^v.$$

- a flype is *non-degenerate* if the braids $\sigma_1^u\sigma_2^v\sigma_1^w\sigma_2^\epsilon$ and $\sigma_1^w\sigma_2^v\sigma_1^u\sigma_2^\epsilon$ are not conjugate in B_3.

A flype on a flype-admissible braid is an operation that preserves the link type of the braid closure, but might change the conjugacy class of the braid. Non-degenerate flypes have been classified by Ko-Lee.

Lemma 3.1 ([53])**.** *A flype is non-degenerate if and only if neither u nor w is equal to 0,ϵ,2ϵ or $v+\epsilon$, and $u \neq w$, and $|v| \geq 2$.*

Moreover, it turns out that a flype is essentially the only move needed to connect distinct conjugacy classes of 3-braids with isotopic closures.

Theorem 3.2 ([15], The Classification Theorem; see also [14])**.** *A link L which is the closure of a 3-braid is represented by exactly one conjugacy class in B_3, unless if:*

- *L is the unknot, which has three classes of representatives: $\sigma_1\sigma_2$, $\sigma_1\sigma_2^{-1}$ and $\sigma_1^{-1}\sigma_2^{-1}$.*
- *L is a torus link $T(2,k)$, $k \neq \pm 1$, which has two classes of representatives, namely $\sigma_1^k\sigma_2$ and $\sigma_1^k\sigma_2^{-1}$.*
- *L is represented by a braid that admits a non-degenerate flype. Such a link has two classes of representatives, $\sigma_1^u\sigma_2^v\sigma_1^w\sigma_2^\epsilon$ and $\sigma_1^w\sigma_2^v\sigma_1^u\sigma_2^\epsilon$.*

Remark 3.1. The statement of the Classification Theorem in [15] seems to contain a minor mistake. A corrected version is presented in [14].

We now go back to positive braids. The representatives of conjugacy classes appearing in Theorem 3.2 are in general not given by positive braid words. To apply it to our setting, we then first have to identify which of those non-positive braids are in fact conjugate to positive braids. This is the object of the following lemma.

Lemma 3.2.

I. For any $k \in \mathbb{Z}$, the braid $\sigma_1^k\sigma_2^{-1}$ is not conjugate to a positive braid.

II. Let $\beta = \sigma_1^u\sigma_2^v\sigma_1^w\sigma_2^\epsilon$ admit a non-degenerate flype. If any of the exponents is negative, then β is not conjugate to a positive braid.

To prove Lemma 3.2, we will again make use of Garside's solution of the conjugacy problem. Recall from Section 2 that a braid β is conjugate to a positive braid if and only if its summit power $P(\beta)$ satisfies $P(\beta) \geq 0$. To prove that a given braid is not conjugate to a positive braid one can hence simply put it in normal form, repeatedly apply cycling to reach the summit set and check that the summit power is strictly negative. We therefore now need a more precise definition of the cycling operation, following [72]. Let $\beta = \Delta^k \tilde{\beta}$ be a braid in normal form, and factor $\tilde{\beta} = P_1 \dots P_n$ as a product of divisors of Δ. We then say that the braid $c(\beta) = \Delta^k P_2 \dots P_n (\Delta^k P_1 \Delta^{-k})$ is obtained by *cycling* β. Notice that, as mentioned before, $c(\beta)$ is indeed obtained from β by elementary conjugations. It is also useful to remark that $\Delta^k P_1 \Delta^{-k}$ is either equal to P_1 (if k is even) or obtained from P_1 by a reflection along the vertical axis (i.e. exchanging $\sigma_1 \leftrightarrow \sigma_2$). To check when we reach the summit set, we will use the following easy lemma.

Lemma 3.3. *If $\beta = \Delta^k \sigma_1^{a_1} \sigma_2^{a_2} \dots \sigma_1^{a_{n-1}} \sigma_2^{a_n}$ or $\beta = \Delta^k \sigma_1^{a_1} \sigma_2^{a_2} \dots \sigma_2^{a_{n-1}} \sigma_1^{a_n}$ with $a_i \geq 2$ for all $1 \leq i \leq n$, then β is in the summit set. The same holds if we exchange $\sigma_1 \leftrightarrow \sigma_2$.*

Proof of Lemma 3.3. First of all, it is clear that the braid $\tilde{\beta} = \sigma_1^{a_1} \sigma_2^{a_2} \dots \sigma_1^{a_{n-1}} \sigma_2^{a_n}$ does not contain the half-twist if $a_i \geq 2$ for all i, as no braid relation can be applied, so this is the only positive word representing $\tilde{\beta}$. Moreover, this is still the case even after performing elementary conjugations on $\tilde{\beta}$. In particular, cycling of $\beta = \Delta^k \sigma_1^{a_1} \sigma_2^{a_2} \dots \sigma_1^{a_{n-1}} \sigma_2^{a_n}$ cannot increase the power. The same argument applies to the other cases. □

Proof of Lemma 3.2.

I. It is clear that we only need to consider $k > 0$, since a negative braid cannot be conjugate to a positive braid. Now,

$$\beta = \sigma_1^k \sigma_2^{-1} = \sigma_1^k \Delta^{-1} \sigma_2 \sigma_1 = \Delta^{-1} \sigma_2^{k+1} \sigma_1$$

is in normal form, and we see that repeated cycling does not increase the power. Hence, β is already in the summit set and $P(\beta) = -1$.

II. We have $\beta = \sigma_1^u \sigma_2^v \sigma_1^w \sigma_2^\epsilon$, with $|v| \geq 2$ and $u, v + \epsilon, w$ pairwise distinct and $u, w \neq 0, \epsilon, 2\epsilon$. Again, if all the exponents are negative β is a negative braid, which cannot be conjugate to a positive braid. There are $14 = 16 - 2$ cases left to be considered, according to the signs of the exponents. All of those can be treated in the same way, as explained in the previous discussion; we will study some in detail, to serve as an example, and sum up the results of the analogous computations for the remaining cases in Tables 3.1 and 3.2. To keep track of the signs, let us replace u, v, w by $\pm p, \pm q, \pm r$, where $p, q, r > 0$.

• $\beta = \sigma_1^p \sigma_2^{-q} \sigma_1^r \sigma_2$: Since the flype is non-degenerate, we know that $q \geq 2$ and $p, r \geq 3, p \neq r$. To find the normal form of β we will use the identities

$$\sigma_2^{-n} = \begin{cases} \Delta^{-n}(\sigma_1\sigma_2^2\sigma_1)^k, & \text{if } n = 2k \\ \Delta^{-n}\sigma_2\sigma_1(\sigma_1\sigma_2^2\sigma_1)^k, & \text{if } n = 2k+1. \end{cases}$$

If $q = 2k$ is even we get

$$\begin{aligned} \beta &= \sigma_1^p(\Delta^{-q}(\sigma_1\sigma_2^2\sigma_1)^k)\sigma_1^r\sigma_2 = \Delta^{-q}\sigma_1^{p+1}(\sigma_2^2\sigma_1^2)^{k-1}\sigma_2^2\sigma_1^{r+1}\sigma_2 \\ &\sim \Delta^{-q}\sigma_1^p(\sigma_2^2\sigma_1^2)^{k-1}\sigma_2^2\sigma_1^r(\sigma_1\sigma_2\sigma_1) = \Delta^{-q+1}\sigma_2^p(\sigma_1^2\sigma_2^2)^{k-1}\sigma_1^2\sigma_2^r = \Delta^{-q+1}\tilde{\beta}_e. \end{aligned}$$

Similarly, if $q = 2k+1$ is odd we get

$$\begin{aligned} \beta &= \sigma_1^p(\Delta^{-q}\sigma_2\sigma_1(\sigma_1\sigma_2^2\sigma_1)^k)\sigma_1^r\sigma_2 = \Delta^{-q}\sigma_2^{p+1}(\sigma_1^2\sigma_2^2)^k\sigma_1^{r+1}\sigma_2 \\ &\sim \Delta^{-q}\sigma_2^p(\sigma_1^2\sigma_2^2)^k\sigma_1^r(\sigma_1\sigma_2\sigma_1) = \Delta^{-q+1}\sigma_1^p(\sigma_2^2\sigma_1^2)^k\sigma_2^r = \Delta^{-q+1}\tilde{\beta}_o. \end{aligned}$$

In both cases, applying Lemma 3.3 we see that the power cannot be further increased by cycling, since all the generators in $\tilde{\beta}_e$ and $\tilde{\beta}_o$ have exponent at least 2. Therefore, the summit set is reached and $P(\beta) = -q + 1 < 0$.

• $\beta = \sigma_1^{-p}\sigma_2^q\sigma_1^{-r}\sigma_2^{-1}$: We know that $q \geq 2$, $p, r \geq 3$ and $p \neq r$. To write β in normal form we will now also need the equalities

$$\sigma_1^{-n} = \begin{cases} \Delta^{-n}(\sigma_2\sigma_1^2\sigma_2)^k, & \text{if } n = 2k \\ \Delta^{-n}\sigma_1\sigma_2(\sigma_2\sigma_1^2\sigma_2)^k, & \text{if } n = 2k+1. \end{cases}$$

Let us assume that $p = 2k$ and $r = 2l$ are both even. We begin by putting β in Garside normal form:

$$\begin{aligned} \beta &= (\Delta^{-p}(\sigma_2\sigma_1^2\sigma_2)^k)\sigma_2^q(\Delta^{-r}(\sigma_2\sigma_1^2\sigma_2)^l)\Delta^{-1}\sigma_2\sigma_1 \\ &= \Delta^{-p-r}(\sigma_2\sigma_1^2(\sigma_2^2\sigma_1^2)^{k-1}\sigma_2)\sigma_2^q(\sigma_2\sigma_1^2(\sigma_2^2\sigma_1^2)^{l-1})\Delta^{-1}\sigma_1\sigma_2\sigma_1 \\ &= \Delta^{-p-r}\sigma_2\sigma_1^2(\sigma_2^2\sigma_1^2)^{k-1}\sigma_2^{q+2}\sigma_1^2(\sigma_2^2\sigma_1^2)^{l-1}. \end{aligned}$$

We can now start cycling to reach the summit set:

$$\begin{aligned} \beta &= \Delta^{-p-r}(\sigma_2\sigma_1^2)(\sigma_2^2\sigma_1^2)^{k-1}\sigma_2^{q+2}\sigma_1^2(\sigma_2^2\sigma_1^2)^{l-1} \\ &\sim \Delta^{-p-r}(\sigma_2^2\sigma_1^2)^{k-1}\sigma_2^{q+2}\sigma_1^2(\sigma_2^2\sigma_1^2)^{l-1}\sigma_2\sigma_1^2 \\ &= \Delta^{-p-r}(\sigma_2^2\sigma_1^2)^{k-1}\sigma_2^{q+2}\sigma_1^2(\sigma_2^2\sigma_1^2)^{l-2}\sigma_2(\sigma_2\sigma_1^2\sigma_2\sigma_1^2) \\ &= \Delta^{-p-r}(\sigma_2^2\sigma_1^2)^{k-1}\sigma_2^{q+2}\sigma_1^2(\sigma_2^2\sigma_1^2)^{l-2}\sigma_2\Delta^2 \\ &= \Delta^{-p-r+2}(\sigma_2^2\sigma_1^2)^{k-1}\sigma_2^{q+2}\sigma_1^2(\sigma_2^2\sigma_1^2)^{l-2}\sigma_2 \\ &\sim \Delta^{-p-r+2}\sigma_2^3\sigma_1^2(\sigma_2^2\sigma_1^2)^{k-2}\sigma_2^{q+2}\sigma_1^2(\sigma_2^2\sigma_1^2)^{l-2} \end{aligned}$$

Now, by Lemma 3.3 we know that the power cannot be further increased by cycling, so the summit set is reached and $P(\beta) = -p - r + 2 < 0$.

All the other braids can be analyzed in a similar manner, with computations that are not harder than the ones we just carried out. The results are presented in Tables 3.1 and 3.2, where we see the original braid and an element in its summit set, from which it is evident that the summit power is always strictly negative.

□

The proof of Theorem 3.1 is now straightforward.

Proof. Let β_1 and β_2 be positive 3-braids with isotopic closures, representing a non-trivial link. By Theorem 3.2, we know that either β_1 and β_2 are conjugate, or they represent a torus link on two strands, or they are in two different conjugacy classes related by a non-degenerate flype. In fact, in the case of a torus link on two strands, by Lemma 3.2 we know that there is a unique class of representatives containing positive braids, so β_1 and β_2 are conjugate.

If β_1 and β_2 are conjugate, the isomorphism ${}^2B(\beta_1) \cong {}^2B(\beta_2)$ follows directly from Proposition 3.2. Otherwise, we can suppose that $\beta_1 = \sigma_1^u\sigma_2^v\sigma_1^w\sigma_2$ and $\beta_2 = \sigma_1^w\sigma_2^v\sigma_1^v\sigma_2$, where $u, v, w > 0$ by Lemma 3.2. We now conclude by noticing that the linking graph of such a flype-admissible braid is a tree and that a flype induces an automorphism of the tree. The secondary braid group is clearly invariant under such a transformation. □

Braid	Parities of (p,q,r)	After cycling
$\sigma_1^p\sigma_2^q\sigma_1^r\sigma_2^{-1}$	(p,q,r)	$\Delta^{-1}\sigma_2^{p+1}\sigma_1^q\sigma_2^{r+1}$
$\sigma_1^{-p}\sigma_2^q\sigma_1^r\sigma_2^{-1}$	$(2j,q,r)$	$\Delta^{-p}(\sigma_2^2\sigma_1^2)^{j-1}\sigma_2^{q+1}\sigma_1^{r+2}$
	$(2j+1,q,r)$	$\Delta^{-p}(\sigma_1^2\sigma_2^2)^{j-1}\sigma_1^2\sigma_2^{q+1}\sigma_1^{r+2}$
$\sigma_1^p\sigma_2^q\sigma_1^{-r}\sigma_2^{-1}$	$(p,q,2l)$	$\Delta^{-r}\sigma_1^{p+2}\sigma_2^{q+1}(\sigma_1^2\sigma_2^2)^{l-1}$
	$(p,q,2l+1)$	$\Delta^{-r}\sigma_1^{p+2}\sigma_2^{q+1}\sigma_1^2(\sigma_2^2\sigma_1^2)^{l-1}$
$\sigma_1^p\sigma_2^{-q}\sigma_1^r\sigma_2^{-1}$	$(p,2k,r)$	$\Delta^{-q-1}\sigma_2^{p+2}(\sigma_1^2\sigma_2^2)^{k-1}\sigma_1^2\sigma_2^{r+2}$
	$(p,2k+1,r)$	$\Delta^{-q-1}\sigma_1^{p+2}(\sigma_2^2\sigma_1^2)^{k}\sigma_2^{r+2}$
$\sigma_1^{-p}\sigma_2^{-q}\sigma_1^r\sigma_2^{-1}$	$(2j,2k,r)$	$\Delta^{-p-q+1}(\sigma_2^2\sigma_1^2)^{j-1}\sigma_2^3(\sigma_1^2\sigma_2^2)^{k-1}\sigma_1^{r+1}$
	$(2j,2k+1,r)$	$\Delta^{-p-q+1}(\sigma_1^2\sigma_2^2)^{j-1}\sigma_1^3(\sigma_2^2\sigma_1^2)^{k-1}\sigma_2^2\sigma_1^{r+1}$
	$(2j+1,2k,r)$	$\Delta^{-p-q+1}(\sigma_1^2\sigma_2^2)^{j-1}\sigma_1^2\sigma_2^3(\sigma_1^2\sigma_2^2)^{k-1}\sigma_1^{r+1}$
	$(2j+1,2k+1,r)$	$\Delta^{-p-q+1}(\sigma_2^2\sigma_1^2)^{j-1}\sigma_2^2\sigma_1^3(\sigma_2^2\sigma_1^2)^{k-1}\sigma_2^2\sigma_1^{r+1}$
$\sigma_1^p\sigma_2^{-q}\sigma_1^{-r}\sigma_2^{-1}$	$(p,2k,2l)$	$\Delta^{-q-r+1}\sigma_1^{p+1}(\sigma_2^2\sigma_1^2)^{k-1}\sigma_2^3(\sigma_1^2\sigma_2^2)^{l-1}$
	$(p,2k+1,2l)$	$\Delta^{-q-r+1}\sigma_1^{p+1}\sigma_2^2(\sigma_1^2\sigma_2^2)^{k-1}\sigma_1^3(\sigma_2^2\sigma_1^2)^{l-1}$
	$(p,2k,2l+1)$	$\Delta^{-q-r+1}\sigma_1^{p+1}(\sigma_2^2\sigma_1^2)^{k-1}\sigma_2^3\sigma_1^2(\sigma_2^2\sigma_1^2)^{l-1}$
	$(p,2k+1,2l+1)$	$\Delta^{-q-r+1}\sigma_1^{p+1}\sigma_2^2(\sigma_1^2\sigma_2^2)^{k-1}\sigma_1^3\sigma_2^2(\sigma_1^2\sigma_2^2)^{l-1}$
$\sigma_1^{-p}\sigma_2^q\sigma_1^{-r}\sigma_2^{-1}$	$(2j,q,2l)$	$\Delta^{-p-r+2}\sigma_2^3\sigma_1^2(\sigma_2^2\sigma_1^2)^{j-2}\sigma_2^{q+2}\sigma_1^2(\sigma_2^2\sigma_1^2)^{l-2}$
	$(2j,q,2l+1)$	$\Delta^{-p-r+2}\sigma_1^3\sigma_2^2(\sigma_1^2\sigma_2^2)^{j-2}\sigma_1^{q+2}(\sigma_2^2\sigma_1^2)^{l-1}$
	$(2j+1,q,2l)$	$\Delta^{-p-r+2}\sigma_1^3(\sigma_2^2\sigma_1^2)^{j-1}\sigma_2^{q+2}(\sigma_1^2\sigma_2^2)^{l-2}\sigma_1^2$
	$(2j+1,q,2l+1)$	$\Delta^{-p-r+2}\sigma_2^3(\sigma_1^2\sigma_2^2)^{j-1}\sigma_1^{q+2}(\sigma_2^2\sigma_1^2)^{l-1}$

Table 3.1: Braids with $\epsilon=-1$

Braid	Parities of (p,q,r)	After cycling
$\sigma_1^{-p}\sigma_2^q\sigma_1^r\sigma_2$	$(2j,q,r)$	$\Delta^{-p}\sigma_1^2(\sigma_2^2\sigma_1^2)^{j-1}\sigma_2^{q+1}\sigma_1^r\sigma_2^2$
	$(2j+1,q,r)$	$\Delta^{-p}(\sigma_2^2\sigma_1^2)^j\sigma_2^{q+1}\sigma_1^r\sigma_2^2$
$\sigma_1^p\sigma_2^q\sigma_1^{-r}\sigma_2$	$(p,q,2l)$	$\Delta^{-r}\sigma_2^2\sigma_1^p\sigma_2^{q+1}(\sigma_1^2\sigma_2^2)^{l-1}\sigma_1^2$
	$(p,q,2l+1)$	$\Delta^{-r}\sigma_2^2\sigma_1^p\sigma_2^{q+1}(\sigma_1^2\sigma_2^2)^l$
$\sigma_1^p\sigma_2^{-q}\sigma_1^r\sigma_2$	$(p,2k,r)$	$\Delta^{-q+1}\sigma_2^p(\sigma_1^2\sigma_2^2)^{k-1}\sigma_1^2\sigma_2^r$
	$(p,2k+1,r)$	$\Delta^{-q+1}\sigma_1^p(\sigma_2^2\sigma_1^2)^k\sigma_2^r$
$\sigma_1^{-p}\sigma_2^{-q}\sigma_1^r\sigma_2$	$(2j,2k,r)$	$\Delta^{-p-q+1}\sigma_1^2(\sigma_2^2\sigma_1^2)^{j-1}\sigma_2^3(\sigma_1^2\sigma_2^2)^{k-1}\sigma_1^{r+1}$
	$(2j,2k+1,r)$	$\Delta^{-p-q+1}\sigma_2^2(\sigma_1^2\sigma_2^2)^{j-1}\sigma_1^3(\sigma_2^2\sigma_1^2)^{k-1}\sigma_2^2\sigma_1^{r+1}$
	$(2j+1,2k,r)$	$\Delta^{-p-q+1}\sigma_2^2(\sigma_1^2\sigma_2^2)^j\sigma_2(\sigma_1^2\sigma_2^2)^{k-1}\sigma_1^{r+1}$
	$(2j+1,2k+1,r)$	$\Delta^{-p-q+1}\sigma_1^2(\sigma_2^2\sigma_1^2)^j\sigma_1(\sigma_2^2\sigma_1^2)^{k-1}\sigma_2^2\sigma_1^{r+1}$
$\sigma_1^p\sigma_2^{-q}\sigma_1^{-r}\sigma_2$	$(p,2k,2l)$	$\Delta^{-q-r+1}\sigma_1^{p+1}(\sigma_2^2\sigma_1^2)^{k-1}\sigma_2^3(\sigma_1^2\sigma_2^2)^{l-1}\sigma_1^2$
	$(p,2k+1,2l)$	$\Delta^{-q-r+1}\sigma_1^{p+1}\sigma_2^2(\sigma_1^2\sigma_2^2)^{k-1}\sigma_1^3(\sigma_2^2\sigma_1^2)^{l-1}\sigma_2^2$
	$(p,2k,2l+1)$	$\Delta^{-q-r+1}\sigma_1^{p+1}(\sigma_2^2\sigma_1^2)^{k-1}\sigma_2(\sigma_2^2\sigma_1^2)^l\sigma_2^2$
	$(p,2k+1,2l+1)$	$\Delta^{-q-r+1}\sigma_1^{p+1}\sigma_2^2(\sigma_1^2\sigma_2^2)^{k-1}\sigma_1(\sigma_1^2\sigma_2^2)^l\sigma_1^2$
$\sigma_1^{-p}\sigma_2^q\sigma_1^{-r}\sigma_2$	$(2j,q,2l)$	$\Delta^{-p-r}(\sigma_1^2\sigma_2^2)^{j-1}\sigma_1^2\sigma_2^{q+2}(\sigma_1^2\sigma_2^2)^{l-1}\sigma_1^2\sigma_2^3$
	$(2j,q,2l+1)$	$\Delta^{-p-r}(\sigma_2^2\sigma_1^2)^{j-1}\sigma_2^2\sigma_1^{q+2}(\sigma_2^2\sigma_1^2)^l\sigma_2^3$
	$(2j+1,q,2l)$	$\Delta^{-p-r}(\sigma_2^2\sigma_1^2)^j\sigma_2^{q+2}(\sigma_1^2\sigma_2^2)^{l-1}\sigma_1^2\sigma_2^3$
	$(2j+1,q,2l+1)$	$\Delta^{-p-r}(\sigma_1^2\sigma_2^2)^j\sigma_1^{q+2}(\sigma_2^2\sigma_1^2)^l\sigma_2^3$
$\sigma_1^{-p}\sigma_2^{-q}\sigma_1^{-r}\sigma_2$	$(2j,2k,2l)$	$\Delta^{-p-q-r+2}(\sigma_1^2\sigma_2^2)^{j-1}\sigma_1(\sigma_1^2\sigma_2^2)^{k-1}\sigma_1^3(\sigma_2^2\sigma_1^2)^{l-1}\sigma_2^3$
	$(2j,2k,2l+1)$	$\Delta^{-p-q-r+2}(\sigma_2^2\sigma_1^2)^{j-1}\sigma_2(\sigma_2^2\sigma_1^2)^{k-1}\sigma_2(\sigma_2^2\sigma_1^2)^l\sigma_2^3$
	$(2j,2k+1,2l)$	$\Delta^{-p-q-r+2}(\sigma_2^2\sigma_1^2)^{j-1}\sigma_2^3(\sigma_1^2\sigma_2^2)^{k-1}\sigma_1^3(\sigma_2^2\sigma_1^2)^{l-1}\sigma_2^3$
	$(2j+1,2k,2l)$	$\Delta^{-p-q-r+2}(\sigma_2^2\sigma_1^2)^j\sigma_1(\sigma_2^2\sigma_1^2)^{k-1}\sigma_1(\sigma_2^2\sigma_1^2)^{l-1}\sigma_2^3$
	$(2j,2k+1,2l+1)$	$\Delta^{-p-q-r+2}(\sigma_1^2\sigma_2^2)^{j-1}\sigma_1^3(\sigma_2^2\sigma_1^2)^{k-1}\sigma_2(\sigma_2^2\sigma_1^2)^l\sigma_2^3$
	$(2j+1,2k,2l+1)$	$\Delta^{-p-q-r+2}(\sigma_1^2\sigma_2^2)^j\sigma_2(\sigma_1^2\sigma_2^2)^{k-1}\sigma_2(\sigma_1^2\sigma_2^2)^l\sigma_2$
	$(2j+1,2k+1,2l)$	$\Delta^{-p-q-r+2}(\sigma_1^2\sigma_2^2)^j\sigma_2(\sigma_1^2\sigma_2^2)^{k-1}\sigma_1^3(\sigma_2^2\sigma_1^2)^{l-1}\sigma_2^3$
	$(2j+1,2k+1,2l+1)$	$\Delta^{-p-q-r+2}(\sigma_2^2\sigma_1^2)^j\sigma_1(\sigma_2^2\sigma_1^2)^{k-1}\sigma_2(\sigma_2^2\sigma_1^2)^l\sigma_2^3$

Table 3.2: Braids with $\epsilon = 1$

Chapter 4

The monodromy group of a positive braid

In this chapter we will introduce and study monodromy groups of positive braids. Its content is mostly taken from [37].

Inspired by the construction of secondary braid groups and their fascinating, conjectural relationship with singularity theory, we will push the parallelism between plane curve singularities and positive braids one step further and consider a braid theoretical analogue of the geometric monodromy group of a singularity. Recall that the generators of the secondary braid group of a positive braid word are in correspondence with the vertices of the linking graph, which in turn correspond to a natural family of curves on the fibre surface. The fundamental observation is that the relations appearing in the definition of secondary braid groups also arise as relations between the Dehn twists around those curves. This is well known for the commutation and braid relations, while the case of the cycle relation is explained in detail in [13]. Having in mind Theorem 2.3, which expresses the geometric monodromy group of a singularity as a quotient of the fundamental group of the discriminant complement, it is therefore natural to associate to any positive braid β a group $MG(\beta)$, which we call the monodromy group of the positive braid, defined as the subgroup of the mapping class group of the fibre surface generated by the Dehn twists around this natural family of curves.

The first result of this chapter shows that the monodromy group of a positive braid is indeed a generalization of the geometric monodromy group of an isolated plane curve singularity.

Theorem 4.1. *Let $f : \mathbb{C}^2 \to \mathbb{C}$ define an isolated plane curve singularity and $L(f)$ be the link of f. Then there exists a positive braid β representing $L(f)$ such that the geometric monodromy group of f is equal to $MG(\beta)$.*

As we have already mentioned in Chapter 2, in [70] Portilla Cuadrado

and Salter proved that the geometric monodromy group of any singularity of genus at least 5 and not of type A_n and D_n is a framed mapping class group. Following their approach, the main result of this chapter is an identification of the monodromy group of a positive braid β whose closure is a knot with a framed mapping class group on the genus minimizing surface Σ_β.

Theorem 4.2. *Let β be a prime positive braid not of type A_n and whose closure is a knot. For all but finitely many such braids, there exists a framing ϕ_β on Σ_β such that the monodromy group $MG(\beta)$ is equal to the framed mapping class group* $\mathrm{MCG}(\Sigma_\beta, \phi_\beta)$.

In particular, it follows from the general theory of framed mapping class groups that, at least for knots of big enough genus, the monodromy group of a positive braid is a well defined knot invariant, which is actually determined by the genus and the Arf invariant of the knot, see Section 3.

Of course, as a consequence of Theorem 4.1 and Theorem 4.2, in the restricted context of singularities we immediately obtain that the geometric monodromy group of an irreducible singularity is controlled by a framing. In fact, as explained in Remark 4.4, one can see that our proof of Theorem 4.2 still applies to links of singularities not of type A_n and D_n, thus recovering the results of [70] up to finitely many exceptions. On the other hand, there are some infinite families of positive braid links for which our methods do not seem to work, see Remark 4.5. Moreover, the monodromy group of a positive braid is proved to be an invariant of the braid closure only if the latter is connected; for braids whose closure is disconnected, the strongest invariance result is Corollary 4.2. In spite of the increased combinatorial difficulty, working in the more general setting of positive braids has some advantages, as we will now explain.

Since the topological type of a singularity is completely determined by its link, a priori every topological invariant of a singularity should be somehow readable from the link. For instance, the Milnor number corresponds to the minimal first Betti number, while the multiplicity corresponds to the braid index [78]. However, this translation is often far from straightforward. Notice that, although not explicitly stated therein, a consequence of the results of Cuadrado and Salter in [70] is that for irreducible singularities the geometric monodromy group is determined by the genus of the Milnor fibre and some Arf invariant associated to the framing, as discussed in Chapter 2. Working with positive braids allows us for explicit calculations that lead to the following corollary, expressing the geometric monodromy group entirely in terms of knot invariants. More precisely, we are able to identify the Arf invariant associated to the framing with the Arf invariant of the knot, see Proposition 4.3.

Corollary 4.1. *Let f define an irreducible isolated plane curve singularity that is not of type A_n and $K(f)$ be the knot of the singularity. For all but finitely*

many such singularities, the geometric monodromy group of f is determined by the genus and the Arf invariant of $K(f)$.

From a purely knot theoretical viewpoint, Theorem 4.2 might seem disappointing. It implies that, if the closure of a positive braid is a knot (up to finitely many exceptions), its monodromy group is an invariant of the knot, but a rather useless one: it is hard to compute, but determined by two classical and much easier invariants, a natural number and a mod 2 class. Its interest lies in negative results such as Corollary 4.1. The geometric monodromy group, which was typically considered a rich yet hard to investigate invariant of a plane curve singularity, turns out, in the case of irreducible singularities, to be determined by two simple knot invariants, and the question whether two irreducible singularities have the same geometric monodromy group can be answered by a direct and easy computation, using existing formulas for the Arf invariant of a knot. Of course, for each fixed genus there are many different irreducible singularities, so there will be different singularities with the same geometric monodromy group. We believe that for big enough genus both values of the Arf invariant are realized, so that there would be exactly two geometric monodromy groups.

Example 4.1. We consider the singularities $f(x,y) = x^p + y^q$ for $(p,q) = (3,46)$, $(4,31)$,$(6,19)$,$(7,16)$,$(10,11)$. The associated knots are the torus knots $T_{p,q}$. They all have genus $\frac{(p-1)(q-1)}{2} = 45$, and the results of Theorem 4.2 hold for each of them (see Proposition 4.6). The Arf invariant of a knot is determined by the Alexander polynomial Δ_K, via the equality (see [58])

$$\mathcal{A}(K) = \begin{cases} 0 & \text{if } \Delta_K(-1) = \pm 1 \mod 8 \\ 1 & \text{if } \Delta_K(-1) = \pm 3 \mod 8 \end{cases}.$$

Knowing that the Alexander polynomial of a torus knot $K = T_{p,q}$ is

$$\Delta_K(t) = \frac{(t-1)(t^{pq}-1)}{(t^p-1)(t^q-1)},$$

it is not hard to check that $\Delta_{T_{p,q}}(-1) = 1$ if p,q are odd and $\Delta_{T_{p,q}}(-1) = q$ if p is even and q is odd. We therefore get

$$\mathcal{A}(T_{p,q}) = \begin{cases} 0 & \text{if } p,q \text{ are odd or } q = \pm 1 \mod 8 \\ 1 & \text{if } p \text{ is even and } q = \pm 3 \mod 8 \end{cases}.$$

Applying Corollary 4.1 we immediately get that for $(p,q) = (3,46)$, $(10,11)$ or $(6,19)$ those singularities have the same geometric monodromy group, while for $(4,31)$ and $(7,16)$ the group is different.

As a final remark, as we have seen the monodromy group of a positive braid word is a quotient of the secondary braid group. It is natural to wonder whether the two groups are isomorphic. This is true if the linking graph is a Dynkin diagram of type A_n or D_n [68], but false for more complicated trees. Indeed, if the linking graph is a tree, the secondary braid group is simply an Artin group, and Labruère [55] and Wajnryb [77] proved that the only Artin groups whose Dynkin diagram is a tree and that geometrically embed in the mapping class group are precisely the ones of type A_n and D_n. Naively, one could hope for the case of linking graphs with cycles to be different, since now the secondary braid group is not an Artin group. However, this is still not correct. For instance, for a positive braid of minimal braid index whose closure is a torus link $T_{p,q}$, Baader and Lönne proved that the secondary braid group is isomorphic to the fundamental group of the discriminant complement of the singularity $f(x,y) = x^p + y^q$, while by Theorem 4.1 we know that the monodromy group is the geometric monodromy group of f, and Portilla Cuadrado and Salter proved that those two groups are never isomorphic as soon as the genus is at least 7 [70]. In fact, the proof of Portilla Cuadrado and Salter can be generalized to all positive braids whose monodromy group is a framed mapping class group on a surface of genus $g \geq 7$: by Proposition 2.4, if $g \geq 7$ the abelianization of a framed mapping class group is $\mathbb{Z}/24\mathbb{Z}$, while every secondary braid group surjects onto $\mathbb{Z}$, by mapping every generator to 1.

Structure of the chapter: In Section 1 we define the monodromy group of a positive braid and prove some basic invariance properties. In Section 2 we discuss the connection to plane curve singularities and, using A'Campo's theory of divides, we prove Theorem 4.1. In Section 3 we construct the framing appearing in Theorem 4.2 and study its Arf invariant. Finally, Section 4 is the technical part of the chapter, in which we prove Theorem 4.2. This basically consists of a lengthy case distinction that allows us to apply the general results on framed mapping class groups discussed in Chapter 2.

1 The monodromy group of a positive braid

Let β be a positive braid word. In what follows we will always assume, mostly without mentioning it, that its closure $\hat{\beta}$ is a non-split link; this is equivalent to ask that every generator appears at least once in the word β. Recall from Chapter 2, Section 3 that in this case $\hat{\beta}$ is a fibred link, and that one can easily construct the fibre surface directly from the positive word β. Let us denote this fibre surface by Σ_β, and let g be its genus and r the number of boundary components. On Σ_β there is a standard family of $2g+r-1$ curves γ_i, forming a

basis of the first homology of Σ_β, and which are in one-to-one correspondence with the vertices of the linking graph of β. In fact, the linking graph precisely records the intersection pattern of those curves.

Definition 4.1. Let β be a positive braid word whose closure is a non-split link. The *monodromy group* $MG(\beta)$ is the subgroup of the mapping class group of Σ_β generated by all the Dehn twists around the curves γ_i, where $i \in \{1, \cdots, 2g + r - 1\}$, i.e.

$$MG(\beta) = \langle T_{\gamma_1}, \cdots, T_{\gamma_{2g+r-1}} \rangle \leqslant \mathrm{MCG}(\Sigma_\beta).$$

Example 4.2. As already mentioned, it follows from [68] that if $\beta = \sigma_1^{n+1}$ then $MG(\beta)$ is isomorphic to the Artin group of type A_n. Similarly, for $\beta = \sigma_1^{n-2}\sigma_2\sigma_1^2\sigma_2$, $MG(\beta)$ is isomorphic to the Artin group of type D_n

Remark 4.1. The fibre surface Σ_β can be constructed by a sequence of plumbings of positive Hopf bands, and the curves γ_i are precisely the core curves of those Hopf bands. The monodromy group of β therefore somehow reflects this plumbing structure. Moreover, the monodromy of the fibration is given by a product of the Dehn twists around those curves, so it is an element of the monodromy group.

A priori, the monodromy group $MG(\beta)$ is associated to a positive braid word β. We will now prove some elementary invariance properties, showing in particular that it depends only on the positive braid represented by β. First of all, from the definition, it is clear that $MG(\beta)$ is invariant under far-commutativity (i.e. $\sigma_i\sigma_j = \sigma_j\sigma_i$ for $|i - j| \geq 2$) and positive Markov move.

Proposition 4.1 (Elementary conjugation invariance)**.** *Let β be a positive braid word on N strands. Then for all $1 \leq i \leq N - 1$, $MG(\beta\sigma_i) \cong MG(\sigma_i\beta)$.*

Proof. Consider the fibre surfaces of $\beta\sigma_i$ and $\sigma_i\beta$. Those surfaces are isotopic, by sliding the topmost band between the i-th and $(i + 1)$-th disks along the back of the disks and bringing it in the lowermost position. Note that this isotopy restricts to the identity outside of the i_{th}-column. The surfaces $\Sigma_{\beta\sigma_i}$ and $\Sigma_{\sigma_i\beta}$ can hence be schematically represented as in Figure 4.1 , where we drew the $i_{th}-$column and the light grey boxes on the two sides represent the remaining parts of the surface.

Let us number the standard curves of the i_{th} column as in Figure 4.1. The isotopy will send each $\gamma_i, i = 1, \cdots, n - 1$ to the corresponding $\tilde{\gamma}_i, i = 1, \cdots, n - 1$ and transform γ_n into the red curve $\tilde{\gamma}_{n+1}$. All we have to prove is then that we can generate the Dehn twists around the curves $\tilde{\gamma}_1, \cdots, \tilde{\gamma}_{n-1}, \tilde{\gamma}_{n+1}$ using $\tilde{\gamma}_1, \cdots, \tilde{\gamma}_{n-1}, \tilde{\gamma}_n$, and vice-versa. But we note that

$$\tilde{\gamma}_{n+1} = T^{-1}_{\tilde{\gamma}_{n-1}} \cdots T^{-1}_{\tilde{\gamma}_2} T^{-1}_{\tilde{\gamma}_1}(\tilde{\gamma}_n),$$

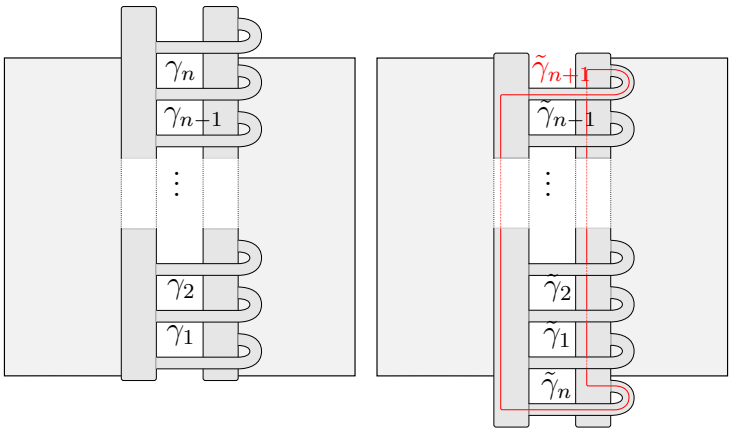

Figure 4.1: The isotopy between $\Sigma_{\beta\sigma_i}$ and $\Sigma_{\sigma_i\beta}$

so that for $h = T_{\tilde{\gamma}_{n-1}}^{-1} \cdots T_{\tilde{\gamma}_2}^{-1} T_{\tilde{\gamma}_1}^{-1}$ we have

$$T_{\tilde{\gamma}_{n+1}} = h T_{\tilde{\gamma}_n} h^{-1}$$

and the result is proved.

□

Proposition 4.2 (Braid relation invariance)**.** *Let α and β be two positive braid words related by a braid relation, then $MG(\alpha) \cong MG(\beta)$.*

Proof. Up to elementary conjugation, we can suppose that $\alpha = \omega\sigma_i\sigma_{i+1}\sigma_i$ and $\beta = \omega\sigma_{i+1}\sigma_i\sigma_{i+1}$, where ω is a positive braid on N strands and $1 \leq i \leq N-2$. At the level of surfaces Σ_α and Σ_β the braid relation can be realized by an isotopy as in Figure 4.2. It is clear that all the standard curves γ_i are fixed by this isotopy but the ones (at most two) passing through the slidden band.

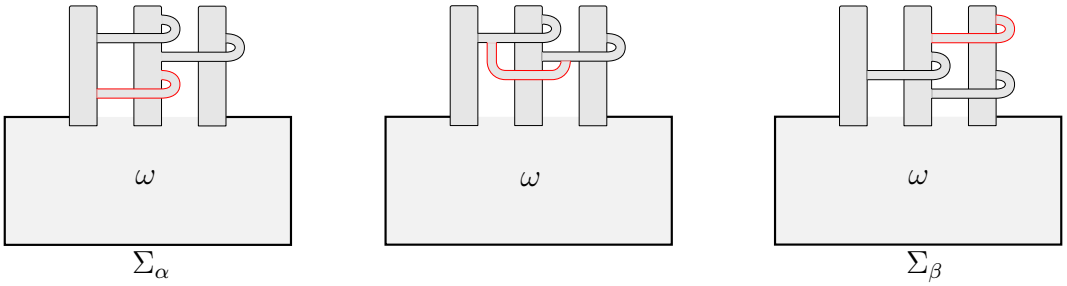

Figure 4.2: The isotopy between Σ_α and Σ_β

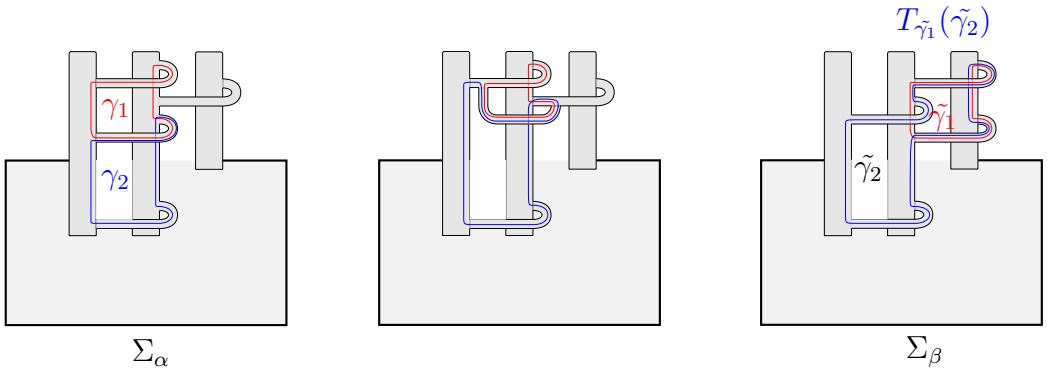

Figure 4.3: First case of braid relation invariance

- There is a generator σ_i in ω: in this case, there are two curves on Σ_α which are modified by the isotopy. Let us call them γ_1 and γ_2, as in Figure 4.3. We see that, after the isotopy, γ_1 is transformed into the corresponding $\tilde{\gamma}_1$, while γ_2 becomes $T_{\tilde{\gamma}_1}(\tilde{\gamma}_2)$. All the other standard curves are fixed. Therefore, we get that $MG(\alpha) \cong MG(\beta)$.

- There is no σ_i in ω: in this case, the only curve modified by the isotopy is γ_1, which as before is transformed into $\tilde{\gamma}_1$. Again, we directly have that $MG(\alpha) \cong MG(\beta)$.

□

To sum up, we have proved the invariance of the monodromy group of a positive braid under braid relations and elementary conjugations. The following corollary now follows directly by an observation of Orevkov about Garside's solution of the conjugacy problem in the braid group, saying that, in the presence of a positive half-twist, two conjugate positive braids can be related by a sequence of braid relations and elementary conjugations, see the proof of Proposition 3.2.

Corollary 4.2. *Let α and β be positive braids such that the closures are braid isotopic and contain a positive half-twist, then $MG(\alpha) \cong MG(\beta)$.*

2 Divides and monodromy of singularities

In this section we will study the relation between monodromy groups of positive braids and geometric monodromy groups of isolated plane curve singularities and prove Theorem 4.1.

Let $f : \mathbb{C}^2 \to \mathbb{C}$ define an isolated plane curve singularity and $\Sigma(f)$ be its Milnor fibre. As we have seen in Chapter 2, the geometric monodromy group

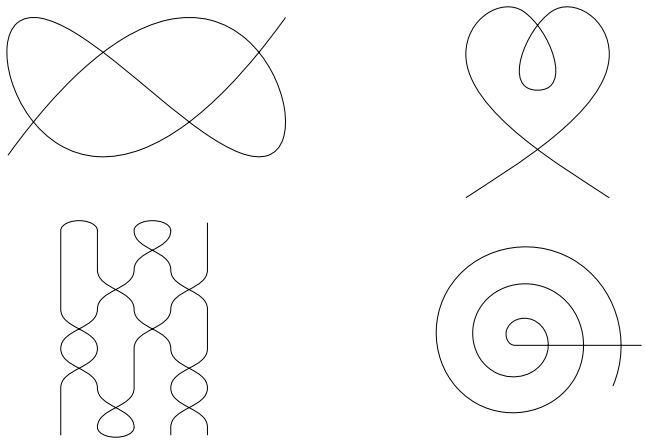

Figure 4.4: The divides on the left are ordered Morse, the divides on the right are not.

of f is a subgroup of $\mathrm{MCG}(\Sigma(f))$ generated by the Dehn twists around a distinguished family of vanishing cycles. Now, links of singularities are closures of positive braids. Since fibre surfaces of fibred links are unique, the Milnor fibre of a singularity f is ambient isotopic to the fibre surface Σ_β of any positive braid β representing $L(f)$. We therefore now have two a priori distinct subgroups of $\mathrm{MCG}(\Sigma_\beta) = \mathrm{MCG}(\Sigma(f))$, the geometric monodromy group of f and the monodromy group of β. Theorem 4.1 says that those two groups coincide for at least one choice of β.

The proof of Theorem 4.1 uses A'Campo's divides and is constructive: we will explicitly find an isotopy between the Milnor fibre, constructed from a divide using Hirasawa's algorithm [48], and the surface of an appropriate positive braid and identify the vanishing cycles on this braid surface. In order to do so, we need to find a divide from which the positive braid is somehow visible.

Definition 4.2. A divide $\mathcal{D} \subset D^2$ is an *ordered Morse divide* if there is a diameter of D^2 such that the orthogonal projection on this diameter is Morse when restricted to $\mathcal{D}$, all the local maxima (resp. minima) have the same critical value b (resp. a) with $b > a$ and all the crossings are mapped in the open interval (a, b).

Basically, a divide is ordered Morse (w.r.t. a given direction) if no local maxima or minima lie in an interior face of the divide. Examples of such divides are given in Figure 4.4.

Remark 4.2. In the literature, ordered Morse divides are sometimes called *scannable divides* [40].

Figure 4.5: Hirasawa's construction of the embedded fibre surface of an ordered Morse divide.

Ordered Morse divides were introduced by Couture and Perron [33], who used a generalization of those to construct a representative braid for any divide link. In particular, ordered Morse divides give positive braid links. Notice that every singularity has an associated divide which is ordered Morse (in fact, the divides originally constructed by A'Campo and Gusein-Zade are ordered Morse, see [33]). The result of Couture and Perron can be obtained geometrically: if we apply the algorithm of [48] to an ordered Morse divide, we get exactly the fibre surface of a positive braid. This was done in [43] for Lissajous divides and torus links, but the same procedure works for an arbitrary ordered Morse divide. The construction of the fibre surface is shown in Figure 4.5: one just has to replace the crossings and minima/maxima of the divide with the corresponding pieces of surface and glue them together following the pattern of the divide. Here we use that all the minima and maxima of the divide are in the exterior face: for general divides the fibre surface is more complicated.

Remark 4.3. The diagrams in Figure 4.5 are the mirror image of those obtained by Hirasawa in [48]. This is due to the different choice of orientation of S^3: Hirasawa uses the orientation induced by the trivialization

$$T\mathbb{R}^2 = \{(x, v) \mid x \in \mathbb{R}^2, v \in T_x\mathbb{R}^2\} \cong \mathbb{R}^2 \times \mathbb{R}^2;$$

we use the identification $T\mathbb{R}^2 \cong \mathbb{C}^2$, where the plane $\mathbb{R}^2$ is identified with the real part of $\mathbb{C}^2$, since this allows to correctly identify the link of a singularity with the link of a corresponding divide.

Proof of Theorem 4.1. Let f be an isolated plane singularity and $\mathcal{D}$ an associated ordered Morse divide. Let Σ be the embedded surface constructed following [48], as explained above. It is an embedded fibre surface whose boundary is the link $L(\mathcal{D}) = L(f)$. To see that this is indeed the fibre surface of a positive braid, we just need to perform the isotopies shown in Figure 4.6 (1) and (2a), getting a collection of disks connected by half-twisted bands, and slide all the bands to the front. Let us remark that an ordered Morse divide is formed of N parallel lines (where N is the number of points in the preimage of a regular value of the Morse projection) connected by the crossings and

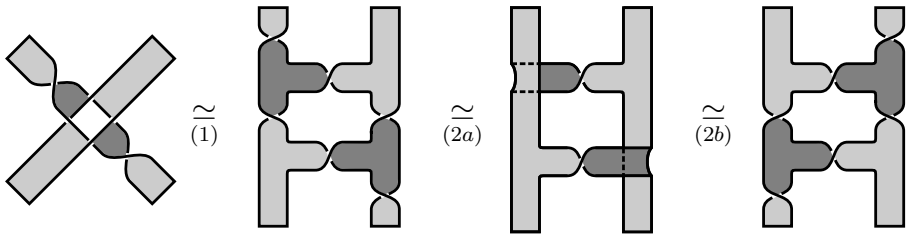

Figure 4.6: A sequence of isotopies.

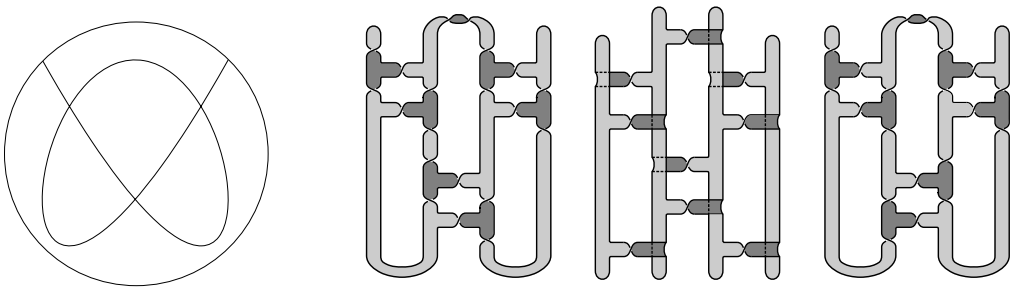

Figure 4.7: An example of the isotopies of Theorem 4.1.

the minima/maxima. The braid obtained will have N strands, a crossing of $\mathcal{D}$ gives a pair of generators while every maximum/minimum gives one generator.

By further performing the isotopies of Figure 4.6, (2b) around all the crossings of $\mathcal{D}$ corresponding to generators σ_i for even i, we can now directly identify Σ with an embedded version of A'Campo's model of the Milnor fibre. A system of vanishing cycles is therefore visible on the braid surface Σ. Those cycles are not exactly the same as the generators of the monodromy group of the braid, but the same arguments as in the proof of Proposition 4.1 show that the two groups are indeed the same. □

Example 4.3. In Figure 4.7, we see an example of the isotopies used in the previous proof. On the left, we start with a divide $\mathcal{D}$; we then construct the Seifert surface following Hirasawa's algorithm. After applying the isotopies of Figure 4.6 (2a), we obtain the surface Σ_β of a positive braid, namely $\beta = (\sigma_1\sigma_2\sigma_3)^3$. On the right, we performed the isotopy of Figure 4.6 (2b) around the central crossing of $\mathcal{D}$. In that way, we clearly see that the surface is composed of twisted cylinders corresponding to the crossings of $\mathcal{D}$ and connected by *half-twisted* bands, as required by A'Campo's construction (compare with Figure 2.1). Notice that it is not relevant that this last step is performed around all the crossings of $\mathcal{D}$ corresponding to generators σ_i for *even* i as opposed to *odd* i; what matters is that it alternates, in order the get the required half-twisting of the bands become visible.

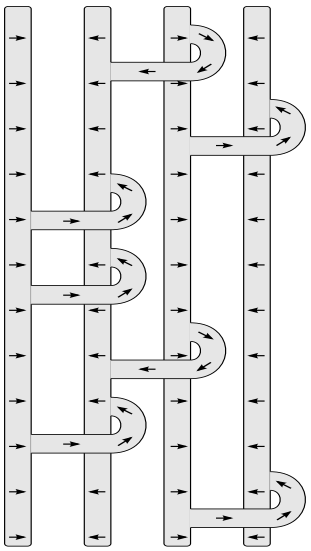

Figure 4.8: The framing on Σ_β for $\beta = \sigma_3\sigma_1\sigma_2\sigma_1^2\sigma_3\sigma_2$. On the vertical disks it is horizontal with alternating directions, on the twisted bands it is parallel to the core.

3 A framing for positive braids

Let β be a non-split positive braid and Σ_β its fibre surface. We can construct a framing ϕ_β on Σ_β as in Figure 4.8. An explicit and straightforward computation now shows that every standard curve γ_i on Σ_β is admissible for ϕ_β. Therefore, the monodromy group of β is contained in the framed mapping class group of ϕ_β:

$$MG(\beta) \leqslant \mathrm{MCG}(\Sigma_\beta, \phi_\beta).$$

We will prove that, at least for positive braids whose closure is a knot of big enough genus, the monodromy group is equal to this framed mapping class group. Let us now recall the discussion in Chapter 2, Section 2, and in particular Proposition 2.3: to each framing on a given surface, one can associate a certain Arf invariant, which distinguishes the conjugacy classe of the corresponding framed mapping class groups. We therefore now want to compute the Arf invariant of ϕ_β.

Proposition 4.3. *Let β be a positive braid whose closure is a knot K. Then*

$$\mathcal{A}(\phi_\beta) = \mathcal{A}(K),$$

where $\mathcal{A}(K)$ is the classical Arf invariant of K.

To prove Proposition 4.3, we will need to discuss a bit more in detail the Arf invariant. Let V be a finite dimensional vector space over $\mathbb{Z}_2$ equipped with a non-singular, symmetric bilinear pairing $\langle \cdot, \cdot \rangle : V \times V \to \mathbb{Z}_2$. A *quadratic refinement* of the bilinear pairing $\langle \cdot, \cdot \rangle$ is a function $q : V \to \mathbb{Z}_2$ such that for all $x, y \in V$

$$q(x + y) = q(x) + q(y) + \langle x, y \rangle.$$

To such a mod 2 quadratic form it is classically associated an invariant $\mathcal{A}(q) \in \mathbb{Z}_2$, called the Arf invariant.

In our context, we will take $V = H_1(\Sigma_\beta, \mathbb{Z}_2)$ and $\langle \cdot, \cdot \rangle$ the mod 2 intersection form. As we have already mentioned, the framing ϕ_β induces a quadratic refinement of the intersection form, whose Arf invariant is $\mathcal{A}(\phi_\beta)$. On the other hand, if the closure of β is a knot K, it is known that the Seifert form also induces such a quadratic refinement. More precisely, if

$$S : H_1(\Sigma_\beta) \times H_1(\Sigma_\beta) \to \mathbb{Z}$$

denotes the Seifert form, we can define $q : V \to \mathbb{Z}_2$ by $q(x) = S(x, x) \mod 2$. It is a classical result that the Arf invariant of this quadratic form is indeed an invariant of K, that we denote by $\mathcal{A}(K)$ (see e.g. Chapter 10 of [58]).

Proof of Proposition 4.3. Let β be a positive braid whose closure is a knot K and Σ_β its fibre surface, equipped with the framing ϕ_β. The family of curves γ_i form a basis of $V = H_1(\Sigma_\beta, \mathbb{Z}_2)$. Since by construction all the γ_i are admissible for ϕ_β, for every i we have the equality

$$\phi_\beta(\gamma_i) + 1 = 1 = S(\gamma_i, \gamma_i) \mod 2.$$

Since $\{\gamma_i\}$ is a basis, it now follows from the defining equation of a quadratic refinement that for every $x \in V$

$$\phi_\beta(x) + 1 = q(x) \mod 2.$$

Therefore the two quadratic forms $(\phi_\beta + 1) \bmod 2$ and q coincide, so their Arf invariants also do. □

4 Proof of the main theorem

In this section we will give the proof of Theorem 4.2, stating that, up to finitely many exceptions, the monodromy group of a positive braid not of type A_n and whose closure is a knot is a framed mapping class group. In the previous section we have constructed a framing ϕ_β on the fibre surface Σ_β and seen that $MG(\beta) \leqslant \mathrm{MCG}(\Sigma_\beta, \phi_\beta)$, so we only need to deal with the opposite

Figure 4.9: Subtrees of $\sigma_1^2\sigma_2\sigma_1^2\sigma_2\sigma_1^2\sigma_2\sigma_1^2\sigma_2\sigma_1^2\sigma_2^2$ and $\sigma_1^2\sigma_2\sigma_1^2\sigma_2\sigma_1^2\sigma_2\sigma_1^3\sigma_2\sigma_1^2\sigma_2$

inclusion. This will be done by applying Proposition 2.2. As a first step, we have to find appropriate subsurfaces supporting an E-arboreal spanning configuration. For this, we will separately consider the case of braids on 3-strands (Proposition 4.4), on at least 11 strands (Proposition 4.5) and finally with an intermediate number of strands (Proposition 4.6).

Proposition 4.4. *Let β be a prime positive 3-braid of genus $g \geq 5$ which is not of type A_n or D_n. Then, excepted finitely many braids, up to positive braid isotopy its linking graph contains an induced subtree which is an E-arboreal spanning configuration on a subsurface of genus $g \geq 5$.*

Proof. Let β be a positive 3-braid which is not of type A_n. Up to elementary conjugation and braid relation we can assume that $\beta = \sigma_1^{a_1}\sigma_2^{b_1}\cdots\sigma_1^{a_m}\sigma_2^{b_m}$, with $a_i \geq 2$ and $b_i \geq 1$ for all $i \in \{1, \cdots, m\}$. First of all, notice that if we can find a suitable subtree for a braid $\sigma_1^{a_1}\sigma_2^{b_1}\cdots\sigma_1^{a_m}\sigma_2^{b_m}$, the result will also hold for any braid $\sigma_1^{a'_1}\sigma_2^{b'_1}\cdots\sigma_1^{a'_m}\sigma_2^{b'_m}$ for $a'_i \geq a_i$ and $b'_i \geq b_i$. We will now prove the result by case distinction over m.

- $m \geq 5$: Every braid with $m \geq 5$ has genus $g \geq 5$ so it is clearly enough to prove the result for $m = 5$. If one of the b_i is at least 2, we can assume that $\beta = \sigma_1^2\sigma_2\sigma_1^2\sigma_2\sigma_1^2\sigma_2\sigma_1^2\sigma_2\sigma_1^2\sigma_2^2$. In the left of Figure 4.9 we now see an induced subtree of the linking graph with the required properties. Similarly if one of the a_i is at least 3 we can assume that $\beta = \sigma_1^2\sigma_2\sigma_1^2\sigma_2\sigma_1^2\sigma_2\sigma_1^3\sigma_2\sigma_1^2\sigma_2$, and we find the induced subtree of the right of Figure 4.9.

  We are now only left with the braid $\sigma_1^2\sigma_2\sigma_1^2\sigma_2\sigma_1^2\sigma_2\sigma_1^2\sigma_2\sigma_1^2\sigma_2$. Here we do not directly find an appropriate subtree, but Figure 4.10 shows a sequence of braid relations that makes it visible.

- $m = 4$: We will treat several cases. Let us first assume that there is an i such that $b_i \geq 2$. If there are $i \neq j$ such that $b_i, b_j \geq 2$, then up to cyclic ordering we only have to deal with the two cases depicted in

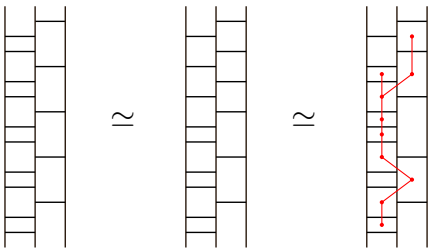

Figure 4.10: The braid $\sigma_1^2\sigma_2\sigma_1^2\sigma_2\sigma_1^2\sigma_2\sigma_1^2\sigma_2\sigma_1^2\sigma_2$

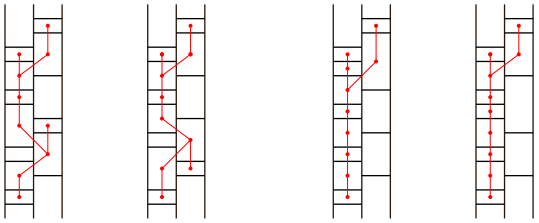

Figure 4.11: The cases when $m = 4$ and $b_i, b_j \geq 2$ (left) or $b_i \geq 2$ and $a_j \geq 3$ (right)

the left of Figure 4.11, where we see the sought subtrees. Similarly, if there is only one b_i greater than 2 but there is one a_j bigger than 3 we will find one of the trees in the right of Figure 4.11. Finally, if all the a_j are equal to 2 and there is only one b_i greater than 2, it is enough to consider the braid $\sigma_1^2\sigma_2\sigma_1^2\sigma_2\sigma_1^2\sigma_2\sigma_1^2\sigma_2^2$, for which we can find the subtree after applying some braid relations as in Figure 4.12.

We are now left with $b_i = 1$ for all i. Notice that in that case there need to be at least one $a_i \geq 3$, otherwise the braid has genus less than 5. If there are two non-consecutive a_i and a_j greater than 3, it is enough to consider the braid $\sigma_1^3\sigma_2\sigma_1^2\sigma_2\sigma_1^3\sigma_2\sigma_1^2\sigma_2$, for which we find an appropriate subtree in the left of Figure 4.13. If not, up to cyclic ordering there must be two consecutive $a_i = a_{i+1} = 2$, in which case we can apply a sequence of braid relations as we did in the right of Figure 4.13 and find our subtree.

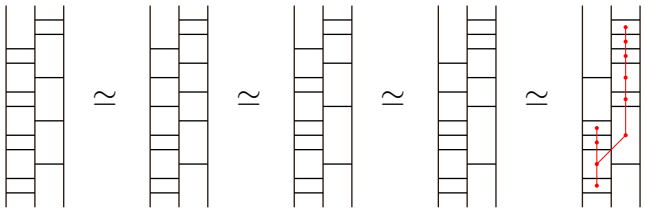

Figure 4.12: The braid $\sigma_1^2\sigma_2\sigma_1^2\sigma_2\sigma_1^2\sigma_2\sigma_1^2\sigma_2^2$

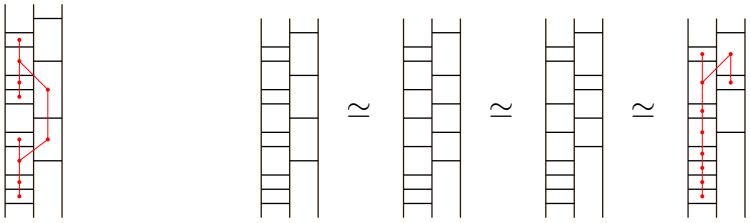

Figure 4.13: The cases $m = 4$ and $b_i = 1$ for all i

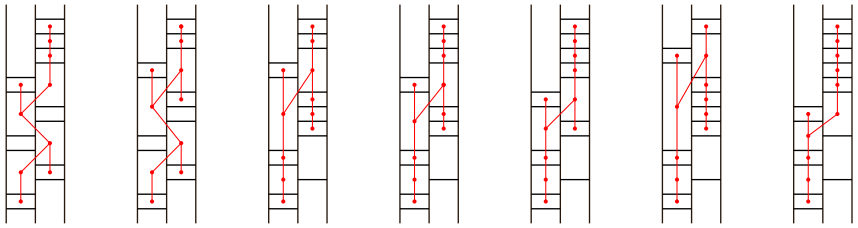

Figure 4.14: When $m = 3$ and $\sum b_i = 8$

- $m = 3$: This will be the lengthier case, since there are many low genus braids that require special treatment. Let $\beta = \sigma_1^{a_1}\sigma_2^{b_1}\sigma_1^{a_2}\sigma_2^{b_2}\sigma_1^{a_3}\sigma_2^{b_3}$ be a braid of genus $g \geq 5$, then a simple argument implies that $\sum a_i + \sum b_i \geq 12$. If $\sum b_i \geq 8$, it is enough to consider the braids in Figure 4.14. Similarly, when $\sum a_i \geq 11$ it is enough to consider the case when all the b_i are equal to 1, and up to elementary conjugation we can assume that $a_3 \geq 3$. In this case, by taking all the vertices in the left column and only the topmost of the right column we will always end up finding a tripod tree $T(1, k, 9-k)$ for $k \geq 2$, which all correspond to subsurfaces of genus 5, see Figure 4.15 for some examples.

  We are now left with the low genus cases.

  - $\sum a_i = 6$: If $\sum b_i = 6$ we always get a link with 3 components and genus 4. If $\sum b_i = 7$ and there is at least one of the b_i equal to one, up to elementary conjugation we can assume that

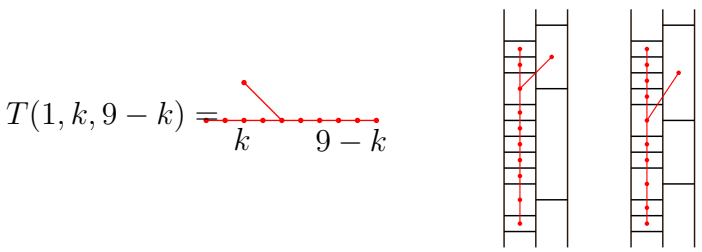

Figure 4.15: The tripod trees for $m = 3$ and $\sum a_i = 11$

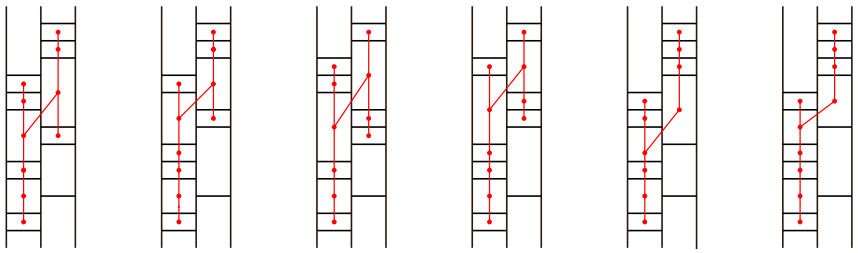

Figure 4.16: When $\sum a_i = 7$ and $\sum b_i = 6$, with $b_1 = 1$

$\beta = \sigma_1^2\sigma_2\sigma_1^2\sigma_2^{b_2}\sigma_1^2\sigma_2^{b_3}$ with $b_2 + b_3 = 6$. Using that $\sigma_1^2\sigma_2\sigma_1^2$ commutes with σ_2 we get $\sigma_2^{b_2}\sigma_1^2\sigma_2\sigma_1^4\sigma_2^{b_3}$, which is conjugate to $\sigma_1^2\sigma_2\sigma_1^4\sigma_2^6$, whose intersection graph is a tree with the required properties. We are now left with $b_i = 2$ for all i. Up to elementary conjugation there is only one such braid, $\sigma_1^2\sigma_2^2\sigma_1^2\sigma_2^2\sigma_1^2\sigma_2^3$. Here there are no possible braid relations to apply and it is not possible to find a subtree of big enough genus.

– $\sum a_i = 7$: Let us first assume that $\sum b_i = 6$. If there is at least one b_i equal to one, we can directly find our subtrees. In Figure 4.16 we see some of the cases. The omitted ones are symmetric and will give the same subtrees. Notice that this will also cover all the braids with $\sum a_i \geq 7$ and $\sum b_i \geq 7$. If $b_i = 2$ for all i, up to elementary conjugation there is only the braid $\sigma_1^3\sigma_2^2\sigma_1^2\sigma_2^2\sigma_1^2\sigma_2^2$, for which again we cannot find any subtree of big enough genus.

If $\sum b_i = 5$, up to conjugation we have $\beta = \sigma_1^3\sigma_2^{b_1}\sigma_1^2\sigma_2^{b_2}\sigma_1^2\sigma_2^{b_3}$. If $b_2 = 1$, using that $\sigma_1^2\sigma_2\sigma_1^2$ commutes with σ_2 we get the braid $\sigma_1^5\sigma_2\sigma_1^2\sigma_2^4$, whose intersection graph is a tree with the required properties. We are left with the three braids $\sigma_1^3\sigma_2\sigma_1^2\sigma_2^2\sigma_1^2\sigma_2^2$, $\sigma_1^3\sigma_2^2\sigma_1^2\sigma_2^2\sigma_1^2\sigma_2$ and $\sigma_1^3\sigma_2\sigma_1^2\sigma_2^3\sigma_1^2\sigma_2$. For the first, up to elementary conjugation and applying the commutativity relation as before we have

$$\sigma_1^3\sigma_2\sigma_1^2\sigma_2^2\sigma_1^2\sigma_2^2 \simeq \sigma_1^2\sigma_2^2\sigma_1^3\sigma_2\sigma_1^2\sigma_2^2 = \sigma_1^2\sigma_2^2\sigma_1\sigma_2^2\sigma_1^2\sigma_2\sigma_1^2 = \\ = \sigma_1^4\sigma_2^2\sigma_1\sigma_2^3\sigma_1^2 \simeq \sigma_1^6\sigma_2^2\sigma_1\sigma_2^3$$

and we get a suitable tree. The second braid is symmetric and will lead to the same intersection tree. For the last, we similarly get

$$\sigma_1^3\sigma_2\sigma_1^2\sigma_2^3\sigma_1^2\sigma_2 = \sigma_1\sigma_2^3\sigma_1^2\sigma_2\sigma_1^4\sigma_2 \simeq \sigma_2\sigma_1\sigma_2^3\sigma_1^2\sigma_2\sigma_1^4 = \\ = \sigma_1^3\sigma_2\sigma_1^3\sigma_2\sigma_1^4 \simeq \sigma_1^7\sigma_2\sigma_1^3\sigma_2.$$

– $\sum a_i = 8$: If $\sum b_i \geq 6$, then either we are already done by the case $\sum a_i = 7$ (if one of the b_i is equal to one) or it is symmetric

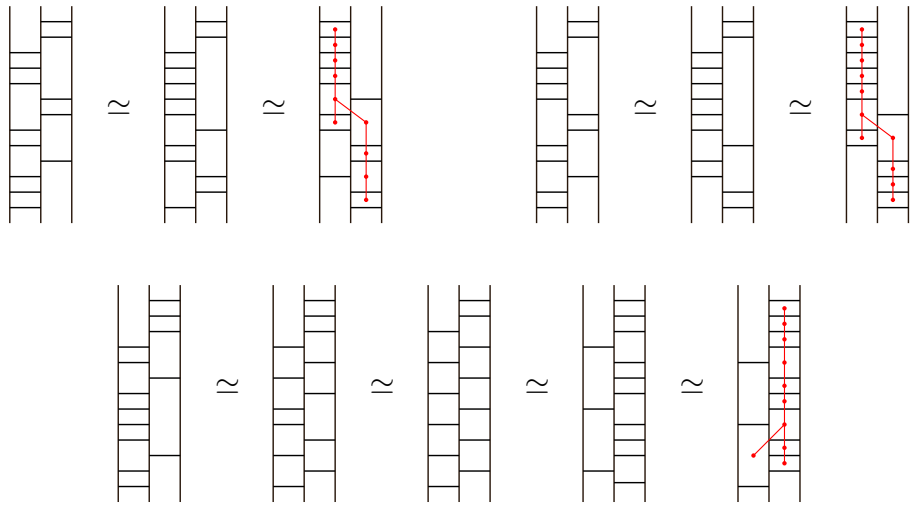

Figure 4.17: When $\sum a_i = 8$ and $\sum b_i = 5$

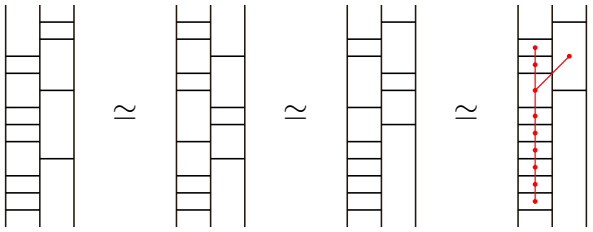

Figure 4.18: The braid $\sigma_1^3\sigma_2\sigma_1^3\sigma_2\sigma_1^2\sigma_2^2$

to the case $\sum b_i \geq 8$. If $\sum b_i = 5$ after applying some positive braid isotopy we can always find an appropriate subtree, with the lone exception of $\beta = \sigma_1^3\sigma_2\sigma_1^3\sigma_2^2\sigma_1^2\sigma_2^2$, for which we couldn't find any. In Figure 4.17 we see some of the cases, the remaining ones being braid isotopic to those. Finally, if $\sum b_i = 4$, we only get links of 3 components and genus 4 excepted for the braid $\beta = \sigma_1^3\sigma_2\sigma_1^3\sigma_2\sigma_1^2\sigma_2^2$ (and the symmetric $\beta = \sigma_1^2\sigma_2\sigma_1^3\sigma_2\sigma_1^3\sigma_2^2$), for which we see the tree in Figure 4.18.

– $\sum a_i = 9$: If $\sum b_i \geq 4$, it is enough to consider $\beta = \sigma_1^{a_1}\sigma_2\sigma_1^{a_2}\sigma_2\sigma_1^{a_3}\sigma_2^2$. By taking all the vertices of the linking graph excepted the lowermost of the right column, according to the value of a_3 we will get one of the tripod trees $T(1,2,6)$, $T(2,2,5)$ and $T(3,2,4)$, which all correspond to surfaces of genus 5. If $\sum b_i = 3$ and there is one even a_i, we only have to consider the three braids $\sigma_1^3\sigma_2\sigma_1^2\sigma_2\sigma_1^4\sigma_2$, $\sigma_1^3\sigma_2\sigma_1^4\sigma_2\sigma_1^2\sigma_2$ and $\sigma_1^5\sigma_2\sigma_1^2\sigma_2\sigma_1^2\sigma_2$. The first two are symmetric, and using that $\sigma_1^2\sigma_2\sigma_1^2$ commutes with σ_2 we see that the first

one is braid equivalent to the last, for which we furthermore have $\sigma_1^5\sigma_2\sigma_1^2\sigma_2\sigma_1^2\sigma_2 = \sigma_1^7\sigma_2\sigma_1^2\sigma_2^2$, whose intersection graph is a tree. Finally, if all the a_i are odd, we get a link of genus 4.

- $\sum a_i = 10$: The only case left is when $\sum b_i = 3$. If one of the a_i is odd we can suppose that a_3 is odd, in which case by taking all the bricks excepted the lowermost of the right column we will get a tripod tree $T(1,2,6)$ or $T(1,4,4)$, which both correspond to subsurfaces of genus 5. If all the a_i are even, up to elementary conjugation we only have the braids $\sigma_1^4\sigma_2\sigma_1^4\sigma_2\sigma_1^2\sigma_2$ and $\sigma_1^6\sigma_2\sigma_1^2\sigma_2\sigma_1^2\sigma_2$. Those are actually related by braid relations and elementary conjugations, and the very same argument used for $\sum a_i = 9$ and $\sum b_i = 3$ will yield the required tree.

- $m = 2$: For a braid $\beta = \sigma_1^{a_1}\sigma_2^{b_1}\sigma_1^{a_2}\sigma_2^{b_2}$ of genus at least 5 the intersection graph is always a tree with at least 10 crossings. Furthermore, by direct inspection we see that those trees will always contain E_6 unless they are of type D_n.

- $m = 1$: In this case we only get non-prime braids.

To sum up, the result holds for all braids excepted $\sigma_1^2\sigma_2^2\sigma_1^2\sigma_2^2\sigma_1^2\sigma_2^3$, its symmetric $\sigma_1^3\sigma_2^2\sigma_1^2\sigma_2^2\sigma_1^2\sigma_2^2$ (which gives the same link with opposite orientation) and $\sigma_1^3\sigma_2\sigma_1^3\sigma_2^2\sigma_1^2\sigma_2^2$ (which gives an invertible link). □

We will now consider braids with big positive braid index.

Proposition 4.5. *Let β be a prime positive braid on $N \geq 11$ strands and whose closure is a knot not of type A_n. Then, up to positive braid isotopy and excepted finitely many braids, its linking graph contains an induced subtree which is an E-arboreal spanning configuration on a subsurface of genus $g \geq 5$.*

The strategy to prove Proposition 4.5 is very simple: we will try to explicitly construct the required subtree and see that, each time our construction fails, either the closure is not a knot or we can reduce the number of strands. The finitely many exceptions come from Proposition 4.4 and Proposition 4.6, in case we can reduce our braid to one of the exceptions therein. We will therefore heavily rely on the following two lemmas.

Lemma 4.1. *Let $\beta \in B_N^+$ be a prime positive braid on $N \geq 3$ strands. If for some i the linking graph of the subword induced by all the generators σ_i and σ_{i+1} is a path, then there exists a positive braid $\beta' \in B_{N-1}^+$ such that $\hat{\beta} = \hat{\beta'}$ and $MG(\beta) = MG(\beta')$.*

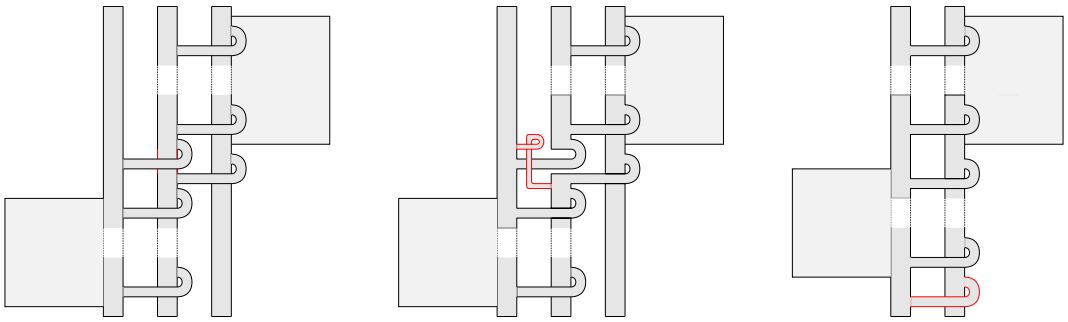

Figure 4.19: An isotopy that reduces the number of strands.

Proof. Up to elementary conjugation and symmetry, we can assume that the subword induced by σ_i and σ_{i+1} is of the form $\sigma_i^a\sigma_{i+1}\sigma_i\sigma_{i+1}^b$. Moreover, we can suppose that all the generators σ_j for $j < i$ appear before the last occurrence of σ_i and all the generators σ_j for $j > i+1$ appear after the first occurrence of σ_{i+1}. In Figure 4.19 we see an isotopy between the fibre surface Σ_β and the fibre surface $\Sigma_{\beta'}$ of a new braid β' with one strand less: the portion of the $(i+1)$-th disk lying between the first occurrence of σ_{i+1} and the last occurrence of σ_i (in red in the leftmost picture) is slid along the last σ_i, becoming a band between the i-th and $(i+1)$-th disk (central image); this band is then slid along the back of the two disks to be brought in the lowermost position. A direct computation now shows that $MG(\beta) = MG(\beta')$.

□

Lemma 4.2. *Let*

- $A = \{\sigma_1^a\sigma_2\sigma_3^b\sigma_2\sigma_1^c\sigma_2\sigma_3^d\sigma_2\sigma_1^e \mid a, b, c, d, e \in \mathbb{N}\}$,
- $B = \{\beta_1\sigma_2\sigma_3\beta_2\sigma_3\sigma_2\beta_3 \mid \beta_1, \beta_3 \in \langle\sigma_3, \sigma_4\rangle, \beta_2 \in \langle\sigma_1, \sigma_2\rangle\}$,
- $C = \{\beta_1\sigma_2\beta_2\sigma_2\sigma_3\beta_3\sigma_3\beta_4 \mid \beta_1, \beta_4 \in \langle\sigma_1, \sigma_4\rangle, \beta_2 \in \langle\sigma_3, \sigma_4\rangle, \beta_3 \in \langle\sigma_1\sigma_2\rangle\}$.

If $\beta \in A \cup B \cup C$, then the closure of β has at least two components.

Proof. In Figure 4.20 we see some schematic drawings of the brick diagrams of braids from the three families, in which one component of the closure is highlighted.

□

Notice that, even though for sake of simplicity we only stated Lemma 4.2 for braids with few strands, the result clearly also applies in case some columns of the brick diagram of a braid on more strands exactly look as in Figure 4.20 (or are symmetric to those).

To construct the trees required in Proposition 4.5, we will also need the following lemma from [59].

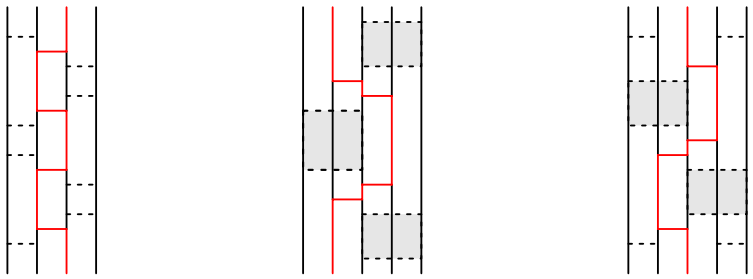

Figure 4.20: Some positive braids with disconnected closure.

Lemma 4.3 ([59], Lemma 7)**.** *Let β be a prime positive braid and v be a vertex of its linking graph. Then there is an induced path in the linking graph connecting v to any other column of the brick diagram.*

We will briefly recall the algorithm for constructing such a path, since this will be used in what follows. Let us say that we want to connect v to a column to its right. Start at v and move up or down its column until reaching the closest brick linked to the right (potentially, already v). Now, move to the right and repeat the procedure. If at the moment of moving to the right there are several possibilities, choose the brick which is the closest to a brick in the same column linked again to its right. It is easy to see that those choices prevent the creation of cycles, so that the result will be a path.

Proof of Proposition 4.5. Let β be a prime positive braid on $N \geq 11$ strands. By Lemma 4.1 we can assume that, for every pair of adjacent columns in the brick diagram, the linking graph restricted to those columns is not a path. Let us furthermore repeatedly apply all the possible braid relations of the form $\sigma_i\sigma_{i+1}\sigma_i \rightsquigarrow \sigma_{i+1}\sigma_i\sigma_{i+1}$, until no subword $\sigma_i\sigma_{i+1}\sigma_i$ is left in β. Our strategy goes as follows: we will start considering an induced path connecting the leftmost column to the rightmost, constructed with the previous algorithm, and try to add to it one single vertex, in order to get a tripod tree containing E_6. Since $b \geq 11$, the tripod tree will have at least 11 vertices and hence correspond to a subsurface of genus at least 5. So, let us fix one such path and look at the third column of the brick diagram. If we can add a brick of this column to the path and get an (induced) tripod tree we are done. There are two reasons why this might not be possible: either because there are no leftover bricks in the third column or because every available brick is linked to more than one brick of the path and adding it would generate a cycle. We will now analyse those cases in detail. By symmetry, we can assume that in the third column our path arrives from the left to a brick v_3, potentially moves *down* to a brick w_3 and then continues to the right.

If there are no leftover bricks in the third column, then by the construction

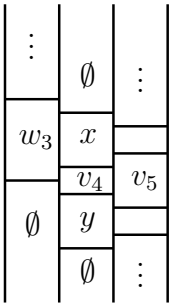

Figure 4.21: We only show the columns $3-5$. The path goes through w_3, v_4, either x or y and v_5.

rule of our paths we know that w_3 is the only brick of column 3 linked to the right. We can now apply elementary conjugations on the right-hand side of the diagram in order to have all the generators σ_i for $i \geq 4$ appear before the last occurrence of σ_3, and perform again all the possible braid moves $\sigma_i\sigma_{i+1}\sigma_i \rightsquigarrow \sigma_{i+1}\sigma_i\sigma_{i+1}$. Those transformations will not affect the first 3 columns and the part of the path therein. We now get that the sub-braid generated by σ_3 and σ_4 is $\sigma_4^a\sigma_3\sigma_4^b\sigma_3^c$, with $c \geq 1$ and $a, b \geq 2$ by Lemma 4.1. Let us denote by v_4 the only brick of column 4 linked to w_3, and let us attach a path connecting v_4 to the rightmost column.

If at least one of the bricks immediately above or below v_4 is not linked to the portion of the path in the fifth column (in particular, if v_4 is itself linked to the right), it can safely be added to get a tripod tree. We directly see that we are left with the case of Figure 4.21. Notice that, up to modifying the path in the fourth and fifth columns, we can always choose whether it passes by x or y. Now, if there is a brick x' above x, either it is not linked to the path in the fifth column, in what case we can directly connect it to x, or it is, in what case we can change our path to $w_3 \to v_4 \to x \to x' \to \{\textit{path in the fifth column}\}$ (thus avoiding v_5) and connect y to v_4. Similarly, we can assume that there is no brick below y.

Let us now consider the fifth column. Notice that there must be at least one brick immediately above and one immediately below v_5 that are not linked to the fourth column, otherwise we could apply one of the forbidden braid relations. By applying the same reasoning as before, we conclude that we can always obtain a tripod tree, unless there are no other bricks in the column. In the latter case, however, the closure of the braid is not a knot by Lemma 4.2 (compare with the leftmost diagram of Figure 4.20).

We can now suppose that there are some leftover bricks in the third column, but adding any of them to our path creates a cycle. The idea is analogous to what we just did: we will try to locally "reconstruct" the linking graph,

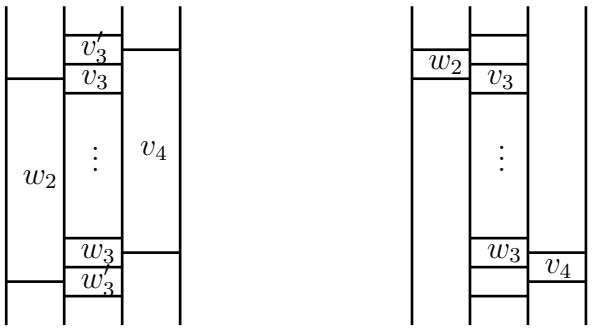

Figure 4.22: In both cases the path arrives from w_2, moves to v_3, then goes down to w_3 and finally to v_4.

successively exclude all the cases where we can find the required tripod and see that in the end we are left with one of the links from Lemma 4.2. However, the analysis gets much more delicate and will need lengthy case distinctions to cover the various ways adjacent columns can be connected. First of all, in the third column there could be bricks left both above and below the path, only above or only below.

I. If there are bricks above v_3 and below w_3, we will be in one of the two cases of Figure 4.22.

I.A. In the left-hand case of Figure 4.22, recalling that the path was constructed with the algorithm of Lemma 4.3, we know that either v_3 and w_3 are adjacent or they coincide. We will analyse those cases in great detail, since they serve as example of the kind of reasoning applied also to the rest of the proof.

I.A.a. If v_3 and w_3 are distinct and adjacent, again by the construction rule of our paths we know that w_3' is not linked to the right at all and v_3' is not linked to the path to the left. Now, if v_3' is linked to the path to the right above v_4, we could change our path to $w_2 \to v_3 \to v_3' \to \{\textit{path in the fourth column}\}$, thus avoiding v_4, and connect w_3 to v_3 to get a tripod. Otherwise, we can instead consider $w_2 \to w_3' \to w_3 \to v_4 \to \{\textit{path}\}$ and connect v_3' to v_4.

I.A.b. If $v_3 = w_3$, then we know that w_2 has to be linked to the first column, otherwise we could perform one of the forbidden braid relations. We will further distinguish according to how w_2 is linked to the first column.

I.A.b.1 Let us suppose first that w_2 is linked to a brick v_1 below it, as in the left-hand side of Figure 4.23 . Notice that the brick

denoted by w_2' needs to exist because of the condition on the possible braid relations. Hence, we can assume that in the first column there are at most two bricks and no bricks below v_1, and that the brick immediately below w_2' (if any) is linked with v_1, otherwise we could immediately find an appropriate tripod. If there is a linking between the second and third columns above v_3, we could modify our path by starting from v_1 and w_2, then moving upwards in the second column until we reach the first connection with the third column above v_3 and finally going down on the third column until the first connection to the original path in the fourth column (which occurs at the latest at v_3'). This will give us a path avoiding v_3. We can now safely connect w_3' to w_2 and get a tripod. If not, up to elementary conjugations on the first two columns, we can suppose that there are no bricks in the second column above v_3, as in the central picture of Figure 4.23. In this case, we can assume that above w_2 there is at most one brick. Now, if in the first column there are two bricks, again by elementary conjugation we are back to the case where there is a brick below v_1 and we are done. We are hence left with just one brick in the first column, as in the right-hand side of Figure 4.23. Notice that in this case the brick w_3' is forced to be linked to w_2', otherwise the closure of the braid is not a knot by the second case of Lemma 4.2. This in turn forces the existence of the brick denoted by b below w_3', otherwise we could apply a forbidden braid relation. If there is a brick a below w_2', we can consider $v_1 \to a \to w_2' \to w_3' \to v_3 \to \{path\}$ and connect b to w_3'. On the other hand, if there are no bricks below w_2' we see that either the closure of the braid is not a knot, if there is a brick above w_2 (third case of Lemma 4.2), or we can reduce the number of strands with Lemma 4.1.

I.A.b.2 We can now suppose that w_2 is linked to a brick v_1 above it, but is not linked with any brick of the first column below it, as in the left image of Figure 4.24. If there are at least two bricks below w_2 we immediately find a tripod. If there is exactly one brick below w_2, we can furthermore assume that v_1 is the only brick in the first column. Let us now consider how v_1 is connected with the second column. If it is only linked to w_2, by applying an elementary conjugation we are back to the previous case where v_1 was below w_2. Notice

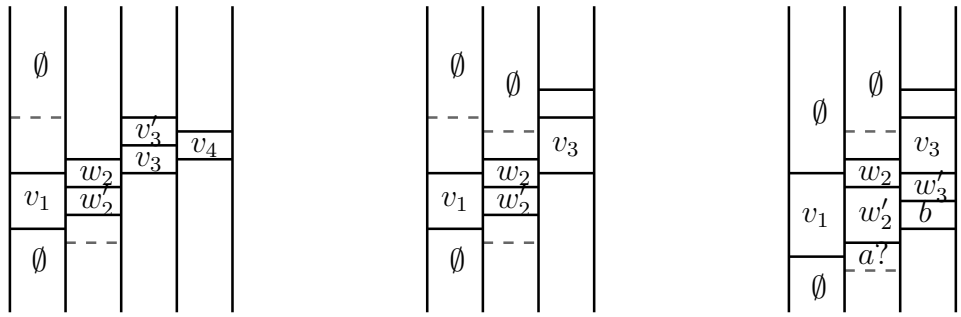

Figure 4.23: The dashed lines show where the following brick (if existing) would be. In the third column, there is still a brick w_3' as in Figure 4.22, which is linked to w_2 and may or may not be linked to w_2'.

that the existence of a brick below w_2 ensures that the condition about the possible braid relations is still satisfied after the conjugation. If v_1 is linked to another brick of the second column above w_2, called a, and a is in the region denoted by $\mathcal{X}$ as in the central image of Figure 4.24, we immediately see that either we find a suitable tripod or the closure is not a knot, depending on how many bricks there are in the second column between w_2 and a (there is at least one by the condition on braid relations; if it is unique, we fall in the second case of Lemma 4.2). Finally, if a is not in the region denoted by $\mathcal{X}$, as in the right image of Figure 4.24, we know that there is a brick between a and w_2 linked to v_3 (potentially, this could be a). We can now consider $v_1 \to a \to \{\textit{second column}\} \to v_3 \to \{\textit{path}\}$ and connect w_3' to v_3. The only case left now is when there are no bricks below w_2. Again, if v_1 is linked to another brick of the second column above w_2 the exact same argument applies. If v_1 is linked only to w_2, this time we cannot simply apply an elementary conjugation to reduce it to a previously treated case. However, if there are no bricks above v_1 (resp. below v_1) we could apply Lemma 4.1, whilst if there are bricks in the first column both above and below v_1 it is immediate to conclude that either we find a tripod or the closure is not a knot, as in the first case of Lemma 4.2.

I.B. In the right-hand case of Figure 4.22, we know that w_2 needs to be linked to a brick v_1 in the first column. Again, we will separately consider whether v_1 is above or below w_2.

I.B.a. Suppose first that w_2 is linked to a brick v_1 above it. By ex-

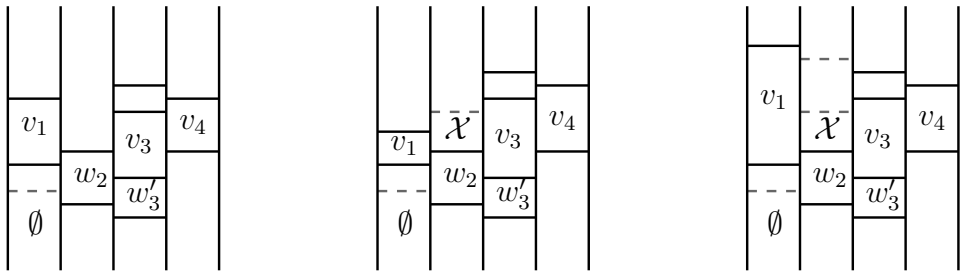

Figure 4.24: Below v_1 there can be bricks only until the dashed line. In the second column, there is at least one brick above w_2 but below v_1.

cluding all the cases where one can immediately find a tripod, we are left with at most two bricks in the first column and we can reduce the study to one of the cases in the left-hand side of Figure 4.25. If there are two bricks in the first column, we either have a brick above v_2, in which case we can find a tripod by simply starting our path from v_1' and adding two bricks above w_2, or we can apply an elementary conjugation to the first column to get a brick below v_1', which again immediately gives a tripod. If in the first column there is just one brick, we know that v_2 needs to be linked to the third column, otherwise the closure is not a knot by Lemma 4.2 (second case). After removing all the trivial cases, we are left with the diagram on the right-hand side of Figure 4.25. Notice that now by Lemma 4.1 there needs to be at least one brick below w_2. If none of the bricks below w_2 are linked to v_3, we see that according to the number of those bricks we either get a tripod or the closure is not a knot by (a symmetry of) the third case in Lemma 4.2. Hence we can suppose that there is a brick w_2' below w_2 linked to v_3. If w_2' is connected to the original path in the third column below v_3, we can instead consider $v_1 \to w_2 \to \cdots \to w_2' \to \{path\}$ and get a tripod by connecting to w_2 the bricks v_3' and v_3''. If not, we can simply take our original path starting from v_3 and connect to it w_2', v_3' and v_3''.

I.B.b. Suppose now that w_2 is only linked to a brick v_1 below it. We immediately see that there can be at most one brick above w_2, and if this brick exists then v_1 is the only brick of the first column. After excluding the trivial cases we are left with the diagrams of Figure 4.26. First, if w_2' is linked to the path in the third column below v_3, we can take $v_1 \to w_2 \to \cdots \to w_2' \to$ *path* and add to it a brick in the third column (which will be

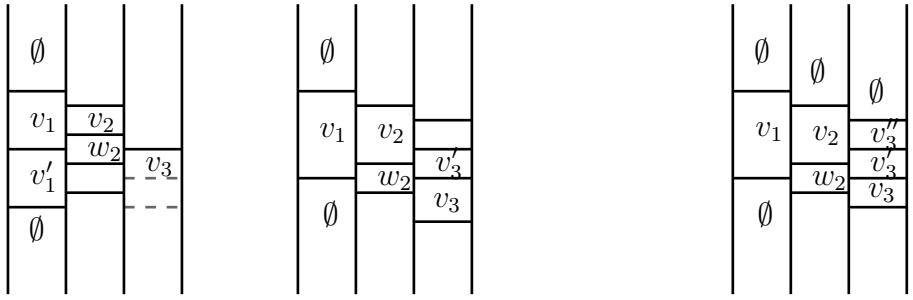

Figure 4.25: The brick v_2 exists by braid relation. In the leftmost image, the dashed lines show where the brick v_3 could end.

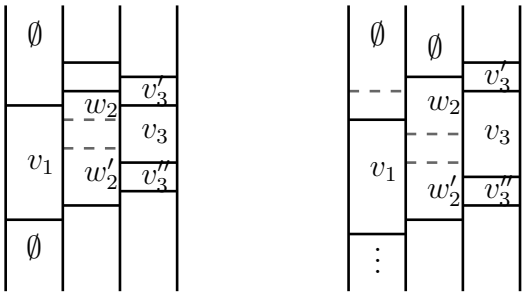

Figure 4.26: Between w_2 and w_2' there can be at most one brick. In the leftmost diagram, the brick above w_2 is not necessarily linked with v_3'.

at most v_3''). Otherwise, if there is a brick w_2'' below w_2', we can simply take our original path from v_3 and add to it v_3', w_2' and w_2''. Finally, let's assume that there are no bricks below w_2'. If there is a brick above w_2 we can apply an elementary conjugation to the first column and get back to the previous case. If not, Lemma 4.1 forces the existence of bricks above and below v_1, in which case either we get a tripod or the closure is not a knot, as in the first case of Lemma 4.2.

II. Let us now consider the case where there is at least one free brick v_3' above v_3, but none below w_3. First of all, if after w_3 our path moves to a brick v_4 of the fourth column which is below it, we are basically in the same situation as Item I.B., and the precise same arguments apply. We can hence suppose that the path moves upwards in the fourth column. We will now treat different cases according to how v_3' is linked to the neighbouring columns.

II.A. If v_3' is not linked to the right, we know that it needs to be linked to a brick w_2 in the second column, which in turns needs to be linked

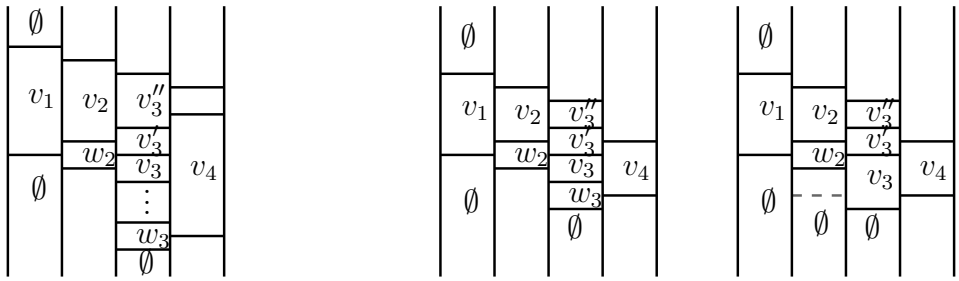

Figure 4.27: Diagrams for Item II.A. and Item II.B..

to a brick v_1 in the first column. Let us suppose first that v_1 is above w_2, then by Item I.B.a., we are left with only one brick in the first column, as in the central image of Figure 4.25. Furthermore, if the brick immediately above v_3' is not linked to its right, all the arguments from Item I.B. still apply. We are hence left with the leftmost diagram of Figure 4.27. Now if v_3'' is not linked to the path above v_4 it can directly be added as additional vertex, otherwise we can instead consider the path $v_1 \to w_2 \to v_3' \to v_3'' \to \{path\}$ and add a brick to this new path in the fourth column. Finally, if v_1 is below w_2, we conclude directly as in Item I.B.b..

II.B. If v_3' is linked to the right (to v_4) and to the left (to a brick w_2), by the construction rules of the path we know that either v_3 and and w_3 are adjacent or they coincide, and by the assumption on the braid relations w_2 is linked to a brick v_1 in the first column.

II.B.a. If v_1 is above w_2, after repeating the arguments of Item I.B. we are left with the two diagrams at the right-hand side of Figure 4.27.

II.B.a.1 Let us first consider the case where v_3 and w_3 are distinct and adjacent. If v_3' is not linked to the path above v_4, we can simply consider $v_1 \to w_2 \to v_3' \to v_4 \to \{path\}$ and add v_3'' (notice that this would also work if v_3 and w_3 did coincide). If v_3' is linked to the path in the fourth column above v_4, take instead $v_2 \to v_3' \to \{path\}$ and add v_3 and w_3.

II.B.a.2 Suppose now that v_3 and w_3 coincide. In this case, notice that no brick below w_2 can be linked to v_3 (otherwise we could perform a forbidden braid relation), and that therefore if there are at least two bricks below w_2 we immediately get a tripod. It follows that there need to be a brick v_2' above v_2, otherwise either we can apply Lemma 4.1 or

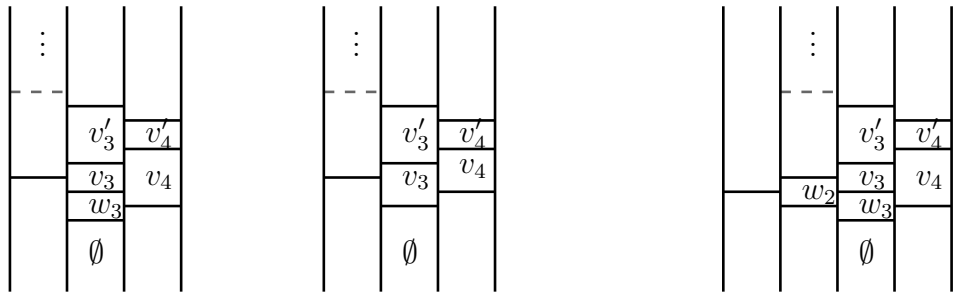

Figure 4.28: Diagrams for Item II.C.; v_3 is linked to the second column, but v_3' is not. On the right, we know that w_2 needs to be linked to some brick v_1 in the first column.

the closure is not a knot, as in the third case of Lemma 4.2. Now, if v_3' is not linked to the path in the fourth column above v_4, we can find the same tripod as in the previous case. If v_3' is linked to the path above v_4, we can instead consider $v_2' \to v_2 \to v_3' \to \{path\}$ and add v_3.

II.B.b. Finally, if v_1 is below w_2, we are left with one of the diagrams of Figure 4.26 (where the brick v_3'' is now w_3). The case where v_3 and w_3 coincide is excluded by the condition on the braid relations. Furthermore, by what was done in Item I.B.b., we know that we can assume the existence of a brick w_2'' below w_2'. Hence, if v_3' is not connected to the path above v_4 we can take $v_1 \to w_2 \to v_3' \to v_4 \to \{path\}$ and add w_3, if v_3' is connected to the path above v_4 we can instead take $w_2'' \to w_2' \to v_3 \to v_3' \to \{path\}$ and add w_3.

II.C. If v_3' is not linked to the left, either v_3 and w_3 are adjacent or they coincide, as in the left hand side of Figure 4.28. In both cases, if v_3' is connected to the path above v_4, we can simply let our path pass by v_3' instead of w_3 (thus skipping v_4) and add a brick in the fourth column (which will be at most v_4').

Suppose now that v_3' is not connected to the path above v_4 and v_3,w_3 are distinct. If w_3 is linked to the left we are in the situation at the right-hand side of Figure 4.28 and we directly find a tripod by considering $v_1 \to w_2 \to w_3 \to v_4 \to \{path\}$ and adding v_3'. If not, then we are in a situation analogous to Figure 4.21 and the same arguments apply.

We are left with the case where v_3 and w_3 coincide and v_3' is not connected to the path above v_4. We will now consider how the third and second column are connected.

II.C.a. Let us suppose first that there is a brick v_2 in the second column below v_3. We know that v_2 needs to be linked to a brick in the first column.

II.C.a.1 If there is a brick v_1 in the first column above v_2, we are in one of the situations in the left of Figure 4.29. In the first one, we directly see that either we find a tripod (if there is at least another brick in the first column) or the closure is not a knot by Lemma 4.2. In the second one, using Lemma 4.1 we furthermore know that there must be a brick in the second column above v_1. By excluding the direct cases, we end up with the diagram on the right-hand side of Figure 4.29. Notice that we can assume that there is no brick below v_2, because otherwise by elementary conjugations we would get two bricks above v_2'' and would find a tripod by taking $\{\textit{second column}\} \to \cdots \to v_2' \to v_3 \to \{\textit{path}\}$ and adding v_1. With similar arguments we can conclude there are no bricks in the second column above v_2'' and v_1 is the only brick of the first column. We now see that there needs to be a brick in the third column above v_2'', otherwise the closure is not a knot by Lemma 4.2. If there are at least two bricks of the third column above v_2', we get a tripod by taking $\{\textit{third column}\} \to \cdots \to v_3' \to v_4 \to \{\textit{path}\}$ and adding v_2' and v_2. Otherwise, we can consider $v_1 \to v_2'' \to \cdots \to v_2' \to v_3 \to \{\textit{path}\}$ and add the other brick in the third column linked to v_2' (which now we know will not link to any other brick of the second column.)

II.C.a.2 If there are no bricks in the first column above v_2, but v_2 is linked to a brick v_1 below it, we can directly conclude that, depending on the number of bricks in the first column, either the closure is not a knot by Lemma 4.2 or we find an appropriate tripod.

II.C.b. Suppose now that there are no bricks in the second column below v_3, which is therefore only linked to a brick v_2 above it.

II.C.b.1 If in the second column there are bricks both above and below v_2, noticing that if there are at least four bricks in the second column we are done, we are only left with the cases of Figure 4.30. For the leftmost diagram, if there is only one brick in the first column the result is not a knot by the second case of Lemma 4.2, otherwise up to elementary conjugation we get a tripod. In the two central diagrams we directly find a tripod. In the rightmost diagram, if v_2'

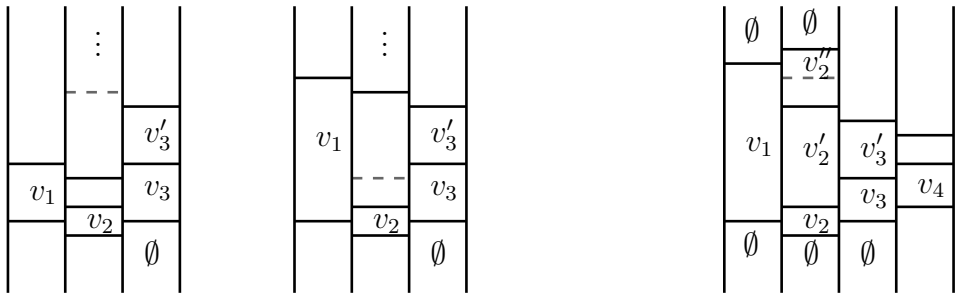

Figure 4.29: More diagrams for Item II.C.a.1, when v_3 and w_3 coincide and there is a brick v_2 below v_3.

is not linked to the third column the closure is not a knot by the first case of Lemma 4.2, otherwise we directly get a tripod (using that v_3' is not linked to the path above v_4, hence all the bricks of the third column above it also are not).

II.C.b.2 If in the second column there are only bricks below v_2, by minimality of the number of strands there must be a brick v_3'' in the third column above v_2. If v_2 is not linked to the first column or if there are at least two bricks in the first column we can simply take our original path and add to it v_3'' (once more, we use that v_3'' is not connected to the path in the fourth column, since by assumption v_3' is not connected to the path above v_4). If there is only one brick in the first column and this brick is linked to v_2, according to the number of bricks of the second column below v_2 we will either get a tripod or a link with at least two components by Lemma 4.2.

II.C.b.3 Finally, if in the second column there are only bricks above v_2, let us consider v_2' the first brick of the second column linked to a brick v_1 of the first column (starting from v_2 upwards, potentially $v_2' = v_2$). If there is still a brick v_2'' above it, up to elementary conjugation on the first column we can assume that v_1 is above v_2'. We now directly see that we are left with only one brick in the first column and that according to whether v_2'' is linked to its right, we either get a link with more than one component by Lemma 4.2 or a tripod, as in the left of Figure 4.31. If there are no more bricks above v_2', we are left with the diagram at the right-hand side of Figure 4.31. By Lemma 4.1, we know that

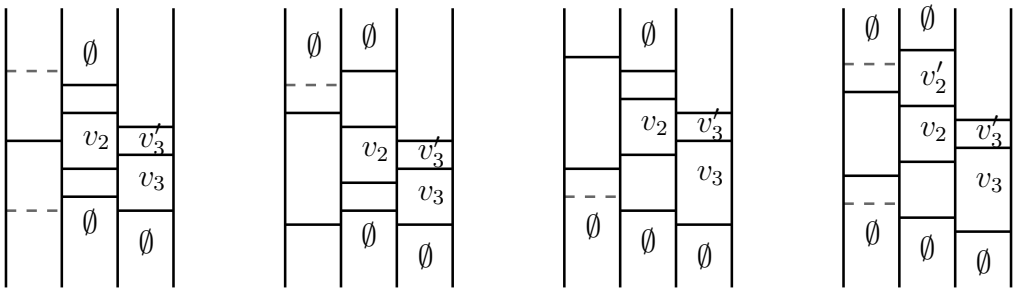

Figure 4.30: More diagrams for Item II.C.b.1, when v_3 and w_3 coincide and there is no brick in the second column below v_3.

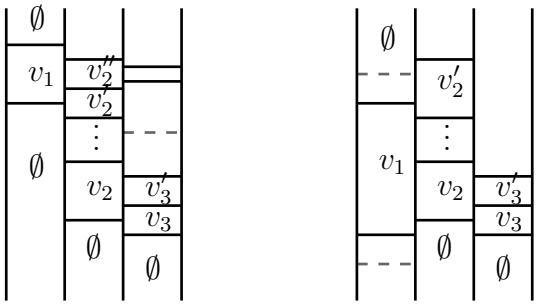

Figure 4.31: Diagrams for Item II.C.b.3: in the left, the case when there is a brick above v_2' which is linked to the right. In the right, when there are no bricks above v_2'.

there must be bricks above and below v_1 and we conclude with an usual argument.

III. We finally have to treat the case where there is a free brick w_3' below w_3, but no brick above v_3. Once more, we distinguish according to how w_3' is connected to the path.

III.A. Let us first suppose that w_3' is linked to a brick w_2 of the original path in the second column (which, by construction, will also be linked to v_3). Then either v_3 and w_3 are adjacent or they coincide, as in the left of Figure 4.32.

III.A.a. If v_3 and w_3 are distinct, by construction we furthermore know that they are not linked to any brick of the fourth column. If v_3 is linked to a brick v_2 of the second column above w_2, we know that v_2 need to be linked to the first column. In this case, we could simply connect the first column to v_3 via v_2 (thus skipping w_2), continue with our original path and add to it w_3' to get a tripod. Similarly, suppose that w_3' is linked to some

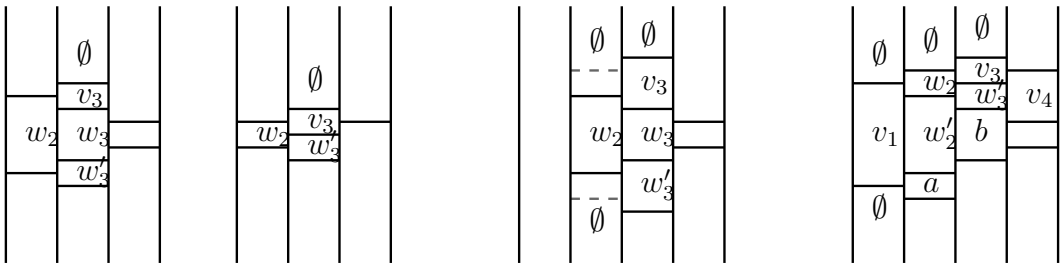

Figure 4.32: In the left, the two main possibilities for Item III.A.. In the centre, the diagram left after treating all the direct cases, for v_3 and w_3 distinct. In the right, the last diagram for $v_3 = w_3$.

brick in the second column below w_2. If there is a connection between the first and second columns below w_2, the previous argument still apply. Otherwise, all the bricks in the second column below w_2 are "free" and can be added to our path. If there are at least two bricks below w_2 we are done; if there is only one, according to the number of bricks in the first column we see that we either find a tripod or the closure is not a knot by Lemma 4.2. We are therefore only left with the diagram in the centre of Figure 4.32. If in the second column there are bricks both above and below w_2, we are basically in the situation of Figure 4.30 (with the appropriate changes in the third column) and the same arguments apply. If there are only bricks above w_2, we end up with diagrams as the ones in Figure 4.31 and we conclude similarly. The case where there are only bricks below w_2 is symmetric.

III.A.b. If v_3 and w_3 coincide, we know that w_2 needs to be linked to a brick v_1 in the first column.

III.A.b.1 If v_1 is above w_2, after removing all the cases where one can directly find a tripod, we are left with diagrams as in the left-hand side of Figure 4.25, and the same arguments apply (remembering that now there are no bricks in the third column above v_3).

III.A.b.2 If w_2 is not linked to any brick in the first column from above, we can reduce to a diagram as in the right-hand side of Figure 4.23. Now, if b is not linked to the path in the fourth column, the same argument as in the corresponding part of Item I.A.b.1 works. If b is linked to the path in the fourth column from below, one can consider $v_1 \to a \to w_2' \to w_3' \to b \to \{path\}$ and add v_3 to get a

tripod. Similarly if w_3' is linked to the path in the fourth column from below. Finally, if b is linked to the path in the fourth column but w_3' is not, we are in the case drawn in the right-hand side of Figure 4.32. If in the third column there are no bricks below a, one can simply perform an elementary conjugation on the second column to get a brick v_2 above w_2, take the original path starting from v_3 and add to it $w_3' \to w_2'$ and v_2 to obtain a tripod. Finally, if in the third column there is a brick below a, in particular w_2' is linked to a brick b' of the third column below b. One can hence take $v_1 \to a \to w_2' \to b' \to \cdots \to b \to v_4 \to \{path\}$ (or potentially skipping w_2' if b' is also linked to a) and connect v_3 to v_4.

III.B. We now suppose that w_3' is not linked to the original path in the second column (and therefore has to be linked to the path in the fourth column). By construction, we know that v_3 is linked to some brick in the second column.

III.B.a. Assume first that v_3 is linked to a brick w_2 above it. We know that w_2 will be linked to a brick of the first column. If it is linked to a brick above it, we conclude as in Item I.B.a., so we can assume that w_2 is only linked to a brick v_1 below it. By Item I.B.b., we are only left with the diagrams of Figure 4.26 (in this case, the brick denoted by v_3' does not exist), and we furthermore can assume that the brick w_2' is not linked to the original path in the third column below v_3 and that there is at least one brick in the second column below v_1. After removing all the cases where one can directly find a tripod, we are left with the leftmost diagram of Figure 4.33. Furthermore, if there are at least two bricks in the first column, up to elementary conjugation we can assume the existence of a brick below w_2'' and can now obtain a tripod by taking $w_2'' \to \cdots \to w_2' \to v_3 \to \{path\}$ and connecting to w_2'' a brick below it and v_1 together with another brick of the first column. We can hence reduce to the central diagram of Figure 4.33. But now we observe that there needs to be a brick in the third column below w_2'', otherwise the closure is not a knot by Lemma 4.2. In particular, w_2' is linked to a brick w_3'' of the third column below v_3. If v_3 is not linked to the fourth column we can simply take $v_1 \to w_2'' \to \cdots \to w_2' \to w_3'' \to \cdots \to \{path\ in\ the\ fourth\ column\}$ and connect v_3 to v_2'. If v_3 is linked to the fourth column (so in particular $v_3 = w_3$), we have the rightmost diagram of Figure 4.33.

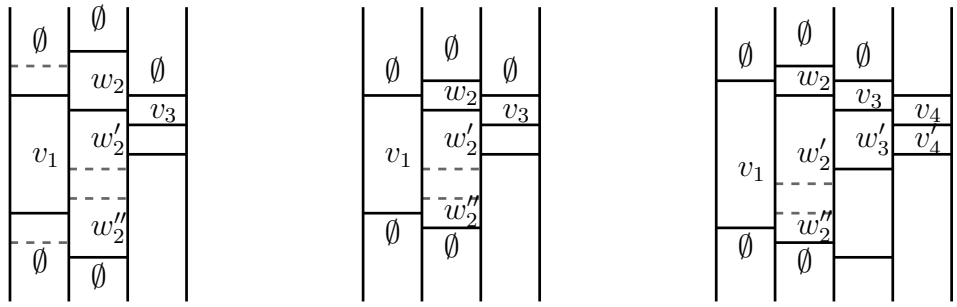

Figure 4.33: The last possibilities for Item III.B.a..

If w_3' is linked to the path in the fourth column under v_4, we can simply consider $v_1 \to w_2 \to v_3 \to w_3' \to \{path\}$ and add v_4'. Finally, if w_3' is not linked to the path in the fourth column below v_4, then all the bricks in the third column under w_3' also are not, and can hence be freely used. If there is still at least one brick in the third column under w_3'', we can take $w_2 \to w_2' \to w_3'' \to \cdots \to w_3' \to v_4 \to \{path\}$ and add a brick below w_3'' to get a tripod. If w_3'' is the last brick of the third column, in particular it is not linked to any of the bricks below w_2', so we can take $v_1 \to w_2'' \to \cdots \to w_2' \to v_3 \to \{path\}$ and connect w_3'' to w_2'.

III.B.b. We can now suppose that v_3 is only linked to a brick w_2 of the second column below it. In particular, our original path was passing by w_2, which is therefore not linked to w_3'. If v_3 and w_3 are distinct, we end up with a diagram similar to Figure 4.21 and the exact same arguments apply. If v_3 and w_3 coincide, we are in a situation perfectly symmetric to Item II.C.b., in particular as in Figure 4.30 and Figure 4.31, and again the same arguments apply.

□

We still have to consider the braids of intermediate positive braid index. One could probably study those by hands, in a similar way to Proposition 4.4 and Proposition 4.5, but the computations would quickly get too complicated. Instead, we will treat them by directly applying Proposition 4.4, at the cost of loosing some low genus cases.

Proposition 4.6. *Let β be a prime positive braid on $4 \leq N \leq 10$ strands whose closure is a knot not of type A_n. Suppose that β has genus $g(\beta) > 4(N-1)$.*

Then there exists a family of curves on Σ_β that is an E-arboreal spanning configuration on a subsurface of genus at least 5.

The curves appearing in Proposition 4.6 will not necessarily be vertices of the intersection graph, but we might need to do some "change of basis", i.e. modify some of the curves by applying appropriate Dehn twists. This will change the intersection pattern of the curves in question, but not the subsurface they span nor the subgroup that the corresponding Dehn twists generate in $\mathrm{MCG}(\Sigma_\beta)$.

Proof. Let β be such a positive braid. Since $g(\beta) > 4(N-1)$, there exists $1 \leq i \leq N-2$ such that the subword induced by all the generators σ_i and σ_{i+1} has first Betti number at least 12, when seen as a 3-braid. Let us denote this subword by $\beta_{i,i+1}$. By Proposition 4.4, either $\beta_{i,i+1}$ is positively isotopic to a 3-braid $\beta'_{i,i+1}$ containing the required spanning configuration, or it is of type A_n or D_n (the other finitely many exceptions have first Betti number 11).

In the first case, the required positive braid isotopy might not be realizable when $\beta_{i,i+1}$ is seen as a subword of β. However, since at the level of curves the effect of braid relations and elementary conjugations is obtained by Dehn twists, we can still find a family of curves in $\Sigma_{\beta_{i,i+1}} \subset \Sigma_\beta$ whose intersection pattern is equal to the linking graph of $\beta'_{i,i+1}$, and the result follows.

If $\beta_{i,i+1}$ is of type A_n, since there are only three strands one can directly verify that up to elementary conjugation its linking graph is a path. We can therefore apply Lemma 4.1 to β and reduce it to a braid with less strands.

If $\beta_{i,i+1}$ is of type D_n, up to elementary conjugation and symmetry it is of one of three forms: $\sigma_i^{n-3}\sigma_{i+1}^2\sigma_i\sigma_{i+1}^2$, $\sigma_i^{n-2}\sigma_{i+1}\sigma_i^2\sigma_{i+1}$ or $\sigma_i^a\sigma_{i+1}\sigma_i\sigma_{i+1}^b\sigma_i\sigma_{i+1}$ with, $a+b=n-2$. This follows from a direct computation, or can be seen by applying the classification of checkerboard graphs of type D_n contained in Lucas Vilanova's PhD thesis [76]. In all the cases one can see that, if the closure is connected, we can always add a brick in a neighbouring column and find the required subtree. We will do it for $\beta_{i,i+1} = \sigma_i^{n-3}\sigma_{i+1}^2\sigma_i\sigma_{i+1}^2$, the others are analogous. In this case, we know that $i < N-2$, otherwise the closure is not a knot by Lemma 4.2. Since β is prime, its intersection graph is connected, so at least one of the three bricks in the $i+1$-th column needs to be linked to its right. After removing the cases where one directly finds an appropriate subtree, we are left with one of the three cases of Figure 4.34. The first one is excluded since the closure is not a knot; in the second one we can find a subtree after braid relation, as shown in the Figure; for the third one, up to elementary conjugation we can suppose that there are no generators σ_{i+2} above the last occurrence of σ_{i+1}. Now we see that if there are at least two bricks in the $i+2$-th column we are done, otherwise either the closure is not a knot (if $i+2 = N-1$) or we can still add one brick further to the right and again find the required subtree.

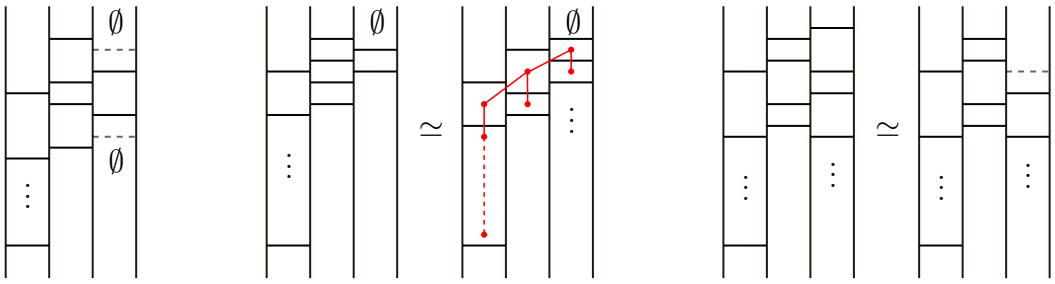

Figure 4.34: The columns $i, i+1$ and $i+2$ of a braid β such that $\beta_{i,i+1} = \sigma_i^{n-3}\sigma_{i+1}^2\sigma_i\sigma_{i+1}^2$.

□

Everything is now ready to prove our main Theorem.

Proof of Theorem 4.2. Let β be a prime positive braid not of type A_n and whose closure is a knot. We want to prove that $MG(\beta) = \mathrm{MCG}(\Sigma_\beta, \phi_\beta)$ by using Proposition 2.2. Let $V = \{\gamma_1, \cdots, \gamma_{2g}\}$ be the family of standard curves on Σ_β corresponding to the vertices of the linking graph of β. In Proposition 4.4, Proposition 4.5 and Proposition 4.6 we have constructed the starting E-arboreal spanning configuration of genus $h \geq 5$ for all but finitely many such prime positive braids. In general, this is obtained by taking a subfamily of curves $V_0' \subset V$ and potentially modifying some of them by applying Dehn twists around other curves of V_0', obtaining a family V_0 of curves in Σ_β. In particular, the subsurface spanned by V_0 is the same as the subsurface spanned by V_0'. It is now clear that the remaining curves of $V \setminus V_0'$ can be attached in an order that respects the definition of h-assemblage, so that

$$\mathrm{MCG}(\Sigma_\beta, \phi_\beta) = \langle T_c \mid c \in V_0 \cup (V \setminus V_0') \rangle = \langle T_c \mid c \in V \rangle = MG(\beta).$$

□

Remark 4.4. In fact, our proof of Theorem 4.2 also applies to many links. Indeed, the requirement of the closure of β being a knot was uniquely used to exclude links as in Lemma 4.2: all these have one unknotted component whose total linking number with the other components is precisely 2. In particular, the proof works without problems for links whose components are all knotted or whose pairwise linking numbers are all big enough.

Interestingly, this is essentially always the case in the special class of links of singularities, if we exclude the special families A_n and D_n. In what follows, the reader can refer to [24] for the background material on plane curve singularities. If f_1 and f_2 are irreducible singularities with associated knots K_1 and K_2, then the link of $f = f_1 f_2$ is $L(f) = K_1 \cup K_2$, and the linking number $lk(K_1, K_2)$

equals the intersection multiplicity of the two branches. It follows that in the link of a singularity all linking numbers are strictly positive. Now, let f be a singularity whose link has a component which is unknotted and has total linking number with the other components equal to 2, as in Lemma 4.2. By the previous discussion, f has at most three branches. Suppose first that $f = f_1 f_2$ has only two branches, and $L(f) = K_1 \cup K_2$. Since one component is the unknot and the multiplicity of a singularity equals the braid index of the associated link by [78], we can assume that $f_2 = y + x\tilde{f}(x, y)$. Let now m be the multiplicity and $y = g(x^{\frac{1}{m}})$ the Puiseux series of f_1, we obtain $2 = lk(K_1, K_2) = \mathrm{ord}(g(t) + t^m \tilde{f}(t^m, g(t))) \geq m$, from which we conclude that K_1 has braid index at most 2. Finally, since the link of a reducible singularity is determined by the components and the pairwise linking numbers, and all the possible pairs of a positive 2-braid and an unknot with linking number 2 are realized by singularities of type A_n or D_n, it follows that f belongs to one of those two families. Similarly, if f has three branches one can conclude that all the components of $L(f)$ are unknotted, so that the link is determined by the triple of linking numbers (where two of the linking numbers are now equal to 1). Since all such triples are realized by singularities of type D_n, f must belong to this family. Therefore, up to finitely many low genus exceptions, we completely recover the main result of [70], saying that the geometric monodromy group of a singularity not of type A_n and D_n is a framed mapping class group.

Remark 4.5. In contrast to the case of singularities, it does not seem possible to extend the proof to all positive braid links. Even excluding the two exceptional families A_n and D_n, there are other infinite families, both with bounded and unbounded braid index, that most likely do not contain an E_6. For example, we could not find such subtrees for the braids

$$\beta_n = \sigma_1 \sigma_2^2 \sigma_1 \sigma_2^{n-4} \sigma_3 \sigma_2^2 \sigma_3 \in B_4^+,$$

whose linking graph is the extended Dynkin diagram $\tilde{D}_n$, nor for

$$\beta_N = (\sigma_1 \cdots \sigma_N \sigma_N \cdots \sigma_1)^2 \in B_{N+1}^+.$$

We do not know whether the corresponding monodromy groups are equal to the whole framed mapping class group.

Chapter 5

Framed mapping class groups and Hopf plumbings

In this short chapter we will see how to extend the methods of Chapter 4 to the setting of surfaces constructed by Hopf plumbings and discuss some applications of the theory of framed mapping class groups to the study of groups generated by finitely many Dehn twists.

Let us first recall some known facts and fix our terminology. The starting datum is a family of simple closed curves $\mathcal{C} = \{c_1, \cdots, c_l\}$ on a surface Σ, taken to be pairwise in minimal position. To such a family one can associate a graph encoding the combinatorial properties of the curves, called the *intersection graph*: each vertex corresponds to a curve of $\mathcal{C}$, and there is an edge between two given vertices for each intersection point between the corresponding curves. In fact, it is sometimes convenient to also record the cyclic order of the edges around each vertex, i.e. the order of the intersection points along each curve; as this is equivalent to choosing an embedding of the graph into a surface (such embedded graphs are sometimes called *maps*, see [56]), we will refer to the intersection graph together with a cyclic order of the edges around each vertex as the *embedded intersection graph*. The basic question is now what group the Dehn twists around the curves of $\mathcal{C}$ generate, and to what extent it depends on the combinatorics of the curves and on the ambient surface Σ.

The case of two curves is completely solved: if the curves are disjoint, they generate $\mathbb{Z}^2$; if they intersect exactly once, they generate either $\mathrm{SL}_2(\mathbb{Z})$ (if on the torus) or the braid group B_3 (on any other surface); if they intersect at least twice, they generate the free group F_2, see Chapter 3 of [36]. In particular, we see that, apart from one low-genus exception, the answer uniquely depends on the intersection number. In general, however, the question is completely open, even in the case of three curves. Moreover, it is known that the answer strongly depends on the ambient surface. For instance, in [50] Humphries

proved that if each pair of curves of $\mathcal{C} = \{c_1, \cdots, c_l\}$ intersects at least twice and no component of $\Sigma \setminus (\bigcup c_i)$ is a disk, then $\langle T_c \mid c \in \mathcal{C} \rangle$ is free of rank l, independently of the intersection graph. However, if one allows disks in the complement, it is not difficult to construct a family of curves with high pairwise intersection numbers but which do not generate a free group; in fact, in striking contrast to the result about groups generated by two Dehn twists, the famous lantern relation induces such an example that requires only three curves with pairwise intersection numbers all equal to two.

A possible strategy to understand those groups is to first look at the curves in $N(\mathcal{C}) \subset \Sigma$, a small regular neighbourhood of $\bigcup c_i$, i.e. understand $\langle T_c \mid c \in \mathcal{C} \rangle$ as a subgroup of $\mathrm{MCG}(N(\mathcal{C}))$, then study the image under the homomorphism $\mathrm{MCG}(N(\mathcal{C})) \to \mathrm{MCG}(\Sigma)$ induced by the inclusion $N(\mathcal{C}) \hookrightarrow \Sigma$; see for instance [73] for a detailed study in the case of curves with intersection graph a cycle. One could optimistically hope that, when working in the neighbourhood $N(\mathcal{C})$, the isomorphism type of $\langle T_c \mid c \in \mathcal{C} \rangle$ should essentially be controlled by the combinatorics of $\mathcal{C}$ (as suggested by the results of [50] and [73]), while the original ambient surface Σ should only influence the additional relations introduced when capping off boundary components of $N(\mathcal{C})$. However, some care is needed, as the homeomorphism type of the neighbourhood $N(\mathcal{C})$ is in general not determined by the (embedded) intersection graph. In the special case where the intersection graph is a tree, $N(\mathcal{C})$ is uniquely determined by the graph, and the embedded intersection graph entirely determines the group $\langle T_c \mid c \in \mathcal{C} \rangle$ in $\mathrm{MCG}(N(\mathcal{C}))$. Nevertheless, notice that if we take two different plane embeddings of the same abstract tree and realize them as embedded intersection graphs of two families of curves $\mathcal{C}$ and $\mathcal{C}'$, while $N(\mathcal{C})$ and $N(\mathcal{C}')$ are homeomorphic, there is in general no homeomorphism mapping $\mathcal{C}$ to $\mathcal{C}'$, so that a priori we cannot conclude that the corresponding groups are isomorphic.

As we have already seen in Chapter 4, thanks to Proposition 2.2 the theory of framed mapping class groups can sometimes be useful to understand groups generated by finitely many Dehn twists. We will now discuss some additional easy applications, focusing in particular on curves with arboreal intersection graph. As a corollary, we show that if a family of curves $\mathcal{C} = \{c_1, \cdots, c_l\}$ with intersection graph a tree has a regular neighbourhood $N(\mathcal{C})$ with connected boundary and $l \geq 10$, the subgroup of $\mathrm{MCG}(N(\mathcal{C}))$ generated by all the Dehn twists around the curves of $\mathcal{C}$ only depends on the abstract intersection graph. In fact, for each such fixed l, we will see that there are at most 3 different isomorphism types of such groups, cf. Theorem 5.1.

Back to framings: In Chapter 4, we were interested in the Dehn twists around a specific family of curves on the fibre surface of a positive braid. To

study the group generated by those Dehn twists, we constructed an explicit framing fixed by all the twists and used the theory of framed mapping class groups. In fact, this is a special case of a more general construction. The starting point is the following easy observation. Consider a surface with boundary Σ' equipped with a framing ϕ'. Let Σ be a surface obtained by attaching a 1-handle h to Σ' and c an oriented simple closed curve on Σ that goes exactly once through the 1-handle (that is, c is the union of an arc in Σ' with the core of h). Then, ϕ' can be extended to a framing ϕ on Σ such that $\phi(c) = 0$. Indeed, consider the arc $a = \Sigma' \cap c$. Up to isotopy, we can assume that ϕ' is orthogonally inwards pointing at the boundary of a. To get the required framing on Σ, we now simply need to compute the winding number $\phi'(a) \in \frac{1}{2}\mathbb{Z}$ and construct a framing on the handle h that is orthogonally outwards pointing on the attaching boundary components and turns $-\phi'(a)$ times.

In particular, whenever a surface Σ is given by a sequence of plumbings of cylinders with core curves $c_1, \dots, c_l$, by iterating this construction one can obtain a framing ϕ on Σ such that $\phi(c_i) = 0$ for all i. This of course applies to h-assemblages, as defined in Chapter 2, Section 2. If we furthermore assume that all the core curves $c_1, \dots, c_l$ are non-separating (a condition needed for the curves to be admissible) we can directly invoke Proposition 2.2.

Corollary 5.1. *Let Σ be a surface and $\mathcal{C} = \{c_1, \cdots, c_l\}$ an h-assemblage of type E on Σ of genus $h \geq 5$. If all the curves in $\mathcal{C}$ are non-separating, then there exists a framing ϕ on Σ such that*

$$\langle T_c \mid c \in \mathcal{C} \rangle = \mathrm{MCG}(\Sigma, \phi).$$

This naturally leads to the following question.

Question 1. *Let Σ be a surface constructed by a sequence of plumbings of cylinders with non-separating core curves $c_1, \dots, c_l$ and ϕ a framing on Σ such that $\phi(c_i) = 0$ for all i. When do we have the equality*

$$\langle T_{c_1}, \dots, T_{c_l} \rangle = \mathrm{MCG}(\Sigma, \phi)?$$

It is clear that we cannot always hope for an equality. For instance, if the curves $c_1, \dots, c_l$ intersect in an A_l pattern, they generate a braid group B_{l+1}, which for l big enough is certainly not a framed mapping class group by Proposition 2.4. This is of course still the case for any family of curves that generates a braid group, even if they do not intersect in an A_l pattern; some examples of such curves are given in [11].

Remark 5.1. The surface Σ obtained by the plumbing construction just discussed is in general not the regular neighbourhood $N(\mathcal{C})$ of the core curves. While this is the case if the intersection graph of $\mathcal{C}$ is a tree, the presence of cycles in the graph will typically be reflected in the presence of disks in $\Sigma \setminus (\bigcup c_i)$.

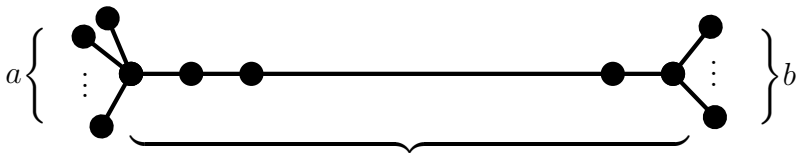

Figure 5.1: The double-star tree $DS(n; a, b)$

When the group in question happens to be a framed mapping class group, the next step is to compute the Arf invariant of the framing. Once again, if the boundary of Σ is connected, the results from Chapter 4 readily generalize to the current setting, as we will now explain. Instead of seeing (Σ, ϕ) as an abstract framed surface, let us represent it as an embedded surface in S^3 constructed by a sequence of plumbing of Hopf bands with core curves $c_1, \ldots, c_l$. There are of course many inequivalent ways of realizing such an embedding, which can for instance result in different boundary links, but this will be irrelevant in the following; let us just choose one. Now, if the boundary is a knot, the same computations as in Chapter 4, Section 3 show that the Arf invariant of the framing is equal to the Arf invariant of the knot. In particular, in this case the framed mapping class group is an invariant of the knot.

Question 2. *Let $\Sigma \subset S^3$ be a surface obtained by plumbing Hopf bands with core curves $c_1, \ldots, c_l$ and $L = \partial\Sigma$ be the boundary link. When is the group*

$$\langle T_{c_1}, \ldots, T_{c_l} \rangle \leqslant \mathrm{MCG}(\Sigma)$$

an invariant of L?

Arborescent plumbings: We will now study the case of curves intersecting in a tree pattern. In order to apply Corollary 5.1, we simply need to understand which trees contain the Dynkin diagram E_6 as a subtree.

Definition 5.1. Let $n \geq 1$, $a, b \geq 0$ be integers. The double-star tree $DS(n; a, b)$ is the tree obtained from an A_n tree by attaching a leaves to one of the vertices of degree 1 and b leaves to the other; if $n = 1$, we simply attach $a + b$ leaves to the unique vertex of A_1 (c.f. Figure 5.1).

A double-star tree $DS(n; a, b)$ has $n + a + b$ vertices. It is clear that the A_n and D_n trees are double-star trees (and can be represented in multiple ways).

Lemma 5.1. *A tree T is a double-star tree if and only if it does not contain E_6 as subtree.*

Proof. One implication is obvious: a double-star tree does not contain E_6. As for the other, we proceed with a simple induction. First, notice that all the trees with up to 6 crossings except E_6 are double-star trees. Now, suppose we have a tree T with $n+1$ vertices, $n \geq 6$, that does not contain E_6. Remove any leaf from T, obtaining a subtree T' with n vertices. By induction hypothesis, T' is a double-star tree. It is easy to verify that adding a leaf to a double-star tree with at least 6 vertices either results in another double-star tree or creates an E_6. □

Now, let T be a plane tree and Σ be a surface constructed by plumbing cylinders with core curves $c_1, \dots, c_l$ according to T. Note that, in our previous notation, $\Sigma = N(\mathcal{C})$. As we have seen, there exists a framing ϕ on Σ such that $\phi(c_i) = 0$ for all i, so, by Proposition 2.2 and Lemma 5.1, if T is not a double-star tree and Σ has genus at least 5 the group $\langle T_{c_1}, \dots, T_{c_l} \rangle \leqslant \mathrm{MCG}(\Sigma)$ is a framed mapping class group. If moreover Σ has a connected boundary, we know that such a framed mapping class group is determined by the genus of Σ (i.e. the number of vertices of T) and the Arf invariant of the framing, which we computed to be the Arf invariant of a knot obtained by plumbing Hopf bands according to T. In particular, as this Arf invariant is clearly independent of the plane embedding of T, the groups we obtain only depend on the abstract intersection graph. Finally, notice that the only double-star trees that give a surface with connected boundary are the A_n trees (for even n). To sum up, we have proved the following.

Theorem 5.1. *Let $\mathcal{C} = \{c_1, \dots, c_l\}$ be a family of curves with intersection graph a tree T and such that the boundary of $N(\mathcal{C})$ is connected. If $l \geq 10$, the group $G(\mathcal{C}) = \langle T_{c_1}, \dots, T_{c_l} \rangle \leqslant \mathrm{MCG}(N(\mathcal{C}))$ is uniquely determined by T. For every fixed l, there are only three possible groups: either $T = A_l$ and $G(\mathcal{C})$ is the braid group B_{l+1}, or $G(\mathcal{C})$ is one of two framed mapping class groups, distinguished by the Arf invariant.*

Remark 5.2. The trees which give a surface with connected boundary can be easily characterized: they are constructed starting from A_2 by consecutively attaching further copies of A_2 (in a similar way as generic trees can be constructed starting from a single vertex by consecutively attaching leaves). At the level of surfaces, this corresponds to so-called trefoil plumbing (cf. [10]).

Remark 5.3. The case of arborescent plumbings with disconnected boundary is much more delicate. Even if one could compute the Arf invariant of the framings, in general choosing a different plane embedding of the same tree will change the value of the framing on the various boundary components, and the theory of framed mapping class groups does not help in comparing the corresponding groups.

A comment on Artin groups: The results of Theorem 5.1 are particularly striking when compared to the analogous situation for Artin groups. Recall that an *Artin group* A is a group generated by a finite set S with generalized braid relations of the form $sts\cdots = tst\ldots$ for each pair of generators $s, t \in S$, where on each side of the equality there are $m(s,t) \in \{2,3,4,\ldots\} \cup \{\infty\}$ generators, and no other relation (having $m(s,t) = \infty$ simply means that there is no relation between s and t). Such a group presentation can be encoded by a finite, weighted graph Γ: the set of vertices is S, between two vertices s and t there is no edge if $m(s,t) = 2$, a simple edge if $m(s,t) = 3$ and an edge with weight $m(s,t)$ if $m(s,t) \geq 4$. Conversely, given such a weighted graph Γ, we will denote by $A(\Gamma)$ the Artin group presented by Γ. We say that an Artin group $A(\Gamma)$ is *irreducible* if Γ is connected. Clearly, a reducible Artin group is simply the direct product of its irreducible components. An Artin group is called of *small type* if all the weights are either 2 or 3. They correspond to classical, unweighted, simple graphs. In spite of the simplicity of their presentation, small-type Artin groups are very poorly understood, but expected to be very rich; in fact, it is conjectured that every Artin group can be realized as a subgroup of a small-type Artin group [63].

As we have already mentioned multiple times in previous chapters, small-type Artin groups are easily related to groups generated by finitely many Dehn twists. Given a simple graph Γ, if we realize it as the intersection graph of a family of curves $\mathcal{C}$, we directly get a group homomorphism

$$A(\Gamma) \to G(\mathcal{C}) \leqslant \mathrm{MCG}(N(\mathcal{C}))$$

by mapping a vertex of Γ to the Dehn twist around the corresponding curve. Such a homomorphism is called a geometric homomorphism. Perron and Vannier [68] proved that the Artin groups of type A_n and D_n admit injective geometric homomorphism, while Labruère [55] and Wajnryb [77] showed that this is not the case for any other tree. Notice that, contrary to what Wajnryb claimed, the question of what Artin groups have geometric embeddings is in general still open, as explained in [73]; Wajnryb's confusion seems related to an ambiguity about the surface in which to look at the Dehn twists.

A basic question about Artin groups is their rigidity, that is, how much does the isomorphism type of A determine its Artin presentations. In other words, if $A(\Gamma)$ and $A(\Gamma')$ are isomorphic, are then the graphs Γ and Γ' also isomorphic? While the answer is negative in full generality, Artin groups are still expected to satisfy rather strong rigidity properties, and rigidity has been proved for several interesting classes. In particular, in [16] the authors define an operation on graphs, called twisting, which leaves the associated Artin groups invariant and can sometimes give rise to examples of non-rigid Artin groups. To the best of our knowledge, this is the only known way of constructing non-rigid Artin groups, and it is an open question whether Artin groups are rigid up

to twisting (see [30], Problem 28). In the case of irreducible small-type Artin groups, a weaker form of rigidity (sometimes referred to as reflection rigidity) can be easily deduced for so-called non-spherical groups from the analogous result for Coxeter groups proved in [29] (see [16], Lemma 7.1). Notice that for spherical Artin groups rigidity was proved in full generality in [67], and that the only spherical, irreducible, small-type Artin groups are the well known groups of type A_n, D_n, E_6, E_7 and E_8. Moreover, irreducible small-type Artin groups do not admit any non-trivial twists [16], which is a further hint of their rigidity.

Now, consider trees satisfying the hypothesis of Theorem 5.1, with a fixed number l of vertices. While we already know that, with the lone exception of A_l, the groups generated by Dehn twists are not geometrically isomorphic to the corresponding Artin groups, if $l \geq 14$ Theorem 5.1 immediately implies that they are also not abstractly isomorphic: again, this follows from Proposition 2.4, as the abelianization of an irreducible small-type Artin group is infinite cyclic. More interestingly, we get a qualitative appreciation of this difference: by the discussion on rigidity, the Artin groups are expected to be all distinct, while the groups generated by the Dehn twists are essentially always the same.

Bibliography

[1] N. A'Campo. "Generic immersions of curves, knots, monodromy and Gordian number". In: *Inst. Hautes Études Sci. Publ. Math.* 88 (1998), 151–169 (1999).

[2] N. A'Campo. "Le groupe de monodromie du déploiement des singularités isolées de courbes planes. I". In: *Math. Ann.* 213 (1975), pp. 1–32.

[3] N. A'Campo. "Le groupe de monodromie du déploiement des singularités isolées de courbes planes. II". In: *Proceedings of the International Congress of Mathematicians (Vancouver, B.C., 1974), Vol. 1*. Canad. Math. Congress, Montreal, Que., 1975, pp. 395–404.

[4] N. A'Campo. "Real deformations and complex topology of plane curve singularities". In: *Ann. Fac. Sci. Toulouse Math. (6)* 8.1 (1999), pp. 5–23.

[5] N. A'Campo. "Sur la monodromie des singularités isolées d'hypersurfaces complexes". In: *Invent. Math.* 20 (1973), pp. 147–169.

[6] V. I. Arnold. "Normal forms of functions near degenerate critical points, the Weyl groups A_k, D_k, E_k and Lagrangian singularities". In: *Funkcional. Anal. i Priložen.* 6.4 (1972), pp. 3–25.

[7] V. I. Arnold, S. M. Gusein-Zade, and A. N. Varchenko. *Singularities of differentiable maps. Volume 1*. Modern Birkhäuser Classics. Birkhäuser/ Springer, New York, 2012. xii+382.

[8] V. I. Arnold, S. M. Gusein-Zade, and A. N. Varchenko. *Singularities of differentiable maps. Volume 2*. Modern Birkhäuser Classics. Birkhäuser/ Springer, New York, 2012. x+492.

[9] S. Baader. "Positive braids of maximal signature". In: *Enseign. Math.* 59.3 (2013), pp. 351–358.

[10] S. Baader and P. Dehornoy. "Trefoil plumbing". In: *Proc. Amer. Math. Soc.* 144.1 (2016), pp. 387–397.

[11] S. Baader, P. Feller, and L. Ryffel. "Bouquets of curves in surfaces". In: *Glasg. Math. J.* 65.1 (2023), pp. 90–97.

[12] S. Baader, L. Lewark, and L. Liechti. "Checkerboard graph monodromies". In: *Enseign. Math.* 64.1 (2018), pp. 65–88.

[13] S. Baader and M. Lönne. "Secondary Braid Groups". In: *arXiv:2001.09098* (2021). arXiv: 2001.09098.

[14] J. S. Birman and W. W. Menasco. "A note on closed 3-braids". In: *Commun. Contemp. Math.* 10 (suppl. 1 2008), pp. 1033–1047.

[15] J. S. Birman and W. W. Menasco. "Studying links via closed braids. III. Classifying links which are closed 3-braids". In: *Pacific J. Math.* 161.1 (1993), pp. 25–113.

[16] N. Brady et al. "Rigidity of Coxeter groups and Artin groups". In: *Geometriae Dedicata*. Vol. 94. 2002, pp. 91–109.

[17] K. Brauner. "Das Verhalten der Funktionen in der Umgebung ihrer Verzweigungsstellen". In: *Abh. Math. Sem. Univ. Hamburg* 6.1 (1928), pp. 1–55.

[18] E. Brieskorn. "Beispiele zur Differentialtopologie von Singularitäten". In: *Invent. Math.* 2 (1966), pp. 1–14.

[19] E. Brieskorn. "Die Fundamentalgruppe des Raumes der regulären Orbits einer endlichen komplexen Spiegelungsgruppe". In: *Invent. Math.* 12 (1971), pp. 57–61.

[20] E. Brieskorn. "Examples of singular normal complex spaces which are topological manifolds". In: *Proc. Nat. Acad. Sci. U.S.A.* 55 (1966), pp. 1395–1397.

[21] E. Brieskorn. "Singular elements of semi-simple algebraic groups". In: *Actes du Congrès International des Mathématiciens (Nice, 1970), Tome 2*. Gauthier-Villars, Paris, 1971, pp. 279–284.

[22] E. Brieskorn. "Sur les groupes de tresses [d'après V. I. Arnol'd]". In: *Séminaire Bourbaki, 24ème année (1971/1972)*. Lecture Notes in Math., Vol. 317. Springer, Berlin, 1973, Exp. No. 401, pp. 21–44.

[23] E. Brieskorn. "Vue d'ensemble sur les problèmes de monodromie". In: *Singularités à Cargèse (Rencontre Singularités Géom. Anal., Inst. Études Sci., Cargèse, 1972)*. Astérisque, Nos. 7 et 8. Soc. Math. France, Paris, 1973, pp. 393–413.

[24] E. Brieskorn and H. Knörrer. *Plane algebraic curves*. Birkhäuser Verlag, Basel, 1986. vi+721.

[25] W. Burau. "Kennzeichnung der Schlauchknoten". In: *Abh. Math. Sem. Univ. Hamburg* 9.1 (1933), pp. 125–133.

[26] G. Burde and H. Zieschang. *Knots*. Second. Vol. 5. De Gruyter Studies in Mathematics. Walter de Gruyter & Co., Berlin, 2003.

[27] A. Calderon and N. Salter. "Framed mapping class groups and the monodromy of strata of Abelian differentials". In: *arXiv:2002.02472* (2020). arXiv: 2002.02472.

[28] A. Calderon and N. Salter. "Higher spin mapping class groups and strata of abelian differentials over Teichmüller space". In: *Adv. Math.* 389 (2021), Paper No. 107926, 56.

[29] P.-E. Caprace and B. Mühlherr. "Reflection rigidity of 2-spherical Coxeter groups". In: *Proc. Lond. Math. Soc. (3)* 94.2 (2007), pp. 520–542.

[30] R. Charney. *Problems related to Artin Groups*. 2008.

[31] D. R. J. Chillingworth. "Winding numbers on surfaces. I". In: *Math. Ann.* 196 (1972), pp. 218–249.

[32] D. R. J. Chillingworth. "Winding numbers on surfaces. II". In: *Math. Ann.* 199 (1972), pp. 131–153.

[33] O. Couture and B. Perron. "Representative braids for links associated to plane immersed curves". In: *J. Knot Theory Ramifications* 9.1 (2000), pp. 1–30.

[34] P. R. Cromwell. "Positive braids are visually prime". In: *Proc. London Math. Soc. (3)* 67.2 (1993), pp. 384–424.

[35] A. H. Durfee. "Singularities". In: *History of topology*. North-Holland, Amsterdam, 1999, pp. 417–434.

[36] B. Farb and D. Margalit. *A primer on mapping class groups*. Vol. 49. Princeton Mathematical Series. Princeton University Press, Princeton, NJ, 2012. xiv+472.

[37] L. Ferretti. "On Positive Braids, Monodromy Groups and Framings". In: *arXiv:2111.08150* (2021). arXiv: 2111.08150.

[38] R. Fintushel and R. J. Stern. "Invariants for homology 3-spheres". In: *Geometry of low-dimensional manifolds, 1 (Durham, 1989)*. Vol. 150. London Math. Soc. Lecture Note Ser. Cambridge Univ. Press, Cambridge, 1990, pp. 125–148.

[39] R. Fintushel and R. J. Stern. "Pseudofree orbifolds". In: *Ann. of Math. (2)* 122.2 (1985), pp. 335–364.

[40] Sergey Fomin et al. "Morsifications and mutations". In: *J. Lond. Math. Soc. (2)* 105.4 (2022), pp. 2478–2554.

[41] M. Furuta. "Homology cobordism group of homology 3-spheres". In: *Invent. Math.* 100.2 (1990), pp. 339–355.

[42] F. A. Garside. "The braid group and other groups". In: *Quart. J. Math. Oxford Ser. (2)* 20 (1969), pp. 235–254.

[43] H. Goda, M. Hirasawa, and Y. Yamada. "Lissajous curves as A'Campo divides, torus knots and their fiber surfaces". In: *Tokyo J. Math.* 25.2 (2002), pp. 485–491.

[44] S. M. Guseın-Zade. "Dynkin diagrams of the singularities of functions of two variables". In: *Funkcional. Anal. i Priložen.* 8.4 (1974), pp. 23–30.

[45] S. M. Guseın-Zade. "Intersection matrices for certain singularities of functions of two variables". In: *Funkcional. Anal. i Priložen.* 8.1 (1974), pp. 11–15.

[46] U. Hamenstädt. "Generating the spin mapping class group by Dehn twists". In: *Ann. H. Lebesgue* 4 (2021), pp. 1619–1658.

[47] U. Hamenstädt. *Quotients of the orbifold fundamental group of strata of abelian differentials*. 2018.

[48] M. Hirasawa. "Visualization of A'Campo's fibered links and unknotting operation". In: *Topology Appl.* 121.1 (2002), pp. 287–304.

[49] F. Hirzebruch and K. H. Mayer. *$O(n)$-Mannigfaltigkeiten, exotische Sphären und Singularitäten*. Lecture Notes in Mathematics, No. 57. Springer-Verlag, Berlin-New York, 1968. iv+132.

[50] S. P. Humphries. "Free products in mapping class groups generated by Dehn twists". In: *Glasgow Math. J.* 31.2 (1989), pp. 213–218.

[51] S. P. Humphries and D. Johnson. "A generalization of winding number functions on surfaces". In: *Proc. London Math. Soc. (3)* 58.2 (1989), pp. 366–386.

[52] D. Johnson. "Spin structures and quadratic forms on surfaces". In: *J. London Math. Soc. (2)* 22.2 (1980), pp. 365–373.

[53] K. H. Ko and S. J. Lee. "Flypes of closed 3-braids in the standard contact space". In: *J. Korean Math. Soc.* 36.1 (1999), pp. 51–71.

[54] P. B. Kronheimer and T. S. Mrowka. "The genus of embedded surfaces in the projective plane". In: *Math. Res. Lett.* 1.6 (1994), pp. 797–808.

[55] C. Labruère. "Generalized braid groups and mapping class groups". In: *J. Knot Theory Ramifications* 6.5 (1997), pp. 715–726.

[56] S. K. Lando and A. K. Zvonkin. *Graphs on surfaces and their applications*. Vol. 141. Encyclopaedia of Mathematical Sciences. Springer-Verlag, Berlin, 2004. xvi+455.

[57] N. Levinson. "A polynomial canonical form for certain analytic functions of two variable at a critical point". In: *Bull. Amer. Math. Soc.* 66 (1960), pp. 366–368.

[58] W. B. R. Lickorish. *An introduction to knot theory*. Vol. 175. Graduate Texts in Mathematics. Springer-Verlag, New York, 1997.

[59] L. Liechti. "On the genus defect of positive braid knots". In: *Algebr. Geom. Topol.* 20.1 (2020), pp. 403–428.

[60] M. Lönne. *Braid Monodromy of Hypersurface Singularities*. 2006. arXiv: `math/0602371`.

[61] M. Lönne. "Fundamental group of discriminant complements of Brieskorn-Pham polynomials". In: *C. R. Math. Acad. Sci. Paris* 345.2 (2007), pp. 93–96.

[62] M. Lönne. "On a discriminant knot group problem of Brieskorn". In: *J. Singul.* 18 (2018), pp. 455–463.

[63] J. McCammond. "The mysterious geometry of Artin groups". In: *Winter Braids Lect. Notes* 4 (Winter Braids VII (Caen, 2017) 2017), Exp. No. 1, 30.

[64] J. Milnor. *Singular points of complex hypersurfaces*. Annals of Mathematics Studies, No. 61. Princeton University Press, Princeton, N.J.; University of Tokyo Press, Tokyo, 1968. iii+122.

[65] D. Mumford. "The topology of normal singularities of an algebraic surface and a criterion for simplicity". In: *Inst. Hautes Études Sci. Publ. Math.* 9 (1961), pp. 5–22.

[66] W. D. Neumann. "A calculus for plumbing applied to the topology of complex surface singularities and degenerating complex curves". In: *Trans. Amer. Math. Soc.* 268.2 (1981), pp. 299–344.

[67] L. Paris. "Artin groups of spherical type up to isomorphism". In: *J. Algebra* 281.2 (2004), pp. 666–678.

[68] B. Perron and J. P. Vannier. "Groupe de monodromie géométrique des singularités simples". In: *Math. Ann.* 306.2 (1996), pp. 231–245.

[69] F. Pham. "Courbes discriminantes des singularités planes d'ordre 3". In: *Singularités à Cargèse (Rencontre Singularités Géom. Anal., Inst. Études Sci., Cargèse, 1972)*. Astérisque, Nos. 7 et 8. Soc. Math. France, Paris, 1973, pp. 363–391.

[70] P. Portilla Cuadrado and N. Salter. "Vanishing cycles, plane curve singularities and framed mapping class groups". In: *Geom. Topol.* 25.6 (2021), pp. 3179–3228.

[71] O. Randal-Williams. "Homology of the moduli spaces and mapping class groups of framed, r-Spin and Pin surfaces". In: *J. Topol.* 7.1 (2014), pp. 155–186.

[72] E. A. El-Rifai and H. R. Morton. "Algorithms for positive braids". In: *Quart. J. Math. Oxford Ser. (2)* 45.180 (1994), pp. 479–497.

[73] Levi Ryffel. "Curves intersecting in a circuit pattern". In: *Topology Appl.* 332 (2023), Paper No. 108522.

[74] N. Salter. "Monodromy and vanishing cycles in toric surfaces". In: *Invent. Math.* 216.1 (2019), pp. 153–213.

[75] J. R. Stallings. "Constructions of fibred knots and links". In: *Algebraic and geometric topology (Proc. Sympos. Pure Math., Stanford Univ., Stanford, Calif., 1976), Part 2*. Proc. Sympos. Pure Math., XXXII. Amer. Math. Soc., Providence, R.I., 1978, pp. 55–60.

[76] L. Vilanova. "Positive Hopf plumbed links with maximal signature". PhD thesis. Bern: Universität Bern, Dec. 2020.

[77] B. Wajnryb. "Artin groups and geometric monodromy". In: *Invent. Math.* 138.3 (1999), pp. 563–571.

[78] R. F. Williams. "The braid index of an algebraic link". In: *Braids (Santa Cruz, CA, 1986)*. Vol. 78. Contemp. Math. Amer. Math. Soc., Providence, RI, 1988, pp. 697–703.

[79] O. Zariski. "On the Topology of Algebroid Singularities". In: *Amer. J. Math.* 54.3 (1932), pp. 453–465.

Declaration of consent

on the basis of Article 18 of the PromR Phil.-nat. 19

,

Name/First Name: Ferretti Livio Clemente Emilio

Registration Number: 14-338-040

Study program: Mathematics

Bachelor ☐ Master ☐ Dissertation ☑

Title of the thesis: On positive braids and monodromy groups of plane curve singularities

Supervisor: Prof. Dr. Sebastian Baader

I declare herewith that this thesis is my own work and that I have not used any sources other than those stated. I have indicated the adoption of quotations as well as thoughts taken from other authors as such in the thesis. I am aware that the Senate pursuant to Article 36 paragraph 1 litera r of the University Act of September 5th, 1996 and Article 69 of the University Statute of June 7th, 2011 is authorized to revoke the doctoral degree awarded on the basis of this thesis.
For the purposes of evaluation and verification of compliance with the declaration of originality and the regulations governing plagiarism, I hereby grant the University of Bern the right to process my personal data and to perform the acts of use this requires, in particular, to reproduce the written thesis and to store it permanently in a database, and to use said database, or to make said database available, to enable comparison with theses submitted by others.

Bern, 29.06.2023

Place/Date

Signature